Scuola Normale Superiore

Classe di Scienze

Anno Accademico 2020

Tesi di Perfezionamento in Fisica

Black Objects without a Vacuum

Candidato

Riccardo Antonelli

Relatore

Prof. Augusto Sagnotti

Ottobre 2020

Abstract

We explore the behavior of gravitational solitons in classical theories with pathological vacua. We first focus on non-tachyonic non-supersymmetric string theories and the construction of brane solutions in the corresponding effective theories, which do not admit a maximally-symmetric vacuum. We then turn to metastable vacua and the holographic interpretation of the vacuum bubbles that may be produced therein by quantum tunneling. Finally, we discuss self-similar collapse solutions, with an eye to analogies with the settings considered in the preceding chapters.

Introduction

In the discussion of solitonic objects within a physical system, the basic notion of a *vacuum* hosting them is rarely put into question, if it is considered at all. This assumption is certainly justified in most contexts. In the quantum case, the existence of a ground state is necessary to grant the absence of tadpoles, and thus finite transition amplitudes. For a classical system, however, the requirement is arguably less precise and typically more philosophically motivated. The very expression *isolated* object implicitly carries a prejudice about the existence of an "emptiness" that the object itself is able to contrast in some sense - it appears contradictory to speak of a "something" without a notion of what is left when that very "something" is removed. A "vacuum-less" classical theory – in any one of the varied forms in which a system can have a lacking, or at the very least, a pathological background – invites to meditate upon this question that is thus elevated beyond mere semantics.

In this work, we report on research results concerning several practical instances when this general phenomenon is realized in varied contexts. All of these relate specifically to gravitational physics, both quantum and classical, and thus the discussion concerning isolated objects is specified as one about black holes, branes, and similar gravitationally-dominated solitons.

Chapter 1 is dedicated to one essential example of contemporary interest, which is provided by the low-energy effective gravitational theories of some non–tachyonic non-supersymmetric string theories in ten dimensions [1–9].

Here String Theory provides strong reasons to expect that the original quantum theory be meaningful, but its ground state is strongly affected by the known quantum corrections. In practice, the effective theories develop unbounded Einstein-frame dilaton potentials of the runaway type,

$$V(\phi) \propto \exp(\gamma\phi)\,, \quad \gamma > 0\,, \tag{1}$$

so that they are driven dynamically away from the maximally symmetric Minkowski vacua where the string theories were originally defined. Nevertheless, such theories do allow form-fluxed solutions of the AdS $\times$ $\mathbb{S}$ type, leading one to conjecture that these are in some way the realisation of brane-like objects, possibly related to the D-branes that can be identified from the worldsheet theory [10]. Part of our contributions to this topic [11] concern specifically the delicate question of extending these candidate near-horizon geometries into full-fledged brane-like profiles, under the limitation that these profiles certainly cannot, as would otherwise be the norm with supersymmetry, interpolate between the AdS $\times$ $\mathbb{S}$ throat and a maximally-symmetric infinity. In fact, *the results suggest that in the full brane geometry space ends abruptly at some finite radius, dissolving into a characteristic type of singularity where the potential of eq.* (1) *drives the dilaton to* $\pm\infty$ *within a finite geodesic distance*. The challenge is to interpret this singularity in such a way that it can physically substitute the original role of empty space – in particular to identify whether some new principles can replace the now lost boundary conditions and eliminate spurious parameters in the solutions. As the standard notion of asymptotic charges, including mass, cannot be relied

upon, one is led to inquire whether generalized replacements to such observables can still be constructed. The limited extent to which this program has been pursued to date suffices to see glimpses of a curious picture for these non-supersymmetric string theories, where the ground state lacks a smooth spacetime, but a sufficiently large stack of charged branes can still support a finite "pocket" of smooth space.

In Chapter 2, instead, we retrace the analysis of [12]. This work focused on the holographic interpretation of a metastable AdS vacuum and its decay to a true AdS vacuum through nucleation and expansion of a vacuum bubble [13, 14]. In this case, the "isolated" object is the bubble itself, which admits a brane-like description, although it is immersed in the highly unusual background of an unstable empty space. In this case, the resulting physical puzzle is whether the celebrated AdS / CFT correspondence can apply throughout the decay process, and if so, how it should be modified to account for the absence of a stable AdS infinity. Through the Ryu-Takayanagi conjecture [15], information-theoretical parameters of the boundary theory, such as the entanglement entropy, map to geometrical properties of the bulk; correspondingly, the work demanded a thorough examination of the geometry of an expanding bubble of true vacuum in a metastable AdS. This geometrical angle of [12] will be our primary focus.

Finally, Chapter 3 is devoted to the study of self-similar collapse in the classical Einstein-axion-dilaton system, following [16, 17]. Starting from [18], a fascinating area of research in classical gravitation arose from the observation, originally motivated by numerical investigations, that *critical* gravitational

collapse – that is to say on the threshold between collapse into a black hole and diffusion – generically develops a space-time self-similarity of some kind. A long series of works [19–26] has further refined the details of a deep and multi–faceted link between initial conditions on the verge of black hole formation and scale-invariant spacetimes, for several matter models, numbers of dimensions and symmetries of the collapse. A strong analogy with parallel phenomena in Statistical Mechanics drives many questions and approaches. In particular, there is a long-held interest into power-law scalings of observables when approaching criticality and in the corresponding exponents as candidate "critical exponents for gravity". Our works [16, 17] were targeted mainly at the specific case of the gravitational collapse of the axion-dilaton system in four and five dimensions, including the classification of continuously scale-invariant geometries and their properties as attractors for critical collapse. Determining the existence, number, and quantitative parameters of these solutions proved a highly non-trivial task. The association with the topic of the present thesis is in this case not much physical in nature, but rather mathematical: the equation of motions that determine a self-similar solution are similar, both in the form of the resulting ordinary differential equations and the specifics of the boundary conditions, to the equations that determine the profile of a brane in the absence of valid boundary conditions at infinity. The rich and unpredictable structure of the solution space for self-similar collapse in the axion-dilaton system can thus shed light on the equally opaque problem of isolated objects in a vacuum-less theory that we outlined previously.

Contents

Chapter 1

On Black branes in non-supersymmetric strings

Despite years of activity, how to effect supersymmetry breaking in String Theory in a controllable fashion remain a puzzle of key importance. Surely for phenomenological applications, but not only. Different mechanisms have been detailed over the years, and the advantages and flaws of each scenario have been extensively investigated [27–38]. A generic undesirable feature is the emergence of instabilities that accompany, in one form or another, the breaking of supersymmetry, which can be of different degrees of severity. The state can be a local minimum of the potential, in which case it is typically a metastable, or false vacuum, which decays via a quantum tunneling process, but a more drastic instability occurs if the effective gravitational theory simply has no viable equilibria to offer, and its own dynamics drives the state

outside the regime of validity of the effective theory itself, specifically to high curvatures or high values of the string coupling. At best the vacuum is then, so to speak, highly stringy, and does not seem to conform to meaningful smooth spacetime. This extreme situation of vacumlessness for the classical theory could be termed "spacelessness", since we do expect a dynamic tendency toward smooth spacetimes to disappear at equilibrium, or in other words for curvature radii to be dynamically driven to shrink towards the string scale. However, strictly speaking these scenarios transcend the range of applicability of the effective field theory, and concern settings where past experience leaves some definite room for surprises.

In this chapter, we focus on a specific class of non–tachyonic string models where supersymmetry is broken at the string scale or not present altogether. We can collect the three relevant models [1–4, 6–9] under the name of **non-supersymmetric non–tachyonic string theories** (NT), since the present analysis, which is limited to low–energy bosonic profiles, is insensitive to this otherwise important distinction. Generally, one builds a non-supersymmetric string theory starting from worldsheet amplitudes and consistency conditions. A special projection compatible with modular invariance thus results in the $\mathrm{SO}(16) \times \mathrm{SO}(16)$, while when open and/or unoriented sectors bring along a more sophisticated world–sheet construction and a space–time picture in terms of orientifold planes and/or D-branes. In the supersymmetric case these objects are mutually BPS, with "brane supersymmetry breaking" [6–9] they are individually BPS but not mutually so, and finally in the $\mathrm{U}(32)$ string they are also individually not BPS. In all cases, the form charges of these filling objects must cancel, but broken supersymmetry manifests it-

self via a vacuum energy reflecting an overall residual tension, and a similar effect emerges from one-loop corrections in the SO(16) × SO(16) model. In all these cases the effective Einstein-frame action features a vacuum energy that scales like a power of $g_s = e^{\phi}$, and thus an (Einstein-frame) exponential dilaton potential [39]

$$V(\phi) = T \exp(\gamma\phi)\,, \quad \gamma > 0\,. \tag{1.1}$$

Consequently, in such effective theories there are no maximally-symmetric vacua at all, but non-maximally metric solutions do exist. However they transcend, in some regions, the regime where the effective field theory can be safely applied.

For the SO(16) × SO(16) heterotic model of [1], [2] the string–frame effective action is

$$S^S_{\rm het} = \frac{1}{2\kappa_{10}^2}\int d^{10}x\,\sqrt{-g}\left(e^{-2\phi}\left(R + 4(\partial\phi)^2 - \frac{1}{12}H_3^2\right) - T\right)\,, \tag{1.2}$$

where $H_3 = dB_2$ is the Kalb-Ramond field strength, and a positive value for T arises from one-loop corrections, and was computed in [1]. Its detailed value, however, is of limited interest for now, as are terms involving other gauge fields, which we have omitted. The dynamics of the effective action (1.2) becomes more transparent upon conversion to the Einstein frame:

$$S^E_{\rm het} = \frac{1}{2\kappa_{10}^2}\int d^{10}x\,\sqrt{-g}\left(R - \frac{1}{2}(\partial\phi)^2 - Te^{\frac{5}{2}\phi} - e^{-\phi}\frac{H_3^2}{12}\right)\,. \tag{1.3}$$

It is then clear that eq. (1.3) has no Minkowski solutions due to the runaway dilaton potential. In fact, there are no maximally-symmetric (AdS_{10} or dS_{10}) solutions either, since the constant curvature can only shift the potential by a constant.

On the other hand, the relevant non-supersymmetric string theories that we can group under the umbrella term of orientifold models, as we have said, as the so-called "0'B" U(32) theory [3, 4] and the Sugimoto USp(32) one [5], which is the prototype of the "brane supersymmetry breaking" scenario of [6–9]. Leeavng aside other gauge fields, the effective theories of these models are actually identical, and are given in the string frame by

$$S^S_{\rm or} = \frac{1}{2\kappa_{10}^2}\int d^{10}x\,\sqrt{-g}\left(e^{-2\phi}\left(R + 4(\partial\phi)^2\right) - \frac{1}{12}F_3^2 - Te^{-\phi}\right)\,, \qquad (1.4)$$

where $F_3 = dC_2$ is now actually a Ramond-Ramond field strength. In this case, the T term reflects a residual tension at the (projective) disk level, and is correspondingly weighed by a $e^{-\phi}$ factor. Since it is not a loop effect for closed strings, T can be estimated much more easily:

$$T = (2\kappa_{10}^2)\,64\,T_{D9} = \frac{16}{\pi^2\alpha'}\,, \qquad (1.5)$$

counting essentially the cumulative tension of 16 D9, 16 $\overline{\rm D9}$-branes, and a balancing orientifold plane. In any case, in the Einstein frame we recover an equally problematic gravitational theory:

$$S^E_{\rm or} = \frac{1}{2\kappa_{10}^2}\int d^{10}x\,\sqrt{-g}\left(R - \frac{1}{2}(\partial\phi)^2 - Te^{\frac{3}{2}\phi} - e^{\phi}\frac{F_3^2}{12}\right)\,, \qquad (1.6)$$

about which similar remarks on instability can be made.

In [11], we made the case for streamlining this discussion by extending our consideration to a larger parametric class of such Einstein-frame systems in a general dimension D and in presence of a p-form potential, given by the action

$$S = \frac{1}{2\kappa_{10}^2}\int d^{D}x\,\sqrt{-g}\left(R - \frac{4}{D-2}(\partial\phi) - Te^{\gamma\phi} - e^{\alpha\phi}\frac{H_{p+2}^2}{2(p+2)!}\right)\,, \qquad (1.7)$$

whose parameters are the spacetime dimension D, rank p, coupling $T > 0$, and exponents $\gamma > 0$ and α. The aforementioned effective models are special cases of the general action (1.7). In fact, both heterotic and orientifold $D = 10$ models afford a double representation in this general action, if one considers the dualization of the form field, which flips the sign of α:

p	Heterotic (RR)	Orientifold (KR)
$p = 1$	$\gamma = \frac{5}{2}$, $\alpha = -1$	$\gamma = \frac{3}{2}$, $\alpha = 1$
$p = 5$	$\gamma = \frac{5}{2}$, $\alpha = 1$	$\gamma = \frac{3}{2}$, $\alpha = -1$

The actions spanned by (1.7) are thus key examples of classical "vacuumless" theories in the sense we have outlined before. It is not excluded that a symmetric vacuum be recovered somehow at the string level, but it must lie outside of the range of applicability of the effective action itself. If this were not the case, this vacuum would be realised as a solution of the latter respecting maximal symmetry, which impossible for these systems.

Still, these effective theories are not necessarily to be discarded, since they arise from tightly constrained string construction, and moreover they hold definitely much interesting physics to be worthy of investigation. One can for example study time-dependent backgrounds for cosmological purposes, as in [40–43]. Alternatively, there is an interesting structure of static compactifications. Moreover, it was first recognized in [44] that the orientifold models support $\mathrm{AdS}_3 \times \mathbb{S}_7$ backgrounds stabilized by a Kalb-Ramond 3-form flux, while the heterotic model allows instead an $\mathrm{AdS}_7 \times \mathbb{S}_3$ geometry with a Ramond-Ramond 7-form flux. The D1-branes of the orientifold model and

the NS5-branes of the heterotic model might thus find a place in supergravity.

In [11] we constructed the parametric generalisation of these solutions to the action (1.7). It is a fluxed $\mathrm{AdS}_{p+2} \times \mathbb{S}_q$ geometry[1], with $q \equiv D - p - 2$:

$$\begin{aligned} ds^2 &= L^2 ds^2_{\mathrm{AdS}_{p+2}} + R^2 d\Omega_q^2 \\ H_{p+2} &= c\, \mathrm{Vol}_{\mathrm{AdS}_{p+2}} \\ \phi &= \phi_0 \end{aligned} \tag{1.8}$$

where $\mathrm{Vol}_{\mathrm{AdS}_{p+2}}$ is the volume form on AdS_{p+2} with radius L. The constants L, R, c, ϕ_0 are all determined by a single flux parameter n, not necessarily an integer, which is defined as

$$n = \frac{1}{\Omega_q} \int_{\mathbb{S}_q} e^{\alpha\phi} H_{p+2} = c e^{\alpha\phi} R^q \,. \tag{1.9}$$

Physically, the solution rests on the balance between the effects of form flux and of the runaway potential. *This equilibrium fixes a unique value for the dilaton and curvature radii, and thus, unlike the supersymmetric fluxed* $\mathrm{AdS} \times \mathbb{S}$ *counterparts, there is no additional string coupling modulus.* This balance, and therefore the solution, exists if and only if

$$\alpha > 0 \,, \quad q > 1 \,, \quad (q-1)\gamma - \alpha > 0 \,. \tag{1.10}$$

[1] We note that in fact the sphere may be replaced with any compact Einstein manifold M_q.

Under the conditions (1.10), the solution reads

$$\begin{aligned} c &= \frac{n}{g_s^\alpha R^q}\,, \\ g_s^{(q-1)\gamma-\alpha} &= \left(\frac{(q-1)(D-2)}{(1+\frac{\gamma}{\alpha}(p+1))T}\right)^q \frac{2\gamma T}{\alpha n^2}\,, \\ R^{2\frac{(q-1)\gamma-\alpha}{\gamma}} &= \left(\frac{\alpha+(p+1)\gamma}{(q-1)(D-2)}\right)^{\frac{\alpha+\gamma}{\gamma}} \left(\frac{T}{\alpha}\right)^{-\frac{\alpha}{\gamma}} \frac{n^2}{2\gamma}\,, \\ L^2 &= R^2\left(\frac{p+1}{q-1}\cdot\frac{(p+1)\gamma+\alpha}{(q-1)\gamma-\alpha}\right) \equiv \frac{R^2}{A}\,, \end{aligned} \tag{1.11}$$

with $g_s \equiv e^{\phi_0}$. Not only can one read off the features of the allowed AdS $\times$ $\mathbb{S}$ flux vacua, but one can also gain some physical intuition about those that could be expected but are nevertheless forbidden. For example, there is no $\mathrm{AdS}_7\times\mathbb{S}_3$ in the orientifold model, corresponding to D5-branes, nor $\mathrm{AdS}_3\times\mathbb{S}_7$ in the heterotic model, corresponding to NS1-branes, even though both these brane species are believed to be present at the string level. In these cases, with $\alpha < 0$, the tadpole dilaton potential and the flux are acting in the same direction on the dilaton itself, which is thus driven to $\phi \to -\infty$, and no equilibrium is possible. The expectation (currently unverified to the best of our knowledge) is that corresponding configurations, if they somehow exist, lie well into the stringy regime, even for large flux n.

In [11] we explored the consequences of pushing the above observations a bit further - that the vacua just described, which balance tadpole potential and form flux pressure, may be near-horizon geometries to brane stacks. It is important to again stress the delicate nature of this claim in the absence of a vacuum in the effective theory. The nature of a possible "full profile" for the brane stack geometry, if such a construction is even sensible, constitutes

a highly non-trivial puzzle.

1.1 Black brane equations in non-supersymmetric strings

The actions of the family (1.7) offer manifold possibilities for the search for useful solutions of particular symmetry, each bringing along particular complications. Therefore, it is essential to narrow the focus to a very specific subset of configurations. We will restrict first of all to geometries with the symmetries of p-branes, fluxed by the H_{p+2} form, and which are "extremal". In this *a priori* context, by extremal we mean that it enjoys full parallel Poincaré symmetry $\mathrm{ISO}(1,p) = \mathbb{R}^{1,p} \rtimes \mathrm{SO}(1,p)$. This may eventually be relaxed to $\mathbb{R} \times \mathrm{ISO}(p)$ for a "non-extremal" brane. With the addition of transverse rotational symmetry, one is left with configurations invariant under the group

$$\mathrm{ISO}(1,p) \times \mathrm{SO}(q)\,, \quad q = D - p - 2\,. \tag{1.12}$$

The general such profile can be written in the following form:

$$\begin{aligned} ds^2 &= e^{2a(r)}\, dx_{1,p}^2 + e^{2c(r)}\, dr^2 + e^{2b(r)}\, R_0^2\, d\Omega_q^2\,, \\ \phi &= \phi(r)\,, \\ H_{p+2}(r) &= h(r)\mathrm{Vol}_{p+2}\,, \qquad \mathrm{Vol}_{p+2} = e^{(p+1)a(r)+c(r)}\, d^{p+1}x \,\wedge\, dr\,, \end{aligned} \tag{1.13}$$

in which we considered an electric flux for the form. We can nevertheless encompass magnetic charges as well within this same form simply by effecting

the duality transformation $p+2 \leftrightarrow q$, $\alpha \to -\alpha$ directly on the original action, so (1.13) is fully general. The equation of motion for H_{p+2} stemming from action (1.7) within the ansatz (1.13) is immediately solved:

$$H_{p+2} = \frac{n}{e^{\alpha\phi(r)}(R_0\, e^{b(r)})^q}\mathrm{Vol}_{p+2}\,, \tag{1.14}$$

where R_0 is an arbitrary constant with units of length, convenient so as to keep $e^{b(r)}$ dimensionless, and which will ultimately drop out of all observables. One is thus left with determining the non-trivial dynamics of the warp functions $a(r)$, $b(r)$, $c(r)$ and the dilaton $\phi(r)$ through the remaining equations of motion. In truth, however, (1.13) is actually still too general, since the gauge transformations corresponding to r diffeomorphisms are available to remove a degree of freedom from the metric functions.

There are several convenient choices at this point, but the most effective in this context is to employ the gauge freedom to impose a linear constraint involving the warp functions, with the specific relationship being determined so as to reduce the field equations to a particularly compact form. Let us review the procedure for the case at hand. The field equations are first computed for the action (1.7) and the ansatz (1.13). Then, collecting the warpings and dilaton in a vector $\vec{a}(r) = (a(r), b(r), c(r), \phi)$, one observes that the equations of motion take the form

$$\vec{a}\,'' + \vec{a}\,' \cdot D\vec{a}\,' = F(\vec{a})\,, \tag{1.15}$$

where D is some constant "drag matrix" and $F(\vec{a})$ are arbitrary force terms. It should be clear that it is generically of interest to perform a change of basis so that D is in diagonal form if possible, or otherwise at least in Jordan

normal form, before taking a decision on the gauge constraint. In the particular situation of action (1.13) this procedure is especially fruitful, as the 4×4 drag matrix D is diagonalizable with three zero eigenvalues, so that the eigenvector to the non-zero eigenvalue can be the one eliminated through gauge freedom. This reduces the equations of motion to a purely Newtonian system for the remaining three fields, say $\vec{v}(r)$:

$$\vec{v}\,'' = F(\vec{v})\,. \tag{1.16}$$

In fact, one can also recognize, after inserting a possible kinetic matrix K (which in Lorentzian signature is not positive-definite), that the force terms themselves stem from a potential:

$$K\vec{v}\,'' = -\frac{\partial U}{\partial \vec{v}}\,. \tag{1.17}$$

Through these instructions one is led to the following parametrization in terms of the three variables $v(r)$, $b(r)$, $\phi(r)$:

$$\begin{aligned} ds^2 &= e^{\frac{2}{p+1}v-\frac{2q}{p}b}\,dx_{1,p}^2 + e^{2v-\frac{2q}{p}b}\,dr^2 + e^{2b}\,R_0^2\,d\Omega_q^2\,, \\ \phi &= \phi(r)\,, \\ H_{p+2} &= \frac{n}{f(\phi)(R_0\,e^b)^q}\mathrm{Vol}_{p+2}\,, \qquad \mathrm{Vol}_{p+2} = e^{2v-\frac{q}{p}(p+2)b}\,d^{p+1}x\,\wedge\,dr\,. \end{aligned} \tag{1.18}$$

Under this choice, which was already well-known in some specific cases[45–47], the Einstein field equations and the dilaton equation of motion admit a very elegant mechanical formulation. Writing $\chi^I \equiv (\phi, v, b)$, they are equivalent to the equations of motion stemming from the action:

$$S = \int dr\,\left(\frac{\mathrm{d}\chi^I}{\mathrm{d}r}K_{IJ}\frac{\mathrm{d}\chi^J}{\mathrm{d}r} - U(\chi)\right)\,, \tag{1.19}$$

with

$$K_{IJ} = \begin{pmatrix} \frac{4}{D-2} & & \\ & -\frac{p}{p+1} & \\ & & \frac{q(D-2)}{p} \end{pmatrix}, \tag{1.20}$$

$$U(\chi) = -Te^{L_I\chi^I} - \frac{n^2}{R_0^{2q}} e^{L_I^{(n)}\chi^I} + \frac{q(q-1)}{R_0^2} e^{L_I^{(q)}\chi^I}. \tag{1.21}$$

$$\begin{aligned} L_I &= (\gamma, \quad 2, -2q/p), \\ L_I^{(n)} &= (-\alpha, \quad 2, -2q(p+1)/p), \\ L_I^{(q)} &= (0, \quad 2, -2(D-2)/p). \end{aligned} \tag{1.22}$$

In addition, the Hamiltonian constraint manifests itself as a zero energy condition:

$$H(r) = \frac{\mathrm{d}\chi^I}{\mathrm{d}r} K_{IJ} \frac{\mathrm{d}\chi^J}{\mathrm{d}r} + U(\chi) = 0. \tag{1.23}$$

This type of formulations for brane equations have been given the name of "Toda systems" because they are similar – though emphatically not identical[2] – to a three-site Toda chain, since the potential U is a sum of exponential of linear combinations of the degrees of freedom.

From now on, we shall employ units such that $T = 1$. While this may appear to potentially obscure a $T \to 0$ limit in which supersymmetric results are recovered, in actuality solutions to the $T > 0$ system are not continuously connected to the $T = 0$ case. The supersymmetry breaking associated to the

[2]in particular, it is worthy of note that the considerations of general integrability of the Toda lattice do not, regrettably, extend to the specific exponentials of the potential (1.21). As we will be able to see further, however, the system is integrable in some limits.

T-term always has drastic consequences that can not be taken to be small perturbations.

The kinetic matrix K_{IJ} has a negative eigenvalue, corresponding physically to the negative energy associated to the gravitational field. This brings an inconvenience in comparison to usual mechanical systems, where one can bound the dynamics to a subregion of configuration space:

$$U(r) \not\leq \frac{\mathrm{d}\chi}{\mathrm{d}r} \cdot K \frac{\mathrm{d}\chi}{\mathrm{d}r} + U(r) = 0\,, \tag{1.24}$$

so that even with the constraint, any point in χ space is in principle accessible.

1.2 The $\mathrm{AdS} \times \mathbb{S}$ vacua

Let us review briefly how the $\mathrm{AdS}_{p+2} \times \mathbb{S}_q$ solution of (1.8), (1.11) is constructed in the context of the Toda system (1.19). In fact, let us seek out all solutions where the dilaton is a constant, and we shall recognise that the aforementioned fluxed vacuum is the unique such solution. If one writes $\phi(r) \equiv \log g_s(r)$, and defines the $\mathbb{S}_q$ radius $R(r) \equiv R_0 e^{b(r)}$, then the potential (1.21) reduces to

$$U(\chi) = e^{2v} \left(\frac{R}{R_0}\right)^{-2\frac{q}{p}} \left(-g_s^\gamma - n^2 g_s^{-\alpha} R^{-2q} + q(q-1)R^{-2}\right)\,. \tag{1.25}$$

Now, g_s can only be a constant iff

$$\partial_{g_s} U = 0 \Rightarrow -\gamma g_s^\gamma + \alpha n^2 g_s^{-\alpha} R^{-2q} = 0 \tag{1.26}$$

which implies that R must be a constant as well, so that the spherical factor of the solution has constant radius. We also observe the requirement that $\alpha > 0$. In any case, one learns that

$$g_s^{\gamma+\alpha} = \frac{\alpha}{\gamma} n^2 R^{-2q} \,. \tag{1.27}$$

We can substitute (1.27) within the R equation of motion:

$$\partial_R U = 0 \Rightarrow g_s^\gamma + (p+1) n^2 g_s^{-\alpha} R^{-2q} - (p+q)(q-1) R^{-2} = 0 \tag{1.28}$$

$$\Rightarrow \left(1 + \frac{(p+1)\gamma}{\alpha}\right) g_s^\gamma = (p+q)(q-1) \left(\frac{\gamma}{\alpha n^2}\right)^{\frac{1}{q}} g_s^{\frac{\gamma+\alpha}{q}} = 0 \tag{1.29}$$

$$\Rightarrow g_s^{(q-1)\gamma-\alpha} = \left(\frac{\alpha(D-2)(q-1)}{(1+\frac{\gamma}{\alpha}(p+1))}\right)^q \frac{\gamma}{\alpha} \frac{1}{n^2} \,, \tag{1.30}$$

which is, up to factors of T, equivalent to that in (1.11). Note also that the factors of R_0 have dropped out, consistently with g_s being an observable. Thus, the dilaton is stabilized to a *fixed* value, and in contrast with usual supersymmetric solutions it is not an additional free parameter of the solutions but depends essentially only on the charge parameter n. The same is true for the sphere radius, which can be now easily explicitly determined from equation (1.27). Physically, the particular values arise as a balance of the tadpole dilaton potential (the T-term), the geometric tension due to the sphere's curvature (the q-term), and the radiation pressure from the form flux (the n-term) in (R, g_s)-space.

Before proceeding with our comments, let us first show that under these conditions $v(r)$ must necessarily trace the profile of an AdS_{p+2} space. From equation (1.25) one can already immediately see that with a constant ϕ and b the potential is proportional to e^{2v}. The behaviour of $v(r)$ under such

a potential can be more easily read from the constraint (1.23), which also implies the v equation of motion in this context:

$$0 = H(r) = v'^2 K_{vv} + U(\chi) = -\frac{p}{p+1} v'^2 + C^2 e^{2v} \tag{1.31}$$

for some constant C^2. A solution is only possible if $C^2 > 0$, in which case the profile is given by

$$v(r) = -\log(r - r_0) - \log \sqrt{\frac{p+1}{p}} C \,. \tag{1.32}$$

Returning back to the metric ansatz (1.18), the line element reduces to

$$ds^2 = c_x \, (r - r_0)^{-\frac{2}{p+1}} \, dx^2_{1,p} + \frac{p}{(p+1)C^2(r-r_0)^2} \left(\frac{R}{R_0}\right)^{-\frac{2q}{p}} dr^2 + R^2 d\Omega_q^2 \,, \tag{1.33}$$

where $R \equiv e^b R_0$ is the constant sphere radius, and c_x is a constant which is irrelevant as it can be reabsorbed with an x^μ rescaling. The change of radial coordinate $\rho^{p+1} = (r - r_0)$ is sufficient to reveal the AdS metric:

$$= \frac{p(p+1)}{C^2} \left(\frac{R}{R_0}\right)^{-2\frac{q}{p}} \frac{c'_x dx^2 + d\rho^2}{\rho^2} + R^2 d\Omega_q^2. \tag{1.34}$$

We thus learn that, provided $C^2 > 0$, the radius L of the AdS_{p+2} factor is

$$L^2 = \frac{p(p+1)}{C^2} \left(\frac{R}{R_0}\right)^{-2\frac{q}{p}} . \tag{1.35}$$

In particular the ratio of curvatures is given by

$$\frac{L^2}{R^2} = \frac{p(p+1) R_0^{2\frac{q}{p}}}{C^2} R^{-2\frac{q+p}{p}} \,. \tag{1.36}$$

The constant C^2 can be recovered by going back to the potential (1.25), and employing relation (1.27) and equation (1.29), so that after some algebra:

$$U = e^{2v} \, R_0^{2\frac{q}{p}} \, R^{-2(q+p)/p} \left(\frac{p(q-1)((q-1)\gamma - \alpha)}{(p+1)\gamma + \alpha}\right) , \tag{1.37}$$

which implies first of all that the solution can only exist under the additional condition that $(q-1)\gamma - \alpha > 0$. If it is satisfied, then the final AdS to $\mathbb{S}$ radius ratio is

$$\frac{L^2}{R^2} = \frac{(p+1)((p+1)\gamma+\alpha)}{(q-1)((q-1)\gamma-\alpha)}\,, \tag{1.38}$$

and the actual form of the constant term in $v(r)$ is as follows:

$$\begin{aligned} v(r) &= -\log(r-r_0) + v_0 \\ v_0 &\equiv \frac{q}{p}\log\left(\frac{R}{R_0}\right) + \log\left(\frac{L}{p+1}\right). \end{aligned} \tag{1.39}$$

Let us review our conclusions. We have shown that the only solutions to the Toda system with constant dilaton is the $\mathrm{AdS}_{p+2}\times\mathbb{S}_q$ vacuum, and that it is unique. It therefore only depends on the original parameters of the general effective action, which is to say p, q, γ, α, T, and the additional charge parameter n which had become embedded in the Toda action (1.19) itself. In addition, the stabilised solution exhibits the following scalings:

$$\begin{aligned} g_s &\sim n^{-\frac{2}{(q-1)\gamma-\alpha}} \\ R &\sim g_s^{-\frac{\gamma}{2}} \sim n^{\frac{\gamma}{(q-1)\gamma-\alpha}} \\ \frac{L}{R} &\sim n^0\,, \end{aligned} \tag{1.40}$$

where, since we recall $(q-1)\gamma - \alpha > 0$, the solution is indeed weakly-coupled and low-curvature for large flux n, so that the effective theory itself is applicable. For example, the case of RR-fluxed 1-branes in the $D = 10$ orientifold models, encoded by $p = 1$, $q = 7$, $\gamma = \frac{3}{2}$, $\alpha = 1$, has the particular scalings

$$g_s \sim n^{-\frac{1}{4}}\,, \quad R \sim n^{\frac{3}{16}}\,, \quad \frac{L^2}{R^2} = \frac{1}{6}\,. \tag{1.41}$$

Notably, the ratio of curvature radii is a flux-independent constant, but unlike the supersymmetric case it is different from one. The heterotic $NS5$ branes, instead, which have $p = 5, q = 3, \gamma = \frac{5}{2}, \alpha = 1$ (magnetic frame) display the scalings:

$$g_s \sim n^{-\frac{1}{2}}\,, \quad R \sim n^{\frac{5}{8}}\,, \quad \frac{L^2}{R^2} = 12\,. \tag{1.42}$$

Normalized equations

Returning to the full set of brane equations, let us show that is actually possible to "factor out" the AdS $\times$ $\mathbb{S}$ solution so as to obtain a normalized system which is independent from both R_0 and n. The former parameter is of course fully unphysical, while the latter only effects overall rescalings of the fields and the radial coordinate, as we will show shortly. First, consider the change of variables:

$$\phi(r) = \Phi(r) + \phi_{\text{AdS}}\,, \quad b(r) = B(r) + \log\left(\frac{R_{\text{AdS}}}{R_0}\right) \tag{1.43}$$

$$v(r) = V(r) + v_0 = V(r) + \frac{q}{p}\log\left(\frac{R_{\text{AdS}}}{R_0}\right) + \log\left(\frac{L_{\text{AdS}}}{p+1}\right) \tag{1.44}$$

where R_{AdS} and L_{AdS} are the radii of the $\text{AdS}_{p+2} \times \mathbb{S}_q$ solution. Note that the uppercase fields $\Phi(r)$ and $B(r)$ are equal to the respective lowercase fields with their constant AdS $\times$ $\mathbb{S}$ values subtracted, but $V(r)$ is defined by only subtracting the constant part of the AdS $\times$ $\mathbb{S}$ solution, without accounting for the logarithmic dependence. Since these new fields are related to the older ones by a simple additive shift, they will obey the same action:

$$S = \int dr\, X'^I K_{IJ} X'^J - U(X)\,, \quad X(r) = (\Phi(r), V(r), B(r))\,, \tag{1.45}$$

and the same zero-energy constraint:

$$X'^I K_{IJ} X'^J + U(X) = 0\,, \tag{1.46}$$

where the potential is simply the pull-back $U(X) = U(\chi(X))$. Substituting this ansatz into the specific reduced form of potential of equation (1.25), and making use of the relationship (1.27) which holds between $g_{s,\mathrm{AdS}}$ and R_{AdS}, the $U(X)$ potential reduces to:

$$\begin{aligned} U(X) \propto e^{-2\frac{q}{p}B+2V}\Bigg(& -e^{\gamma\Phi} - \frac{\gamma}{\alpha}e^{-2qB-\alpha\Phi} \\ & + g_{s,\mathrm{AdS}}^{\frac{\alpha+\gamma(1-q)}{q}} n^{-\frac{2}{q}} q(q-1)\left(\frac{\gamma}{\alpha}\right)^{\frac{1}{q}} e^{-2B}\Bigg) \end{aligned} \tag{1.47}$$

where the proportionality constant includes powers of n and $g_{s,\mathrm{AdS}}$. The only non-trivial dependence on n is in the coefficient of the last term. However, because of the scaling

$$g_{s,\mathrm{AdS}}^{a+\gamma-q\gamma} \sim n^{2/q} \tag{1.48}$$

from equation (1.40),the coefficient is actually n-independent. Thus, one can conclude that

$$U(X) \propto e^{2V} f(B,\Phi) \tag{1.49}$$

where $f(B,\Phi)$ is specifically an R_0 and n-independent linear combination of three exponentials, though the constant coefficients are unwieldy to report explicitly. It then suffices to rescale the r coordinate by a suitable factor so as to eliminate the n and R_0 dependence in the overall proportionality constant.

The final system is thus rendered universal across all flux numbers, and the conclusion is that therefore all brane stacks of a given p in a given theory

are qualitatively identical, simply related by rescalings, and that the analysis that follows is really unaffected by this value. This also implies that no qualitatively distinct behaviours occur for very small or very large flux number (of course, only at the classical level). From a practical standpoint, the large symbolic complexity of the various constants in the normalized system means it is only a viable option with the help of a computer algebra system and/or for the purpose of numerical studies. In the following dissection of the Toda system we will not employ this frame, choosing instead to continue carrying factors of n and R_0, but with the implicit understanding that these parameters do not affect the problem at an essential level.

1.2.1 Radial perturbations and throat egress

We seem to be presented with a somewhat unusual problem: a candidate near-horizon $\mathrm{AdS}_{p+2} \times \mathbb{S}^q$ solution is available, but a full brane solution, of which the former would be the near-horizon limit, is unknown. Short of approaching the complete, non-linear equations of motion (which we shall attempt in the following sections) there is a simpler test to estimate the likelihood that the $\mathrm{AdS}_{p+2} \times \mathbb{S}^q$ metric connect smoothly to a complete brane metric. As we shall now show, important information is encoded in the perturbation theory of a candidate near-horizon metric.

Let us assume an existing full p-brane profile for a gravitational theory, given for the sake of clarity as a Toda system solution $\chi^I(r)$. Let us also assume that the brane is "extremal" with the meaning employed so far, so that it has

a near-horizon metric which possesses an AdS_{p+2} factor. Since in the Toda parametrization the AdS horizon is located at $r = -\infty$, the brane solution generically admits an asymptotic expansion for $r \to -\infty$ of the following form:

$$\chi^I(r) = \chi^I_{\mathrm{AdS}\times\mathbb{S}}(r) + \dots \tag{1.50}$$

where $\dots$ includes generic terms subleading to the $\mathrm{AdS} \times \mathbb{S}$ solution as $r \to -\infty$. The precise nature of these subleading terms is of particular interest.

As one begins tracing the geometry from the horizon at $r = -\infty$ and moving outwards to increasing r, the subleading component will allow to interpolate from the throat profile to the outer portion of the brane metric. We term this process **throat egress**, and the subleading mode through which it is effected an **egress channel**. In [11] we attempted to reverse-engineer standard extremal brane solutions within this picture, with the aim of extracting a useful criterion. We have observed that, when known examples are rewritten in the Toda chart and expanded near the horizon to subleading order, the egress channel is always realized as a negative power of r:

$$\chi^I(r) = \chi^I_{\mathrm{AdS}\times\mathbb{S}} + A^I(-r)^\lambda + o((-r)^\lambda)\,, \quad r \to -\infty \tag{1.51}$$

where A^I is a constant vector, and the exponent $\lambda < 0$. This is true for example for extremal Reissner-Nordström black holes with an $\mathrm{AdS}_2 \times \mathbb{S}^2$ near-horizon metric, and for type-II D5-branes and their $\mathrm{AdS}_5 \times \mathbb{S}^5$ throat, though the value of λ is dependent on the specific type of solution.

Now, recall that both $\chi(r)$ and $\chi_{\mathrm{AdS}\times\mathbb{S}}(r)$ are solutions, by the initial assumption. Therefore, inserting the expansion (1.51) into the equations of motion

implies that the egress channel $A^I(-r)^\lambda$ must then be a solution to the *linearization* of the equations around the AdS $\times$ $\mathbb{S}$ background. *This yields a necessary condition for a given solution to be a candidate near-horizon limit of a full brane profile: its linear perturbation theory must allow a mode scaling like* $(-r)^\lambda$, $\lambda < 0$. *If this mode is not present, egress is impossible and the throat cannot be completed into a full brane profile.*

We perform this test on the $\mathrm{AdS}_{p+2} \times \mathbb{S}_q$ solutions of Section 1.2 in the non-supersymmetric models. We study the radial perturbation theory of the near-horizon throat and verify the existence of at least one viable egress channel. Specifically, perturbing the AdS $\times$ $\mathbb{S}$ background with a general power-law mode

$$\chi^I(r) = \chi^I_{\mathrm{AdS}\times\mathbb{S}} + \epsilon(-r)^\lambda\,, \quad \epsilon \ll 1\,,\, r < 0 \tag{1.52}$$

the spectrum of λ eigenvalues must contain at least one which is negative.

Note that this perturbative study with radial dependence has partial, but not complete, overlap with the scope of previous investigations that focused, for example, on the stability in AdS time of modes generically carrying $\mathbb{S}^q$ angular momentum, see for example [48, 49]. The present discussion is limited to modes with no angular dependence. In any case, as the system is (pseudo-)mechanical, the perturbation theory can be extracted by expanding the potential (1.21) to quadratic order. Because of the factorization

$$U(\chi) = e^{2v}\hat{U}(\hat{\chi})\,, \quad \hat{\chi} = (\phi, b)\,, \tag{1.53}$$

to that order the v perturbations and the (ϕ, b) perturbations will not mix, so that they can be considered separately. For what concerns v, let us perturb

the constraint (1.23) first, keeping in mind that (ϕ, b) are constant in the background:

$$2\frac{p}{p+1}v'\delta v' = \partial_v U \delta v = 2U\delta v = 2\frac{p}{p+1}v'^2\delta v\,, \tag{1.54}$$

$$\Rightarrow \delta v = A(-r)^{-1}\,, \tag{1.55}$$

where everything is computed on $\mathrm{AdS}\times\mathbb{S}$. We thus observe that a mode with $\lambda = -1$ is *always* present, independently of all other parameters, and would appear to be viable as an egress channel. However, this mode is merely a generator for a gauge freedom of the Toda system, namely r translations, or equivalently the arbitrariness in the location of the AdS horizon r_0. Indeed, performing an infinitesimal translation on the AdS $\times$ $\mathbb{S}$ solution generates such a term:

$$v(r) = -\log(-r) + v_0 \to v(r+\epsilon) = -\log(-r) + \frac{\epsilon}{r} + v_0\,, \tag{1.56}$$

and thus, it can always be reabsorbed by a gauge transformation. Physical modes are therefore limited to the $\hat{\chi} = (\phi, b)$ sector.

The linearized equations of motion for $\hat{\chi}$ reduce, on the background $\mathrm{AdS}\times\mathbb{S}$, to

$$2K\cdot\hat{\chi}'' = -\frac{\partial^2 U}{\partial\hat{\chi}\partial\hat{\chi}}\cdot\hat{\chi} \tag{1.57}$$

$$\Rightarrow \hat{\chi}'' \equiv -\frac{1}{r^2}H_0\hat{\chi} \tag{1.58}$$

which defines the constant matrix H_0. To solve equation (1.58), one can employ the change $t = \log(-r)$:

$$\left(\frac{\mathrm{d}^2}{\mathrm{d}t^2} - \frac{\mathrm{d}}{\mathrm{d}t}\right)\hat{\chi} = H_0\hat{\chi}\,, \tag{1.59}$$

so that modes are of the form $\hat{\chi} \sim (-r)^{\lambda}$, where λ is an eigenvalue of the 4×4 matrix

$$M = \begin{pmatrix} 1 & -H_0 \\ 1 & 0 \end{pmatrix}. \tag{1.60}$$

Since the characteristic polynomials of M and H_0 are related as follows:

$$P_M(\lambda) = P_{H_0}(\lambda - \lambda^2) \tag{1.61}$$

The four eigenvalues $\lambda_i^{\pm}$, $i = 1, 2$ of M can be extracted from those of H_0, say h_1, h_2:

$$h_i = \lambda_i^{\pm} - (\lambda_i^{\pm})^2\,, \quad \Rightarrow \lambda_i^{\pm} = \frac{1 \pm \sqrt{1 - 4h_i}}{2} \tag{1.62}$$

As for the explicit form of h_1, h_2, they do not easily yield to simplification for general values of the parameters. Nevertheless, they are as follows:

$$\begin{aligned} \lambda_{1,2}^{\pm} &= \frac{1 \pm \sqrt{1 - 4\,h_{1,2}}}{2}\,, \\ h_{1,2} &\equiv \frac{\mathrm{tr}(H_0) \pm \sqrt{\mathrm{tr}(H_0)^2 - 4\det(H_0)}}{2}\,, \end{aligned} \tag{1.63}$$

with the trace and determinant of H_0 being

$$\begin{aligned} \mathrm{tr}(H_0) &= -\frac{\alpha\left(\gamma\left(\alpha+\gamma\right)(D-2)^2 - 16\right) + 16\,\gamma\,(p+1)\,(q-1)}{8\,(p+1)\left((q-1)\gamma - \alpha\right)}\,, \\ \det(H_0) &= \frac{\alpha\,\gamma\,(D-2)^2((p+1)\gamma + \alpha)}{4\,(p+1)^2\left((q-1)\gamma - \alpha\right)}\,. \end{aligned} \tag{1.64}$$

Note that $\mathrm{tr}(H_0) < 0$ with the known bounds on the parameters, which guarantees that at least one of h_1, h_2 has negative real part. This in turn means that amongst the $\lambda_i^{\pm}$ there will always be at least one eigenvalue with nega-

tive real part[3]. *Therefore, all* $\mathrm{AdS} \times \mathbb{S}$ *solutions of the general action* (1.7) *do possess at least one viable egress mode, which means that the possibility exists for a more general solution for which* $\mathrm{AdS} \times \mathbb{S}$ *is a near-horizon limit.* This is a significant and non-trivial result, and is a necessary condition for bringing forward an interpretation of these vacua as near-horizon metrics for brane-like geometries.

In the specific case of the $\mathrm{AdS}_3 \times \mathbb{S}_7$ (purported D1-brane stack) of (1.41), solution to the orientifold models, the eigenvalues are computed as

$$\lambda_i^{\pm} = \frac{1 \pm \sqrt{13}}{2}\,, \quad \lambda_2^{\pm} = \frac{1 \pm \sqrt{5}}{2}\,, \tag{1.65}$$

thus sporting two candidate egress modes. And for the $\mathrm{AdS}_7 \times \mathbb{S}_3$ (would-be NS5-brane stack) of the heterotic models, they are

$$\lambda_i^{\pm} = \pm\sqrt{\frac{2}{3}}\,, \quad \lambda_2^{\pm} = 1 \pm \sqrt{\frac{2}{3}}\,, \tag{1.66}$$

again with two viable modes.

1.3 Dynamics of Lorentzian Toda-like systems

In the previous section we observed that egress from the throat is possible. Therefore, it is possible to explore the question of global extensions of the $\mathrm{AdS} \times \mathbb{S}$ throat into a full r-dependent profile. This condition, that $\mathrm{AdS} \times \mathbb{S}$

[3]There is no general guarantee for the $\lambda_i^{\pm}$ to be real. In fact, there exist values for the parameters such that the eigenvalues have an imaginary part. However, in the physically-relevant cases that we have investigated in [11], the $\lambda_i^{\pm}$ are all real.

is recovered for $r \to -\infty$, constitutes only half of the necessary boundary conditions for uniquely determining the solution; the rest would be provided by imposing that the metric approaches a constant-dilaton D-dimensional Minkowski space (or AdS_D or dS_D) as $r \to \infty$. This, however, is impossible as such a background is not itself a solution. Thus, we are naturally invited to consider a classification of possible final states of r-evolution.

These may either occur as $r \to +\infty$, or as singularities presenting for a finite $r = r_0$. For what concerns solutions that can be extended to $r \to +\infty$, we distinguish two sub-cases:

- $\lim_{r\to\infty} \phi(r) = \phi_\infty$ finite, in which case the final state must be $\mathrm{AdS}_p \times \mathbb{S}_q$ as previously proven in Section 1.2, except with the flux changed in sign as the volume form on the AdS space is flipped. The case of interpolating between two antipodal, oppositely-charged near-horizon geometries is not physically relevant.

- $\lim_{r\to\infty} \phi(r) = \pm\infty$. If the vector $\chi(r)$ in general becomes unbounded for large r, the potential of eq. (1.21) will be asymptotically $U(\chi) \sim \pm A \exp(\pm B|\chi|)$

1.3.1 Prototype Equation

To better map out the complex dynamics of the Toda system (1.19), it will prove very convenient to first perform a cursory examination of its fundamen-

tal component, which takes the form of a simple, one-dimensional ordinary differential equation:

$$y''(r) = 2e^{y(r)}\,. \tag{1.67}$$

Many of the limiting regimes of the system reduce ultimately to equation (1.67), which we therefore call **prototype equation**, or to its first-order equivalent:

$$y'(r)^2 = 4e^{y(r)} + 4E\,. \tag{1.68}$$

Depending on the sign of the mechanical energy E, the solution is readily found:

$$y(r) = \begin{cases} \log(\epsilon^2 \csc^2(\epsilon(r-r_0))) & E = -\epsilon^2 \\ -\log((r-r_0)^2) & E = 0 \\ \log\big(\epsilon^2 \operatorname{csch}^2(\epsilon(r-r_0))\big) & E = \epsilon^2 \end{cases} . \tag{1.69}$$

Some comments are in order. To begin with, all solutions display at least one singularity, of the specific asymptotic character

$$y \sim -\log\big((r-r^*)^2\big)\,, \quad r \to r^*\,, \tag{1.70}$$

which is independent from E. $E < 0$ solutions have infinite identical branches, of finite extent $\frac{\pi}{\sqrt{E}}$, each bound on both sides by such a singularity at $r^* = r_0 + \pi n$, $n \in \mathbb{Z}$. Instead, $E \geq 0$ solutions have two mirrored branches, one from $r = -\infty$ to a singularity at $r^* = r_0$, and another from r_0 to $+\infty$.

We can thus observe that initial conditions with either $E < 0$, or $E \geq 0$ but $y'(0) > 0$ will develop a runaway singularity at a finite r and will not be able to be continued further - we term these **blowups**. The remaining solutions with $E < 0$ and $y'(0) < 0$ are instead smooth towards positive infinity, and

we call them **drifts**, as y will slowly approach $-\infty$. We further refine the nomenclature by specifying that the non-generic $E = 0$ case is a **logarithmic drift**, and $E > 0$ is a **linear drift**, since $y(r) \sim -2\epsilon r$ asymptotically.

1.3.2 Single-term system

Let us consider a system of intermediate complexity between the prototype equation and the Toda system, in which there are N degrees of freedom but only one potential term:

$$2\chi_I'' = -\frac{\partial U}{\partial \chi^I}\,, \quad U = A\exp\bigl(V_I\chi^I\bigr)\,. \tag{1.71}$$

The indices $I = 1, \ldots, N$ and are raised and lowered with the mass matrix K_{IJ}, which we assume is specifically of Lorentzian signature, with exactly one negative eigenvalue, as is always the case for gravitational systems. One can then, optionally, also study the combination with a zero-energy constraint:

$$\chi_I'\chi'^I + U = 0\,. \tag{1.72}$$

First of all, one can effect a classification based on whether V_IV^I vanishes, as several details are qualitatively distinct.

Non-null term

If $V^2 \equiv V_IV^I \neq 0$, then we can complete it into an orthogonal basis $(V, E_{(i)})$, $i = 2, \ldots, N$. We decompose χ into this basis

$$\chi^I(r) = \frac{y(r)}{V^2}V^I + z^{(i)}(r)E^I_{(i)}\,, \tag{1.73}$$

with the factor of V^2 included for convenience. If one then plugs (1.73) into the equation of motion and dots with the basis vectors, one obtains the equations

$$2y'' = -AV^2\, e^y\,, \quad (z^{(i)})'' = 0\,, \tag{1.74}$$

from which it is clear that a blow-up can occur if and only if $AV^2 < 0$. The direction of blowup is along the vector $\frac{V^I}{V^2}$.

Now let us include the energy constraint (1.72). In the basis, it reduces to:

$$(y')^2 = -AV^2\, e^y + Z^2\,, \quad Z^I \equiv (z^{(i)})'\, E^I_{(i)}\,. \tag{1.75}$$

Thus, y behaves according to the prototype equation with a mechanical energy given by the constant Z^2. Limiting ourselves to the relevant case where a blowup *does* occur, then as seen in Section 1.3.1, the asymptotic form of y will be independent from Z^2, which will only affect subleading terms. Such a leading part will be of the following form:

$$\chi^I \sim -\log\big(\rho^2\big)\frac{V^I}{V^2}\,, \quad \rho = r_0 - r \tag{1.76}$$

In addition, by expanding the general solution (1.69) one can see that the next corrections to $y(r)$ are at most of order $\mathcal{O}((r-r_0)^2)$ independently on the value of Z^2, so that we can write the more precise asymptotic form

$$\chi^I = -\log\big(\rho^2\big)\frac{V^I}{V^2} + Z^I_0 - Z^I\rho + \mathcal{O}(\rho^2)\,, \tag{1.77}$$

for some integration constants Z^I_0, Z^I that are orthogonal to V^I. These amount to a total number of $2(N-1)$ free parameters in the blowup. All higher orders are instead determined from these by further expanding the equations of motion.

Null term

If, instead, V^I is null, we can complete it to a basis $(V, Y, E_{(i)})$, $i = 3, \ldots, N$, with the following properties:

$$V \cdot Y = 1\,, \quad Y^2 = 0\,, \quad V \cdot E_{(i)} = 0\,, \quad Y \cdot E_{(i)} = 0\,, \quad E_{(i)} \cdot E_{(j)} = \delta_{ij} \tag{1.78}$$

and decompose χ as follows:

$$\chi(r) = x(r)V + y(r)Y + z^{(i)}(r)E_{(i)}\,. \tag{1.79}$$

The choice of vector Y is not unique, but we will see eventually that the results are independent of this choice. Again inserting into the equations of motion and contracting with the basis, we obtain the equations

$$2x'' = -Ae^y\,, \quad y'' = 0\,, \quad (z^{(i)})'' = 0\,, \tag{1.80}$$

and immediately the general solution[4] for x and y:

$$y = y_1 r + y_0\,, \quad x = -\frac{A}{2y_1^2} e^{y_0} \left(e^{y_1 r} - 1 - y_1 r\right) + x_1 r + x_0\,. \tag{1.81}$$

We have made the unusual choice of integration constants to connect smoothly to the special solution in the $y_1 \to 0$ limit more transparently:

$$y = y_0\,, \quad x = -\frac{A}{4} e^{y_0} r^2 + x_1 r + x_0\,, \quad (y_1 = 0)\,. \tag{1.82}$$

Therefore, in the case of a null exponential term, no blowup is possible, and the solution is smooth towards $r \to \infty$. Nevertheless, χ can grow exponentially with r, and this will happen along the direction of $\pm V^I$, with the sign this time determined by that of $-A$.

[4]The provided form is also valid for $y_1 \to 0$ as a limit

Let us now again include the Hamiltonian constraint (1.72). Inserting the solutions and simplifying we see that the r-dependence cancels

$$Ae^{y_0} + 2x_1y_1 + Z^2 = 0\,, \quad Z^I \equiv (z^{(i)})' \, E^I_{(i)}\,, \tag{1.83}$$

or

$$x_1 = -\frac{Ae^{y_0} + Z^2}{2y_1}\,. \tag{1.84}$$

It is therefore again true that the leading asymptotic behaviour of χ is unaffected by the constraint, which only involves corrections to the next order; the difference in this case is that the asymptotic expansion is for $r \to \infty$, instead of a singularity at finite r, and that the subleading terms are actually determined by successive orders of the equations of motion. The leading part asymptotics

$$\chi = -\frac{A}{2y_1^2}e^{y_1 r + y_0} + \mathcal{O}(r) \tag{1.85}$$

are therefore complete in terms of free parameters, of which the only ones are y_0 and y_1.

1.3.3 Orthogonal two-term system

By providing an exact solution to the one-term Toda system, we have in fact equivalently shown that it is integrable. Generally, two exponential terms in the potential are enough to ruin integrability. However there is a rather simple subcase which is actually of physical relevance. Consider the two-term potential

$$U(\chi) = A_1 e^{V_I \chi^I} + A_2 e^{W_I \chi^I} \tag{1.86}$$

where the two vectors V and W are not null and orthogonal under the kinetic matrix:

$$V_I V^I \neq 0 \neq W_I W^I \,, \quad V_I W^I = 0 \,. \tag{1.87}$$

In this case, the system is exactly solvable through what should by this point be a familiar technique. Complete (V, W) into an orthogonal basis $(V, W, E_{(i)})$, $i = 3, \ldots, N$ and decompose the degrees of freedom:

$$\chi(r) = x(r)\frac{V^I}{V^2} + y(r)\frac{W^I}{W^2} + z^{(i)}(r)E^I_{(i)} \,, \tag{1.88}$$

from which we can plug into the equations of motion and contract with the basis vectors. The result is

$$2x'' = -A_1 V^2 e^x \,, \quad 2y'' = -A_2 W^2 e^y \,, \quad (z_{(i)})'' = 0 \,. \tag{1.89}$$

The degrees of freedom are completely decoupled. As before, the x part will be able to support a blowup iff $A_1 V^2 < 0$, and the y part iff $A_2 W^2 < 0$. The Hamiltonian constraint is

$$0 = H_x + H_y + Z^2 = (x')^2 + (y')^2 + U + Z^2 \,, \tag{1.90}$$

a statement not as eloquent as it was in the one-term case.

1.4 Eventual evolution of brane equations

Let us return to the specific system (1.19) of the three-site Toda system describing a p-brane in a non-supersymmetric string theory, and apply the notions accumulated in the previous sections.

The first observation is that, as evidenced by a quick calculation, the n-term (arising from form-flux pressure) and the q-term (arising from the curvature of the sphere) are orthogonal for any values of the parameters

$$L_I^{(n)} K^{IJ} L_J^{(q)} = 0\,, \quad \forall p, q\,. \tag{1.91}$$

It can also be seen that neither of these covectors is ever null. Thus, the n- and q-terms form an integrable two-term system of the type mapped in section 1.3.3. This is in fact fully expected: this system is what would be left after removing the supersymmetry-breaking tension and thus the T-term, and is therefore just the corresponding supersymmetric brane equation involving a form flux and a gravity, which is known to be fully integrable. We have then re-encountered this fact in the abstract language of the Toda system formulation.

A second observation is less trivial, and depends on the specific parameters of the models. The square of the T-term covector is

$$L^2 = \frac{D-2}{4}\gamma^2 - \frac{4(D-1)}{D-2}\,, \tag{1.92}$$

depending only on the dimension of spacetime and not on the dimensionality of the brane itself. But what is truly remarkable is that this quantity vanishes precisely for the orientifold models

$$D = 10\,,\ \gamma = \frac{3}{2} \quad \Rightarrow \quad L^2 = 0\,, \tag{1.93}$$

a fact whose specific significance still eludes us, but which implies that the orientifold brane dynamics require a more delicate treatment. In the heterotic models, instead

$$D = 10\,,\ \gamma = \frac{5}{2} \quad \Rightarrow \quad L^2 = 8\,, \tag{1.94}$$

so that the analysis is likely to be simpler.

1.4.1 Tadpole-dominated asymptotics

Let us consider eventual evolution asymptotics in which the dilaton tadpole component of the potential dominates over the n-term and q-term, to thus reduce to a system of the type of section 1.3.2. We would have a potential

$$U(\chi) \sim -\exp\big(L_I\chi^I\big) = -\exp\left(\gamma\phi + 2v - 2\frac{q}{p}b\right), \tag{1.95}$$

and dominance is guaranteed in the following region of configuration space:

$$L_I\chi^I \gg L_I^{(n)}\chi^I\,, \quad L_I\chi^I \gg L_I^{(q)}\chi^I\,. \tag{1.96}$$

Now, the coefficient of equation (1.95) is $A = -1$. In the orientifold models, L_I is null (see eq. (1.93)), which means that the solution will grow exponentially as $r \to \infty$ in the direction of $-AL^I = L^I$ – provided that the integration constant $y_1 \geq 0$. To evidence that the dominance is preserved asymptotically, one just then needs to verify that

$$L^2 = 0 > L_I^{(n)}L^I\,, \quad L^2 = 0 > L_I^{(q)}L^I\,, \tag{1.97}$$

but this is always true, in fact

$$L_I^{(n)}L^I = -\frac{(D-2)\alpha\gamma}{4} - \frac{4(p+1)}{D-2}\,, \quad L_I^{(q)}L^I = -4\,, \tag{1.98}$$

for all values of the parameters. Thus, in the orientifold models, and actually in all models with $L^2 = 0$ which may appear in different dimensions, we

will have an eventual evolution for $r \to \infty$ with the following leading order asymptotics for the fields:

$$\chi \sim \frac{e^{y_0}}{2} f(r) L^I \,, \quad L^I = \left(\tfrac{D-2}{4}\gamma, -\tfrac{2(p+1)}{p}, -\tfrac{2}{D-2} \right), \tag{1.99}$$

where

$$f(r) = \begin{cases} e^{y_1 r} & y_1 > 0 \\ \\ \frac{r^2}{2} & y_1 = 0 \end{cases} . \tag{1.100}$$

The total radial arc length up to $r = \infty$ is actually finite:

$$\sqrt{g_{rr}} \sim \exp\left(v - \frac{q}{p} \right) = \exp\left(\frac{e^{y_0}}{2} f(r)(-2) \left(1 + \frac{1}{D-2} \right) \right) \tag{1.101}$$

$$\Rightarrow \quad \int^{\infty} dr \, \sqrt{g_{rr}} < \infty \tag{1.102}$$

which means, physically, that it is actually impossible to have an infinite amount of space in the theory with the exception of the AdS throat itself – one eventually must encounter one such "wall" where space ends, after a finite geodesic distance. Because $b(r)$ is asymptotically very negative, and thus the radius of the sphere quickly shrinks to zero, we call such a singularity a **pinch off**. There is no hope for this singularity to be a coordinate artifact, since the dilaton (a scalar) always diverges to positive infinity.

Since, as seen previously, null L_I blow-ups will form a two-parameter family, the same is true for the tadpole-dominated pinch-off singularities in the orientifold models. We note that these two parameters are physical, as they cannot be changed with a residual gauge transformation, which would consist in a constant shift in $b(r)$ or $v(r)$ by rescaling x^μ or R_0.

Let us have a look at the case where $L^2 > 0$, which includes the heterotic models. Here one can have a proper blowup at a finite r coordinate, since

$AL^2 = -L^2 < 0$, and it will be in the direction of $\frac{L^I}{L^2} \propto L^I$. For dominance to be preserved in the blowup and thus the approximation to be self-consistent, it is required that L^2 be larger than both $L_I^{(n)} L^I$ and $L_I^{(q)} L^I$, but we have already shown that the latter quantities are always negative. Therefore $L^2 > 0$ models allow for a tadpole-dominated singularity at some $r = r_0$ with leading profile

$$\chi \sim -\log\left(\frac{L^2(r-r_0)^2}{4}\right) L^I\,, \quad L^I = \left(\tfrac{D-2}{4}\gamma, -\tfrac{2(p+1)}{p}, -\tfrac{2}{D-2}\right). \tag{1.103}$$

We examine the geodesic radial length here as well:

$$\sqrt{g_{rr}} \sim \exp\left(v - \frac{q}{p}\right) = \exp\left(-\log\left(\frac{V^2(r-r_0)^2}{4}\right)(-2)\left(1 + \frac{1}{D-2}\right)\right), \tag{1.104}$$

or

$$\sqrt{g_{rr}} \sim (r-r_0)^c\,, \quad c = 4\left(1 + \frac{1}{D-2}\right) > 0\,, \tag{1.105}$$

which is yet again integrable. Therefore, this singularity also lies at a finite radial distance. In addition, it is again true that the sphere radius shrinks to zero and that the dilaton diverges to positive infinity, so that $L^2 > 0$ models also display a pinch-off singularity.

The heterotic pinch-off is at first glance a 4-parameter family according to our analysis of the blowup of the prototype equation. However, two of these parameters correspond directly to the constant terms in the expansion of $b(r)$ and $v(r)$ near r_0, and they can be shifted with a suitable rescaling of x^μ or R_0. They are therefore unphysical. We are thus left with a 2-dimensional space of physically distinct pinch-offs.

1.4.2 Flux/geometry dominated asymptotics

Consider, instead, the case in which during radial evolution the (n, q)-part of the potential eventually dominates over the T-term,

$$e^{L_I\chi^I} \ll \left| -\frac{n^2}{R_0^{2q}} e^{L_I^{(n)}\chi^I} + \frac{q(q-1)}{R_0^2} e^{L_I^{(q)}\chi^I} \right| . \tag{1.106}$$

This could happen if χ diverges in a direction satisfying

$$L_I^{(n)}\chi^I \gg L_I\chi^I , \quad \text{or } L_I^{(q)}\chi^I \gg L_I\chi^I . \tag{1.107}$$

If this is assumed as true, then we are justified in approximating χ by means of the solution to the system including only the (n, q)-terms, which as we have observed is integrable. The n-term has negative coefficient, and $(L^{(n)})^2 = (4(1+p)(-1+q))/(p+q) + 1/4(p+q)\alpha^2 > 0$, therefore it is able to develop a blowup in the direction of $+L^{(n)}$. The q-term has a positive coefficient, but $(L^{(q)})^2 = -\frac{4(q-1)}{q} < 0$, so that it is also susceptible to blowup, in the direction $-L^{(q)}$.

Generically, the two blowups will not be located at the same value of r, so that we can assume that at the first singularity the leading part of χ will be either parallel to $+(L^{(n)})^I$ or $-(L^{(q)})^I$. The n-term dominated blowup is self-consistent, as divergence along $+L^{(n)}$ will preserve dominance:

$$0 < (L^{(n)})^2 > L_I(L^{(n)})^I < 0 \tag{1.108}$$

while the same is false for the q-term, since

$$-(L^{(q)})^2 = -L_I(L^{(q)})^I - \frac{4}{q} . \tag{1.109}$$

In other words, a q-term blowup is actually driving the system into a tadpole-dominated region. Therefore, the Toda system surely does not allow such asymptotic configurations at all. There is a much simpler physical picture of this fact. When the T-term is excluded, the q-term-driven blowups include regular Minkowski space. In fact, imagine a general q-term blowup of the following asymptotic form:

$$\chi^I \sim_{s\to 0} -\log\big((s)^2\big)\frac{(L^{(q)})^I}{(L^{(q)})^2} + \mathcal{O}(s) \tag{1.110}$$

where $s \equiv r - r_0$. The assumption of the q-term blowup preceding that of the n-term implies that the $L^{(n)}$ which is

$$\chi^I \sim -\frac{1}{q-1}\log s \begin{pmatrix} 0 \\ \frac{q(p+1)}{p} \\ 1 \end{pmatrix} + o(s)\,. \tag{1.111}$$

The dilaton is trivially asymptotically constant. Omitting constant factors the asymptotic metric is

$$ds^2 \sim s^0 dx^2 + s^{-\frac{2q}{q-1}} ds^2 + s^{-\frac{2}{q-1}} d\Omega_q^2\,, \tag{1.112}$$

which after a change of variables into the arc-length $\rho = s^{-\frac{1}{q-1}}$ (again, foregoing irrelevant constants) is revealed as flat space:

$$ds^2 = dx^2 + d\rho^2 + \rho^2 d\Omega_q^2\,. \tag{1.113}$$

The subleading part then includes information relevant to how the constant-dilaton Minkowski metric can be asymptotically approached, like the tails of the profile of a charged brane. It is then no surprise that with the inclusion of the T-term such asymptotic solutions become forbidden. More informative is the fact that *all* configurations (solving the equations of motion or

otherwise) where the metric is asymptotically flat, with any behaviour on the dilaton, take specifically the form above in the Toda system, and are therefore never solutions in the presence of a dilaton tadpole. The relevance is, for example, that one could posit on the basis of intuition a solution where the metric is asymptotically Minkowski, but the dilaton slowly drifts to $-\infty$ (say, as $-\log\rho$) – it would appear to be the natural generalization of the supersymmetric Minkowski with $\phi = -\infty$ as a sort of pathological minimum of the potential. This scenario is categorically excluded, as we will now show. If a metric is asymptotically Minkowski, then we know that the parallel warp factor $\frac{1}{2}\log g_{tt}$ must be asymptotically constant, thus

$$\frac{v(r)}{p+1} - \frac{q}{p}b(r) = k \tag{1.114}$$

Under this condition, the rest of the metric describes flat $\mathbb{R}^{q+1}$ if and only if

$$b'e^b = e^{v-\frac{q}{p}b} \Rightarrow b'(r) = \exp((q-1)b + (p+1)k)\,. \tag{1.115}$$

The differential equation (1.115) has solutions that are asymptotically

$$b(r) \sim -\frac{\log(r_0 - r)}{q-1}\,, \tag{1.116}$$

which is precisely the profile of solution (1.111). Combining with (1.114), we see that also the asymptotics of $v(r)$ must match. Therefore, these are the only realizations of asymptotically Minkowski metrics, and only exist for $T = 0$.

As for the flux-dominated singularity, it is indeed possible, though unphysical, as we will now argue. The dilaton diverges to $-\infty$, and the $\mathbb{S}_q$ radius vanishes. The total arclength is finite, since

$$\sqrt{g_{rr}} \sim (r - r_0)^c\,, \quad c = -2\left((L^{(n)})^v - \frac{q}{p}(L^{(n)})^b\right) = \frac{4(p+1)}{D-2}\,. \tag{1.117}$$

Nevertheless, the solution has to be discarded on physical grounds. First of all, it is by construction also a valid solution to the supersymmetric brane equations. In that context, one is able to exclude it thanks to the boundary conditions that are available. Since this singularity involves an increase in the flux energy density and the associated gravitational effect, it is clear that it appears going *inwards* towards a charged brane stack and not when moving away from it.

It is indeed featured as a generic asymptotic solution if one integrates the supersymmetric brane equations starting from some finite radius and going inwards, while retaining the assumption of parallel Poincaré symmetry $\mathrm{ISO}(1,p)$. Such a symmetry is actually physically only realized for strictly extremal branes. But in turn, extremality is a condition relating asymptotic charges, and thus automatically encoded in asymptotic behaviour at $r=\infty$. When the supersymmetric brane equations with $\mathrm{ISO}(1,p)$ symmetry are integrated with the condition that Minkowski space is recovered as $r\to\infty$, then such pathological singularities are excluded. In a vacuumless theory, instead, this procedure turns rather opaque, and extremality appears to be a much more elusive notion. The correct methodology, in any case, would be to explicitly break $\mathrm{ISO}(1,p)\to\mathbb{R}_t\times\mathrm{ISO}(p)$ by distinguishing a time warping and a parallel space warping, and then verifying *a posteriori* when the original symmetry is consistent, that is to say when it is preserved in evolution. Indeed, the n-term blowup solutions just described do not extend to solutions of such a more general system, and are thus physically untenable. In the full split system, starting from non-extremal boundary conditions near infinity and integrating inwards, the two warpings eventually differ and one

approaches either a Rindler near-horizon, or a superextremal naked Reissner-Nordström singularity. Only for an extremal solution do the warpings actually remain equal throughout evolution, thus justifying a posteriori the use of the assumption of Poincaré symmetry.

For the sake of our discussion, however, we remain focused on AdS $\times$ $\mathbb{S}$ as a candidate near-horizon for extremal branes, and therefore we will not pursue this explicit investigation; it is sufficient to observe that the n-term blowups are certainly to be discarded as physically-meaningful *final* states when integrating outwards from an AdS $\times$ $\mathbb{S}$ throat.

1.4.3 Null and logarithmic drifts

One last situation to consider is for all three terms in the potential to be negligible with respect to the kinetic energy $(\chi')^2$. In that case, the equations of motion and the zero energy constraint imply that the fields will drift linearly in r along a null direction:

$$\chi^I(r) = \chi_1^I r + \chi_0^I\,, \quad (\chi_1)^2 = 0 \tag{1.118}$$

The potential is suppressed if the following conditions hold:

$$L_I \chi_1^I < 0\,, \quad L_I^{(n)} \chi_1^I < 0\,, \quad L_I^{(q)} \chi_1^I < 0\,. \tag{1.119}$$

This asymptotic solution class is certainly a subset of the following linear drift configurations which ignores the Hamiltonian constraint:

$$ds^2 = e^{2Ar} dx^2 + e^{2Cr} dr^2 + e^{2Br} R_0^2 d\Omega^2\,, \quad \phi = \Phi r \tag{1.120}$$

or, equivalently

$$ds^2 = \rho^{2\frac{A}{C}} dx^2 + \frac{d\rho^2}{C^2} + R_0^2 \rho^{2\frac{B}{C}} d\Omega^2 \,, \quad \phi = \frac{\Phi}{B} \log(\rho) \,. \tag{1.121}$$

These geometries are similar to a Kasner metric, but with a time-like singularity. We shall now argue that these solutions are fully unphysical as well. While one would intuitively expect to discover the Minkowski solution (foregoing the T-term, of course) within this class, this is not the case. Indeed, Minkowski requires $A = 0$, $B = C$, which leads to a contradiction already when comparing the metric (1.121) with the ansatz (1.18). The special flat space solution is instead obtained as a non-generic logarithmic drift where the q-potential is only marginally suppressed. This is important conceptually, as it means that from the point of view of the radial equation of motion integrated outwards flat space appears as a liminal solution, precisely on the threshold of runaway and collapse under the tension of the sphere factor. The Kasner-like solutions described above lie indeed on the other side of this threshold, with the potential decaying too quickly. In the usual treatment, these singularities can be excluded on the basis of the conical defect they carry at $r = \infty$, which has no associated physical source, and this fixes the actual physical solution at large distance to be Minkowski space (or AdS or dS in the presence of a cosmological constant).

In our case, of course, we do not possess the luxury of the Minkowski solution, as it does not satisfy the first suppression condition of (1.119) at all. Let us see which logarithmic drifts are allowed in the Toda system. Consider a generic asymptotic logarithmic drift solution

$$\chi^I(r) \sim \chi^I_\ell \log r + \chi^I_0 + o(r^0) \,, \tag{1.122}$$

under which the zero-energy condition takes the form

$$\frac{\chi_\ell^2}{r^2} + U_{(T)} + U_{(n)} + U_{(q)} = 0\,, \quad U_{(T)} \sim r^{L_I \chi_\ell^I}\,, \ldots \tag{1.123}$$

This can only be satisfied at leading order if all the potential terms scale as r^{-2} or smaller[5], i.e.:

$$L_I \chi_\ell^I \leq -2\,, \quad L_I^{(n)} \chi_\ell^I \leq -2\,, \quad L_I^{(q)} \chi_\ell^I \leq -2\,, \tag{1.124}$$

These equations can actually be shown to admit solutions. However, note that as per our previous analysis of the prototype equation, logarithmic drifts arise as special limits of blowup singularities. Therefore, they must be connected continuously to them. A logarithmic drift where $\phi_\ell < 0$ would be connected to blowups that do not involve the T-term; as such, it cannot be physical since otherwise it would also be in the supersymmetric case. Limiting ourselves to $\phi_\ell > 0$, which are necessarily T-term logarithmic drifts, note that by the first condition in equation (1.124) the radial arc-length is finite just as it is for the blowups proper, since

$$\sqrt{g_{rr}} = r^{v_\ell - \frac{p}{q} b_\ell} \leq r^{-1 - \frac{\gamma}{2}\phi_\ell}\,, \tag{1.125}$$

which is integrable. Therefore, a logarithmic drift offers no conceptual advantage and does not prevent the inevitable demise of space at finite distance.

[5]It should be noted that in principle one should also consider the (rather odd) possibility that two potential terms are of the same order and do dominate over the kinetic energy, and then these leading terms cancel each other. Only the (T, n) and (T, q) pair can cancel due to the overall signs, and in each case one can verify that the condition for equality of the exponents actually sets those exponents themselves to be subdominant to the kinetic energy.

As such, there is no benefit in considering them separately from the regular blow-ups, instead of including them implicitly as limits of the blowup parameters.

1.5 The full brane profile

With these foundations in place, we are now in a position to speculate as to the actual nature of D-brane stacks in the effective description of non-supersymmetric strings, with a special eye to $D1$-branes in the orientifold systems and $NS5$-branes in the heterotic model. The more precise question we would like to examine is whether there exist a "valid" and unique brane profile, namely a static solution to the equations of motion with brane symmetries $\mathrm{ISO}(1,p)\times\mathrm{SO}(q)$ which has the near-horizon $\mathrm{AdS}_{p+2}\times\mathbb{S}_q$ throat as a limit, and whose behaviour on the other end of the radial coordinate is somehow "physical", in a way to be determined.

As seen in thorough detail, the standard definition of "physical" eventual evolution, which is to converge to maximally-symmetric space, is impossible to satisfy in this context. One must therefore replace this with a generalized notion of non-pathological "far away". We argue that amongst all choices presented, only those that result in the tadpole-generated potential term becoming large must be considered: if the T-term is eventually negligible, then that eventual evolution profile is also a solution of the supersymmetric equations, and must therefore be equally unphysical in the non-supersymmetric case. The only possibility is then to conjecture that the tadpole-dominated

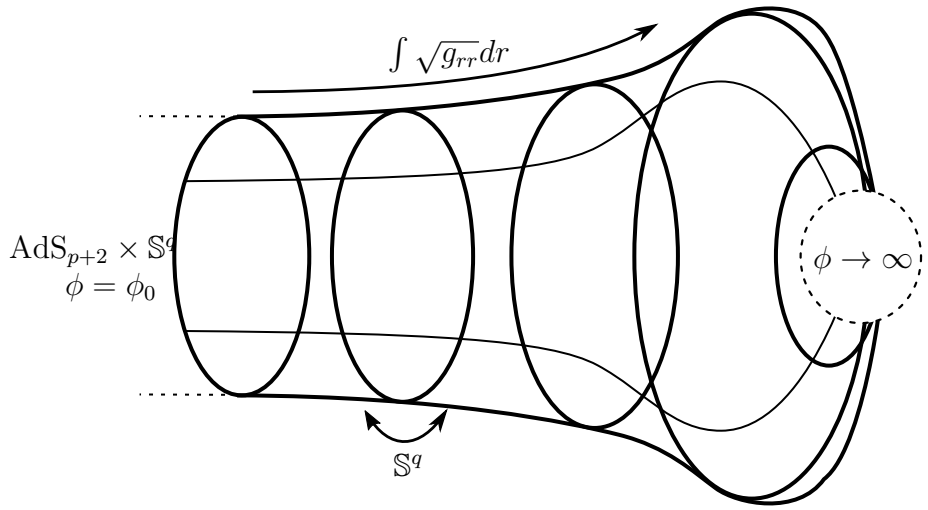

Figure 1.1: A schematic depiction of the geometry of an extremal p-brane geometry in a non-supersymmetric string theory, in the radial and $\mathbb{S}^q$ dimensions. The profile interpolates between an infinite $\mathrm{AdS}_{p+2} \times \mathbb{S}^q$ throat and a finite-distance pinch-off singularity.

pinch-off singularities are to be taken as the most physically reasonable eventual evolutions of a brane profile. Let us try and provide a qualitative picture of the consequences for the shape of branes in such theories.

Pinch-offs occur at finite radial distance, as observed. If a metric interpolates between $\mathrm{AdS} \times \mathbb{S}$ and a pinch-off, then there is only a finite amount of space outside of the throat. That amount of space scales with a positive power the brane flux n, as shown in Section 1.2. This suggests a picture where the brane's form-charge is blowing up a pocket of smooth space with a small g_s, balancing the force of the tadpole potential, which drives space to contract and the dilaton to diverge to $+\infty$. As one moves outwards from the throat,

the stress-energy density of the form-field becomes low enough that it is overcome by the tadpole potential and space collapses into a pinch-off. The physical scenario that is painted by these properties is that the vacumlessness of non-supersymmetric string effective theories has a specific, non-obvious character: empty space is naturally driven to shrink to string-scale curvature radii, and thus the effective theory dynamically undermines its own validity. Smooth spacetime only appears when *out* of equilibrium, in the presence of additional objects, and exists only localized to those very objects.

1.5.1 Solution parameters

In the standard treatment of brane profiles in a context that admits a Minkowski vacuum, integration constants appear in the general asymptotically-flat solutions that correspond to the physical parameters of mass (or better, tension) and charges of the brane, plus possibly moduli of the flat vacuum itself. The identification is transparent thanks in particular to the asymptotic infinity, where they can be immediately matched to parameters in the fall-off behaviour of the perturbation from the empty Minkowski solution at large distance, by comparison with the corresponding linearized theory. Similar notions can be defined in an asymptotically dS or AdS backgrounds, with suitable modifications to the interpretations of these quantities. In a system like the present one, where one only accounts for the effects of gravity and a p-form field, a p-brane would possess exactly three such quantities in the tension and form flux, appearing as the coefficients for the Newton and Coulomb fields for large r, and the asymptotic constant value of the dilaton. An

extremal brane satisfies a condition involving tension and charge, and is parametrized by two values, say, the flux number n and the string coupling at infinity $g_{s,0}$.

No such luxury is allowed in our specific vacuumless scenario, as there is no way to reach a large distance from the throat nor any linearized regime around a certain infinite-size solution of higher symmetry. The brane charge is embodied straightforwardly by the parameter n, and while the physical meaning of tension is rather obscure without a Newtonian regime, one could still argue that the presence of the AdS_{p+2} factor in the throat is related to some form of extremality condition that fixes its value, so that it will not appear as a parameter in the solutions with such initial conditions. Nevertheless, there are still residual parameters in the solutions to the Toda system. We argue that these are to be taken as the generalization of the supersymmetric flat-space modulus given by the vacuum string coupling, since they do affect the radial evolution of the dilaton when exiting the throat and when approaching the pinch-off.

While these parameters are fully encoded in the linearized perturbation when approaching a Minkowski vacuum in the conventional picture, it is also true that they are equivalently determined by perturbations of an $\mathrm{AdS} \times \mathbb{S}$ throat when *exiting it*. In Section 1.2.1, when we determined the egress modes for the near-horizon throat, we have shown that not only does at least one such mode exists, but that specifically the orientifold $D1$-branes and the heterotic $NS5$-branes possess exactly two. These two coefficients match non-trivially with the two parameters of distinct pinch-off singularities in both orientifold

and heterotic models as determined in Section 1.4.1. While it's impossible, because of the highly exotic context, to extricate which are properties of the branes and which are properties of the vacuum, one can still conclude that two scalar "charges" exist parametrizing a two-dimensional space of brane solutions.

A contrast arises upon comparison with the equivalent string theory picture, where only the original background g_s in the supersymmetric theory exists as a parameter. Our expectation so far has been that of the two pinch-off parameters, one may be fixed by a "physicality" condition, by direct analogy with the equivalent situation with supersymmetry, where the assumption of no conical defects at infinity allows to fix an integration constant and determine regular Minkowski space as the only physical asymptotic metric. The remaining parameter would then match with the string theory original modulus. However, so far the search for such a physicality condition has not been fruitful.

1.6 Conclusions

In the present chapter, we have outlined the present state of affairs concerning the determination of analogs of the supersymmetric classical brane profiles for effective field theories of non-supersymmetric strings. Not all details concerning these vacuumless brane solutions can be worked out at present. Nevertheless, we were able to extract sufficient information to attain a partial understanding of how physically-motivated "isolated" objects work, in what

is essentially the minimal example of a vacumless effective theory of this type.

In a vacuumless effective theory, isolated objects in the original string theory such as D or NS-branes may (depending on the coupling between the form field and the dilaton) blow up finite pockets of spacetime via the pressure associated with the flux. *These pockets reach an end at some radial distance from the brane stack, where the dilaton potential overcomes the flux density and blows up, while the spacetime "boils away" in a pinch-off singularity where $\phi \to \infty$ (see again Figure 1.1).* The picture appears reasonable, and provides a picture of the spontaneous compactification at work in the Dudas–Mourad vacuum [50], but these considerations remain tentative since they involve a regime that lies outside the applicability of the effective field theory.

We have identified two arbitrary parameters for such pocket solutions that are independent of the flux number. We have conjectured that these replace the single modulus of the dilaton at infinity of the supersymmetric case, arguing that perhaps it may be possible to reproduce these two degrees of freedom in the string configuration, or more likely to show how an additional constraint reduces them to a single one.

Chapter 2

Vacuum bubbles in AdS

Effective theories around metastable vacua provide a more subtle notion of classical "vacumlessness". More specifically, it is conceivable for a quantum theory (especially gravitational) to display multiple maximally-symmetric solutions that are stable to small perturbations, but which nevertheless have different vacuum energy. In these case, a potential barrier may somehow prevent the higher-energy vacuum from transitioning to the lower-energy one at the classical level, and yet a decay may still occur via quantum tunneling. The higher-energy metastable solution provides an unusual scenario where a classical description based on it manages to capture most of the dynamics quite accurately. Still, a semi-classical improvement introduces localized events which occur with very low probability, but can bring forth nonetheless catastrophic global consequences.

Such events are called vacuum bubbles [13, 14]. These are "pockets" of the

true, lower-energy vacuum within a bulk of the metastable one, which are bounded by a thin and highly-energetic membrane where the field values travel across the potential barrier. In a semi-classical, or equivalently thin-wall, approximation, they are first created by a quantum tunneling process (nucleation), whose amplitude is well captured by a Euclidean instanton[1]. When their nucleated size is so large that the vacuum energy difference due to the internal volume overcomes the tension of the surface membrane, bubbles become classical object that expand approaching the speed of light, and eventually replace [2] the metastable space with the true vacuum.

In [12] we set out to give an interpretation for vacuum bubbles in terms of the celebrated AdS/CFT correspondence[51], and propose holographically dual notions for metastability and vacuum decay. In this work we focused on such a scenario involving a metastable AdS vacuum, specifically AdS_3 for the sake of simplicity. It should be clear that such a setup is very difficult to produce within the context of a consistent theory of quantum gravity – for metastability, one requires both broken supersymmetry and some non-perturbative understanding of the dynamics. For example, we started from

[1]The instanton in Euclidean signature is also, confusingly, often called a "vacuum bubble", because it possesses radial symmetry and a radial profile matching that of the actual bubble.

[2]More precisely, if the metastable space is dS, only a fraction of it will eventually be replaced with true vacuum, and it will always be possible to escape crossing the bubble surface. A metastable Minkowski is always completely replaced, albeit in infinite time, while a metastable AdS is erased in a finite time.

a simple and surely academic example of a minimally-coupled scalar field

$$\mathcal{L} = R - \frac{1}{2}(\partial\Phi)^2 - V(\Phi)\,, \tag{2.1}$$

where $V(\phi)$ is a double-well potential, with two different minima where $V < 0$. Such an effective Lagrangian, or one containing a sector of this type, does indeed give rise to a truly stable AdS vacuum and a distinct, metastable AdS of larger curvature radius. A sufficiently steep potential wall between the two minima will then guarantee that the decay process will occur through quantum tunneling and can be treated in a semi-classical approximation in the standard fashion[14]. However, extracting a Lagrangian of the kind (2.1) as an effective description to a string configuration, is a highly non-trivial matter. Some interesting considerations were already made in this regard in the preceding chapter, in particular in connection with the decay of a metastable stack of $D1$-branes in non–tachyonic orientifolds in [16]. These provided an example of an $\mathrm{AdS}_3 \to \mathrm{AdS}_3$ transition with a possibly accessible CFT_2 dual. One ought to consider also the $D3$-brane scenario of [**Kachru2002Brane/fluxTheory**]. These may well entail some general lessons, since the "bubble holography" program should proceed along lines that are independent of fine details of the metastable setup.

The core of the proposed correspondence in [12] is that the expansion of a vacuum bubble and the gradual replacement of a metastable AdS space with a more stable one of higher curvature is dual to a renormalization group (RG) flow between two conformal field theories, where the first has a higher central charge and the second has a lower one. The leaping stone for the holographic investigation of vacuum bubbles comes from the information-

geometry program, specifically the connection between minimal surface areas and entanglement entropy [15]. This approach allows one to bypass the specific construction of metastable configurations, as it is only really sensible to the presence of metastability and on the initial and final curvature radii. That the transition is in particular an RG-flow through non-conformal theories, seeded by a relevant deformation, is the less trivial statement. It was suggested by the construction of an explicit example of c-function as predicted by Zamolodchikov's C-theorem [52]. The C-theorem in two dimensional quantum field theories states, in brief terms, that a function $C(g, \mu)$ depending only the couplings g and on the scale μ exists, which is monotonically decreasing over all RG-flows, and which at fixed points of the flows equals the CFT central charge c. Intuitively, such a c-function counts the available degrees of freedom, extending the concept of central charge to non-conformal configurations, and the C-theorem embodies the idea that theories can only *lose* degrees of freedom under RG flows, not gain them.

For vacuum bubbles, the computation of minimal surface areas is approachable, and the Ryu-Takayanagi formula opens a portal to compute entanglement-entropies of the boundary theory along the transition, and thus to examples of physically-motivated candidate c-functions. The formula relates the areas of minimal surfaces in the bulk of given holonomy with the entanglement entropy associated with binary partitions of the boundary degrees of freedom. For any given such partition, the entanglement entropy provides itself a quantitative tool to estimate the effective number of degrees of freedom, which in the CFT case reduces to the central charge, up to a multiplicative constant. If all of the entanglement entropies are in addition monotonically decreasing

during the bubble expansion, they all constitute candidate c-functions, and support the existence of an otherwise inaccessible RG-flow. In fact, this is what we shall ultimately conclude from our computations. The following section are therefore devoted to the problem of computing some geometrical quantities entering the Ryu-Takayanagi formula in the background of a expanding AdS expanding in a metastable AdS space.

It is both convenient and more effective to perform these computations in the lowest possible non–trivial dimension, thus focusing on the AdS_3/CFT_2 correspondence. First of all, the theory of minimal surfaces in asymptotically AdS_3 metrics reduces to the study of geodesics in asymptotically $\mathbb{H}_2$ surfaces, which allows the direct application[3] of the insightful approach of integral geometry, which we shall summarize in Section 2.2.1. In addition, for two-dimensional conformal field theories one can resort to both the classic form of the c-theorem and the universality of entanglement entropies, which follow the Calabrese-Cardy formula [53, 54]. For a CFT_2 on a cylinder, which is relevant to the $AdS_3 \times CFT_2$ correspondence, an interval of angular size 2θ has with its complementary interval the entanglement entropy

$$S_{\text{ent}} = \frac{c}{3} \left(\log \sin \theta + \Lambda \right) \ , \tag{2.2}$$

where Λ is a divergent regulator that will be defined more precisely in the following. Our purpose is to find the behaviour of the entanglement entropy, interpolating between these known values at the initial and final CFT_2, for any value of $0 < \theta < \frac{\pi}{2}$, and verify its monotonic behavior.

[3]The formalism is significantly less transparent in higher dimension, though still functional.

2.1 AdS $\rightarrow$ AdS **Bubble geometry**

We first consider the anatomy of the vacuum decay process. We take two AdS_d vacua, AdS_d^- of radius L_- and AdS_d^+ of radius L_+. We imagine that the AdS_d^- vacuum is metastable, and susceptible to decay induced by tunneling into the true vacuum AdS_d^+. This implies that the cosmological constant of AdS_d^+ is more negative than that of AdS_d^-, and thus $L_- > L_+$.

At the beginning, the space is AdS^-. A quantum-gravitational tunneling process creates a localized bubble containing a region of AdS^+. For the current purposes this initial nucleation size can be considered negligible. The differences in vacuum energy exert a pressure that drives the bubble to expand. Quickly the bubble surface will both thin out and accelerate to ultrarelativistic speed, replacing an ever increasing volume of AdS^- with AdS^+. Because of the particular geometry of anti-de Sitter spacetime, the bubble will actually reach infinity in a finite (in fact, bounded) time for any inertial observer. Therefore a vacuum decay from a metastable AdS space has a distinct "finalization" event where the bubble actually reaches the boundary at infinity and the space inside is fully replaced with AdS^+. After finalization, it is difficult to confidently talk about what the correct outcome is. We argue that since stress-energy has leaked outside of the conformal boundary, one has to apply explicit conditions for the boundary's reaction if existence and uniqueness in the bulk has to be preserved. In [12] we implicitly chose to assume that the boundary never radiates any stress-energy back into the bulk, which means the stress-energy carried by the bubble is simply lost and spacetime is pure AdS^+ from then on. If different boundary conditions are chosen, other out-

comes are possible, see for example [55]. In any case, our interest is limited to the expansion phase stretching between nucleation and finalization, and the question of the outcome is less relevant.

In [12], we employed an approximation where the bubble's surface can be treated as infinitely-thin and moving at c throughout expansion. While we employed the name of "thin-wall" approximation, this is emphatically not the same limit as the homonymous approximation in the classic literature on vacuum bubbles [14]. In any case, if the bubble's surface is indeed a null hypersurface, specifically a cone, to construct the spacetime metric in the expansion phase one must then perform a gluing of AdS^- and AdS^+ on such a hypersurface. It is non-trivial that such a gluing can be even effected, and in fact the gluing surface being null turns out to be an essential requirement.

To perform a gluing, one has to excise the gluing surface from both spacetimes, then construct a bijection between the two newly created boundaries so that their induced metrics match. Consider having to glue across a general spherically symmetric hypersurface, defined by a time-dependent radius $R_-(t)$ in AdS_- (given) and $R_+(t)$ in AdS_+ (to be determined). When gluing, one would have to match lengths both in the $d-2$ rotational directions and the single remaining tangent direction:

$$g^-_{ij}(R_-(t)) = g^+_{ij}(R_+(t))\,, \tag{2.3}$$

$$g^-_{\mu\nu}(R_-(t))V^\mu_- V^\nu_- = g^+_{\mu\nu}(R_+(t))V^\mu_+ V^\nu_+\,, \quad V^\mu_\pm(t) = (1, R'_\pm(t), 0, \ldots)\,. \tag{2.4}$$

Generically, these two conditions form an over-constrained system for the radius, and the gluing cannot be performed. However, if the tangent vector

V_-^μ is null, then the system degenerates and a solution can be found. Let us show that explicitly by employing the following Schwarzschild-like chart for both $\mathrm{AdS}_\pm$ spaces

$$ds_\pm^2 = -\left(1+\frac{r^2}{L_\pm^2}\right)\frac{d\eta^2}{\left(1+\frac{\eta^2}{L_\pm^2}\right)^2}+\frac{dr^2}{1+\frac{r^2}{L_\pm^2}}+r^2d\Omega^2\,. \tag{2.5}$$

This chart is not global, but it does map the entirety of the decay process up to finalization. Having placed the nucleation at $(\eta, r) = (0, 0)$, the two sides of the null bubble surface are simply parametrized as

$$R_\pm(\eta) = \eta\,, \tag{2.6}$$

satisfying both gluing conditions. In other, more geometric terms, such a null spherically-symmetric excision can always be glued, and the gluing is determined by ensuring the areas of the spheres are matching. The advantage of chart (2.5) is that it allows to write the entire geometry in a single expression involving a piecewise-defined curvature radius:

$$ds_\pm^2 = -\left(1+\frac{r^2}{L_{\text{eff}}^2}\right)\frac{d\eta^2}{\left(1+\frac{\eta^2}{L_{\text{eff}}^2}\right)^2}+\frac{dr^2}{1+\frac{r^2}{L_{\text{eff}}^2}}+r^2d\Omega^2\,, \tag{2.7}$$

$$L_{\text{eff}}(\eta, r) = \begin{cases} L_- & r > \eta \\ \\ L_+ & r < \eta \end{cases}. \tag{2.8}$$

The bubble metric breaks the original $\mathrm{SO}(2, d-1)$ isometry group of AdS_d into the isotropy group of the nucleation event, which is the Lorentz group $\mathrm{SO}(1, d-1)$. These rotations and boosts keep invariant the bubble surface and the AdS metrics on either side. The ring on the boundary where finalization occurs is also invariant.

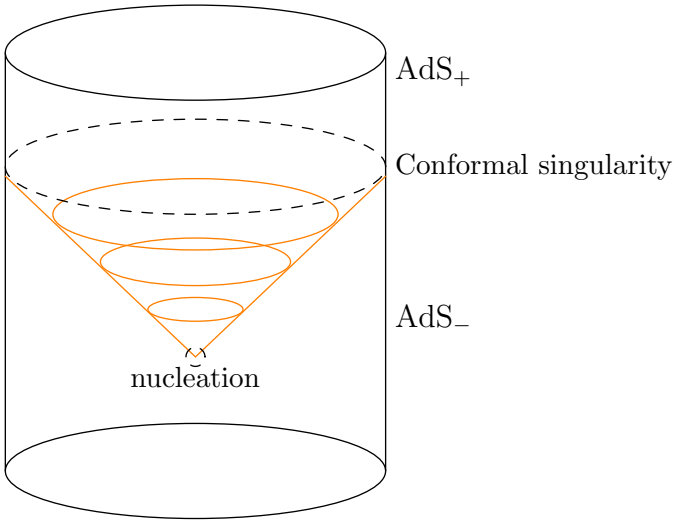

Figure 2.1: The quasi-conformal diagram of the $AdS_{\rightarrow}AdS_{+}$ bubble geometry.

2.1.1 Conformal Structure

Since the interest is in probing a holographic description, it is important to gain an understanding of how the bulk and boundary are **geometrically** related, and in which sense the relationship is exotic, in comparison to the standard construction. Typically, the boundary theory lives in a space which is the conformal boundary of the bulk, which in turn is formally defined as the boundary of its conformal compactification[4]. The glued geometry of (2.7), however, does not have a well-formed conformal compactification. It is pos-

[4]For the sake of precision it should be reminded that for infinite-time AdS space, the caveat to the formal definition is made that the time dimension is not required to be compact, as this is impossible for this space, and the same holds for the conformal boundary itself. Compactness is therefore reduced to a limitation of closure and boundedness in the spacial dimensions only.

sible to perform the conformal compactification of both $AdS^{\pm}$ sides, but no matter how this is done, a hole is produced, located at the finalization events when the bubble reaches infinity, where no suitable conformal structure can be defined. Therefore we are left with a conformal boundary composed of two semi-infinite cylindrical spaces, separated by a "conformal singularity" at the finalization ring (see Figure 2.1). As we will see in section 2.1.2, this is not an artefact of the "thin-wall" approximation but an unavoidable geometrical limitation of vacuum transitions in AdS space.

In [12], we argued that this fact is to be interpreted holographically as a hint that the boundary theory is undergoing a process that it is carrying it from an initial CFT_-, dual to AdS_- and with a larger central charge, into a final CFT_+, dual to AdS_+ and with smaller central charge, and that the transition must happen by passing through non-conformal theories. This non-conformal flight mirrors the temporary breakdown of the bulk conformal structure on the geometric side. This general description then points strongly at the possibility that this process is in fact a renormalization group flow.

2.1.2 Symmetry groups and smooth bubbles

Consider discarding the "thin-wall" approximation we employed thus far, but maintaining full $SO(1, d-1)$ symmetry. The bubble would now have to be described as a full spacetime-dependent field configuration, but because of the number of symmetries, fields will only depend on a single variable. We can isolate said variable by constructing an explicitly $SO(1, d-1)$-invariant

quantity, which is unique up to diffeomorphisms.

This is most convenient to do in a chart that makes the symmetries manifest. Embed AdS_d space in $\mathbb{R}^{2,d-1}$ as the hyperboloid

$$X^\mu X_\mu = -1\,, \tag{2.9}$$

and call Y^μ the coordinates in this chart of the nucleation event. Then, the following quantity

$$\xi^2 = (X^\mu - Y^\mu)(X_\mu - Y_\mu) \tag{2.10}$$

is an explicit scalar of $\mathrm{SO}(2, d-1)$, provided that Y^μ is transformed as a vector as well. If, instead, Y^μ is kept fixed, ξ^2 is only invariant for the isotropy subgroup of Y^μ, which happens to be the sought $\mathrm{SO}(1, d-1)$.

Having this special coordinate defined, we can write the general $\mathrm{SO}(1, d-1)$-invariant deformation of AdS space:

$$ds^2 = L^2(\xi^2) ds^2_{\mathrm{AdS}} \tag{2.11}$$

And the expansion of a smooth vacuum bubble can be formed by taking some smooth $L^2(\chi^2)$ interpolating between the radii when going from spacelike to timelike separation:

$$\lim_{\chi^2 \to \mp\infty} L(\chi^2) = L_\mp\,. \tag{2.12}$$

While this obviates the flaws of the approximation of a discrete jump, it is not a particularly practical construction for the purposes of holography. First of all, the bubble has finite extent at nucleation time, which means the solution must be explicitly glued to a nucleation trajectory violating

both the equations of motion and $\mathrm{SO}(1, d-1)$ symmetry, for example the Wick-rotated Euclidean instanton. In addition, this smoothing produces no equivalent interpolation on the boundary, because of the following geometric considerations:

- All of the level sets of ξ^2 meet at infinity on the finalization ring on the boundary. Physically, for an inertial observer the bubble's wall, even if initially thick, ultimately thin out to zero width approaching finalization. All previous and later boundary points are not reached at all.
- The conformal boundary structure of the smoothed bubble metric determined by (2.12) is exactly the same as that of the thin-wall metric.

The smoothing actually complicates our following computations considerably, without procuring a conceptual advantage according to the aforementioned remarks. For the sake of producing concrete results, we will continue employing the "thin-wall" approximation, though we maintain that the procedure sketched in this section would likely prove to be the correct methodology to effect a smooth vacuum bubble.

2.2 Minimal curves in asymptotically AdS_3 spaces

2.2.1 Integral Geometry of the Hyperbolic Plane

For the purpose of our calculations, it is very useful to review the basics of integral geometry, which is a handy mathematical tool in the context of the information-geometry connection, most transparently in $\mathrm{AdS}_3/\mathrm{CFT}_2$. We follow the treatment of [56] and [12].

Let γ be a rectifiable curve in the Euclidean plane. Now parametrize a generic oriented line by its angle ϕ and its signed distance from the origin p. Let $n_\gamma(\phi, p)$ be the the number of intersections of the line described by (ϕ, p) and the curve γ, and consider the following integral over all possible signed lines:

$$\iint d\phi \wedge dp\, n_\gamma(\phi, p)\,. \tag{2.13}$$

Let us examine the properties of the quantity of eq. (2.13). If γ is a finite line segment, and since the quantity is invariant under isometries, it can only be a function of the segment's length. It is also easily seen to be additive over curve concatenation, which implies first and foremost that for a line segment it is actually proportional to the length, and for a rectifiable curve that it must be proportional to the arc length. Therefore

$$\mathrm{length}(\gamma) = C \iint d\phi \wedge dp\, n_\gamma(\phi, p)\,. \tag{2.14}$$

In the case of γ being the unit circle,

$$n_\gamma = \begin{cases} 2 & |p| < 1 \\ \\ 0 & |p| > 1 \end{cases}, \tag{2.15}$$

so that

$$2\pi = 2C \int_{-1}^{1} dp \int_{0}^{2\pi} d\phi \Rightarrow C = \frac{1}{4}\,, \tag{2.16}$$

which therefore proves the **Crofton formula** for the arclength of curves in the Euclidean plane:

$$\text{length}(\gamma) = \frac{1}{4} \iint d\phi \wedge dp\, n_\gamma(\phi, p)\,. \tag{2.17}$$

The formula is suggestive because it appears to encode metric information, embodied in the length functional, in terms of properties of the space of oriented lines, or **kinematic space**. The core of the argument rests on the isometries of the plane, which are reflected into kinematic space itself – thus, it is conceivable that it can be repeated in two-dimensional spherical and hyperbolic geometry, which enjoy the same number of symmetries. Let us attempt to extend this same argument to the hyperbolic plane. For it to go through, it's necessary to replace the two-form $d\phi \wedge dp$, which acted as an ISO(2)-invariant volume form for kinematic space, with an $\mathrm{SL}(2,\mathbb{R})$-invariant two-form ω on the space of hyperbolic lines. Thankfully, there is an elegantly simple way to visualize this 2-form. We are seeking ω on the kinematic space of $\mathbb{H}_2$ such that

$$\text{length}(\gamma) = \frac{1}{4} \int_{\mathcal{K}} \omega\, n_\gamma\,, \tag{2.18}$$

for any rectifiable curve γ on $\mathbb{H}_2$.

The set of ideal points, or conformal boundary, of the hyperbolic plane is topologically a circle. An oriented line is identified uniquely by an ordered pair of the two ideal points that it connects. In the Poincaré disk model, we can parametrize using the positions u and v of these points on the unit

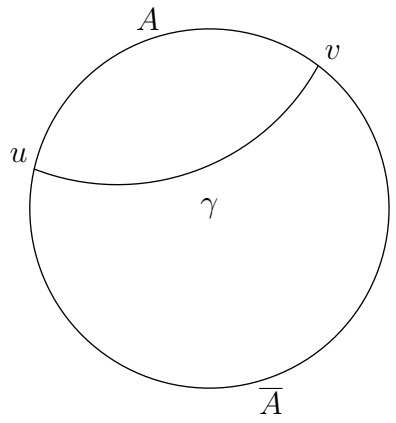

Figure 2.2: An oriented geodesic of $\mathbb{H}_2$ in the Poincaré disk model, with the ideal endpoints u, v marked. The curve is associated with the boundary interval $A = (u, v)$, with complementary $\bar{A} = (v, u)$.

circle, with the exclusion of all pairs with $u = v$ (see Figure 2.2). We can then define a mean position $\phi = \frac{u+v}{2}$ and a half-aperture angle $\theta = \frac{u-v}{2}$, which establish a chart for the Kinematic space of the hyperbolic plane. Shifts of ϕ are rotations of the disk and therefore isometries, so that the sought form must be

$$\omega = f(\theta)\, d\theta \wedge d\phi\,. \tag{2.19}$$

To fix $f(\theta)$, take γ to be a circle centered in the origin and of geodesic radius r. Let $\bar{\theta} < \frac{\pi}{2}$ be the half-aperture of a line tangent to the circle. Then (2.18) reads

$$2\pi \sinh(r) = \frac{1}{4} \int_0^{2\pi} d\phi \int_{\bar{\theta}}^{\pi-\bar{\theta}} d\theta\, f(\theta) \cdot 2\,, \tag{2.20}$$

$$\Rightarrow f(\bar{\theta}) = -\frac{\mathrm{d}}{\mathrm{d}\bar{\theta}} \sinh(r)\,. \tag{2.21}$$

In the diagram 2.3 we see highlighted the right triangle with vertices on the origin, the point of tangency, and the endpoint at infinity of the line.

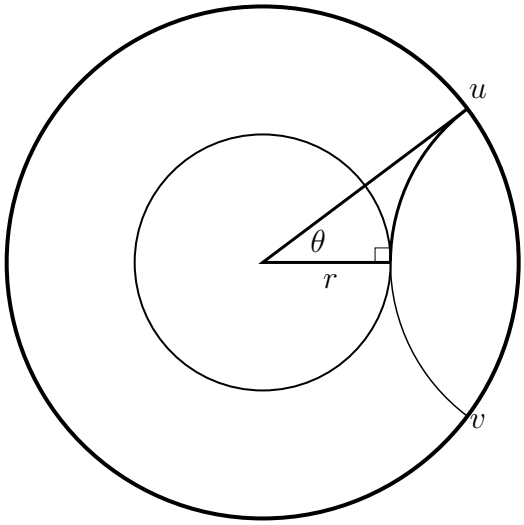

Figure 2.3: Displaying how the half-aperture θ of a line is the angle of parallelism for its distance r from the origin.

Therefore, $\bar{\theta}$ is the angle of parallelism[5] for perpendicular distance r, and the relationship

$$\cot \bar{\theta} = \sinh(r) \tag{2.22}$$

holds. Therefore, we are led to the determination of the correct 2-form for the hyperbolic plane

$$\omega = -\frac{1}{\sin^2 \theta} d\theta \wedge d\phi \,, \tag{2.23}$$

with the corresponding Crofton formula

$$\text{length}(\gamma) = \frac{1}{4} \int_{\mathcal{K}} \omega \, n_\gamma \,. \tag{2.24}$$

There is a very interesting geometrical structure at play, hinted at by the

[5]We remind briefly that the angle of parallelism $\Pi(x)$ for perpendicular distance x is the angle that a line must make with a segment AB of length x to be exactly parallel (i.e. meeting at infinity) to the orthogonal line to the segment passing through B.

fact that if ω is interpreted as a volume 2-form, then the kinematic space of $\mathbb{H}_2$ is naturally endowed with the structure of a de Sitter space[6]. Consider the hyperboloid model of $\mathbb{H}_2$ as a surface in $\mathbb{R}^{1,2}$ given by the equation

$$x^\mu x_\mu = -1\,, x^0 > 0\,. \tag{2.25}$$

Lines in the hyperboloid model are given by intersection of (oriented) planes passing through the origin; these will only intersect the hyperboloid if their normal vector is spacelike. The mapping of each oriented plane into its oriented unit normal determines a bijection between oriented hyperbolic lines and the set

$$x^\mu x_\mu = 1\,, \tag{2.26}$$

which is the natural embedding of de Sitter 2-space. In addition, since all isometries of $\mathbb{H}_2$ actually descend from $\mathbb{R}^{1,2}$ Lorentz transformations, then we know that the dS metric that kinematic space is endowed with is invariant under hyperbolic isometries. Thus, the volume form of de Sitter space must also be the Crofton form, up to a constant. Then the coordinates α and ϕ are simply recognized as a conformal closed slicing of dS_2:

$$ds^2 = \frac{-d\theta^2 + d\phi^2}{\sin^2\theta}\,, \tag{2.27}$$

while the null chart (u, v) is in fact the well-known ruling of the one-sheeted hyperboloid.

This can be generalized further. Imagine some surface which possesses some notion of "lines" - for our purposes, we request that it is asymptotically flat or

[6]While of course $\mathrm{dS}_2 = \mathrm{AdS}_2$ up to exchanging time and space, the higher-dimensional equivalent of $\mathcal{K}_{\mathbb{H}_d}$ is dS_d, so that the de Sitter picture is more practical.

hyperbolic, but may have some localized warping. We define the lines of the surface as the geodesics extending to infinity in both direction. In particular, in the asymptotically hyperbolic case a line is the geodesic between two ideal points. Then we can attempt imposing that the Crofton formula holds for all curves γ

$$\text{length}(\gamma) = \frac{1}{4}\int_{\mathcal{K}} \omega\, n_\gamma\,, \tag{2.28}$$

and determine whether a suitable ω form exist. Indeed, (2.28) appears to be an integral transform from Crofton form on $\mathcal{K}$ to the length functional, or equivalently the metric tensor, on the original surface, so that one may consider the possibility of inverting the transform. Let us show how to effect this inversion in the asymptotically hyperbolic case. First, we introduce a radial cutoff a certain geodesic distance $\Lambda \gg 1$ from the origin, and consider the length of the portion of a line inside of the cutoff. This defines a function on kinematic space, which we parametrize with (u, v)-coordinates:

$$L_{(\Lambda)}(u, v)\,. \tag{2.29}$$

It can be defined as the shortest distance between the points u and v on the cutoff surface. Now, we insert the line itself as the curve γ into the Crofton formula.

$$L_{(\Lambda)}(u, v) = \frac{1}{4}\int_{(u^*,v^*)\in\mathcal{K}} \omega(u^*, v^*) n(u, v, u^*, v^*)\,. \tag{2.30}$$

The intersection number is easy to compute: for very large Λ, given the oriented boundary interval $I = [u, v]$, and its complement $\bar{I} = [v, u]$, then $n = 1$ if one of (u^*, v^*) is in I and the other in $\bar{I}$, and $n = 0$ otherwise. We can assume $u^* \in I$ and $v^* \in \bar{I}$ by accounting for a factor of 2, and (2.30)

becomes

$$L_{(\Lambda)} = \frac{1}{2}\int_{u^*=u}^{v}\int_{v^*=v}^{u} \omega(u^*, v^*)\,, \tag{2.31}$$

and differentiating with respect to u and v yields

$$\frac{\partial^2 L}{\partial u \partial v} du \wedge dv = \omega(u, v)\,. \tag{2.32}$$

The identity (2.32) is the sought inversion of the Crofton formula, allowing to compute the corresponding Crofton 2-form starting from an asymptotically hyperbolic metric. We can omit the Λ subscript on the length, because it's easily verified that the second derivative in (2.32) is finite for $\Lambda \to \infty$, even though the length itself diverges. In aperture-center coordinates, this takes the form

$$\frac{1}{2}\left(\partial_\phi^2 - \partial_\theta^2\right) L(\phi, \theta) d\theta \wedge d\phi = \omega(\phi, \theta) \tag{2.33}$$

Let us display this inversion explicitly in the vacuum case of an exactly $\mathbb{H}_2$ metric. Take again the cutoff to be at geodesic distance Λ from the origin. The segment of line of half-aperture θ stretching between two points on the cutoff surface is twice the leg of a hyperbolic right triangle with a vertex in the origin, an opposite angle of θ, and a hypotenuse of Λ. Thus, by hyperbolic trigonometry its length is

$$L = 2\sinh^{-1}(\sin\theta \sinh\Lambda) \tag{2.34}$$

Now note that for any real x we have the asymptotic expansion for large Λ:

$$\sinh^{-1}\left(x\frac{e^\Lambda}{2} + \mathcal{O}(e^{-\Lambda})\right) = \log x + \Lambda + \mathcal{O}\left(e^{-\Lambda}\right)\,, \tag{2.35}$$

so that the length can be expanded as

$$L = 2\left(\log(\sin\theta) + \Lambda + \mathcal{O}\left(e^{-\Lambda}\right)\right)\,. \tag{2.36}$$

It is then clear that the Crofton form extracted through application of (2.33) is finite in the $\Lambda \to 0$ limit:

$$\omega = -\partial_\theta^2 \log(\sin(\theta)) d\theta \wedge d\phi = \frac{d\theta \wedge d\phi}{\sin^2 \theta} = \frac{du \wedge dv}{2 \sin^2(\frac{u-v}{2})}\,, \tag{2.37}$$

and that it is indeed the Crofton form of $\mathbb{H}_2$.

The framework described so far establishes a dictionary between the surface with its asymptotically hyperbolic metric and its kinematic space with the symplectic (and equivalently, Lorentzian) structure given by its Crofton form. In turn, the Crofton form is a two-form on $\mathcal{K}$ that asymptotes to the volume form of dS_2 for very large absolute de Sitter times:

$$\omega \to -\frac{d\theta \wedge d\phi}{\sin^2 \theta}\,, \quad \sin\theta \to 0\,, \tag{2.38}$$

since, of course, this is the limit in which lines become distant from the origin.

2.2.2 Holographic Integral Geometry

The previous discussion of integral geometry in the hyperbolic plane takes a much more physical meaning in the context of the AdS/CFT correspondence, specifically in a much more clear fashion in the $\mathrm{AdS}_3/\mathrm{CFT}_2$ case, thanks to the Ryu-Takayanagi[15] formula, which connects the area of specific minimal surfaces in the asymptotically AdS bulk with entanglement entropies across partitions of the boundary CFT. The precise statement of the formula for $\mathrm{AdS}_{p+2}/\mathrm{CFT}_{p+1}$ is as follows. Take a constant-time slice Σ of the bulk, and a corresponding boundary slice $\partial\Sigma$, which has $\mathbb{S}^p$ conformal structure. Consider a p-dimensional region A of $\partial\Sigma$, its complement $\bar{A}$, and the boundary

cycle ∂A separating A from $\bar{A}$. Take then all possible p-dimensional surfaces γ in the bulk that are homologous to A; by this we mean both that they have ∂A as a boundary and that A and γ are connected by a continuous homology of the closure of the bulk. Then, we have that

$$\frac{1}{4G} \min_{\gamma \cong A} \text{Area}(\gamma) = S_E(A)\,, \tag{2.39}$$

where $S_E(A)$ is the entanglement entropy of the subsystem of the degrees of freedom in A with those in $\bar{A}$. For the equation to be sensible, the d-dimensional area has to be regulated with a spherical cutoff at a large radial distance Λ, and the entropy must also be correspondingly regulated with a UV cutoff at momentum Λ. The CFT state on which the entanglement entropy is computed is the one corresponding to the bulk metric in which the minimal surfaces are sought, according to the holographic dictionary. We recall that the entanglement entropy of a subsystem A of a larger system, itself in a generic state given by the state matrix ρ, with its complement $\bar{A}$ is given by the Von Neumann entropy of the reduced state:

$$S_E(A) = S_{\text{VN}}(\rho_A) = -\,\text{Tr}(\rho_A \log \rho_A)\,, \quad \rho_A = \text{Tr}_{\bar{A}}(\rho)\,, \tag{2.40}$$

where $\text{Tr}_{\bar{A}}$ denotes a partial trace over only the degrees of freedom of $\bar{A}$. If the overall system happens to be in a pure state, so $\rho = |\Psi\rangle\langle\Psi|$, then the entanglement entropy is also symmetric:

$$S_E(A) = S_E(\bar{A}) \tag{2.41}$$

as can be easily observed by the Schmidt decomposition of $|\Psi\rangle$ over the state sub-spaces of A and $\bar{A}$. In this case, the name entropy of entanglement

is accurate, as it is a quantitative measure of the amount of information encoded strictly in the entanglement between A and $\bar{A}$.

Through the Ryu-Takayanagi formula, entanglement entropy in a conformal field theory maps to the area of minimal surfaces in the bulk. If the CFT state is pure, the entanglement entropy will be symmetric, and thus the bulk will have to be homologically trivial, i.e. devoid of horizons, so that minimal surfaces of complementary boundary regions will have to coincide. If instead the CFT is in a mixed state, for example thermal, that will mark the presence of horizons in the bulk, such as a black hole, which separate the two complementary surfaces. In such a way one can then provide a very picturesque proof of the equality of the CFT state's entropy and the area of horizon divided by $4G$[57].

The implications of this dictionary are manifold, but our attention is concentrated on the relationship with integral geometry. While we could perform the following construction in any dimension, it is arguably significantly more transparent in the case of $\mathrm{AdS}_3/\mathrm{CFT}_2$, where the minimal "surfaces" coincide with geodesic lines, so we shall restrict ourselves to that dimensionality. Combining the Ryu-Takayanagi formula with the inverse Crofton formula one obtains a remarkable identity:

$$\omega(u,v) = \frac{1}{4G}\frac{\partial^2 S_E(u,v)}{\partial u \partial v} du \wedge dv \tag{2.42}$$

allowing one to compute the Crofton form for the bulk's kinematic space, evaluated at the line stretching between boundary points u and v, in terms of the entanglement entropy of the CFT interval from u to v. Since ω in turn allows by definition to compute lengths of arbitrary bulk curves, it is

thus possible to reconstruct the whole geometry of the bulk entirely from the information of entanglement entropy.

Also useful us that the equation (2.42) involves only finite quantities independent of a regulator. The finite form $4G\,\omega$ has, in addition, an information-theoretical interpretation for the CFT as conditional mutual information, see [56].

2.3 Geodesics in the bubble geometry

The purely geometrical question that we have ultimately reduced to in the discussion of the holography of bubbles is that of determining the (regulated) length of geodesics of given endpoints, and in particular the absolute minimum length when multiple local minima exist. This search is performed on time-slices of the bubble geometry, which take the shape of two hyperbolic planes of different radii of curvature L_- and L_+ which are glued at a circular surface concentric with the cutoff. As explained above, the gluing is effected in such a way that the surface has the same circumference as measured from either plane, and this fixes all parameters except for one, which we can take as the instantaneous radius of the bubble. More specifically, let $\mathcal{C}$ be the circumference of the bubble. This determines the inner and "outer" radii:

$$\mathcal{C} \equiv 2\pi L_+ \sinh(\rho_+) = 2\pi L_- \sinh(\rho_-)\,. \tag{2.43}$$

The inner radius ρ_+ is the geodesic distance from the surface of the bubble to its centre in units of L_+, while the "outer" radius ρ_- is the radius of the

bubble's circle if the bubble itself was not there, measured in units of L_-. Any of the two can be taken as a parameter, as they are related by (2.43).

Directly attempting to solve the geodesic equation in the bubble geometry is at best wasteful, and at worst flawed. This comes to be first of all because the geometry is not smooth and the geodesic equation will not thus be a well-defined differential equation. It is potentially manageable distributionally, but this grows unnecessarily unwieldy. In addition, almost all points of the geometry consist of a locally $\mathbb{H}^2$ space, where geodesics are already known. We take instead a different, more geometric approach.

We first work out a useful lemma, which we name the **no-kink condition**. The statement is as follows: if a geodesic γ crosses the gluing surface, the angle γ makes with the bubble as measured from the outer plane coincides with the angle as measured from the inner plane. This means that if the entire geometry is depicted with a conformal model, then the curve γ will appear graphically to not have a kink at the intersection. The proof is simple: consider two points A and B on γ on the two sides of the bubble, at a distance less than ϵ from the intersection. In the limit of ϵ very small, the curvatures of the two hyperbolic planes can be neglected, as can the curvature of the bubble itself, while the kink angle is, of course, unchanged. In this limit the glued geometry actually becomes the smooth Euclidean plane. Therefore, if γ is a geodesic between A and B, it must be the straight line segment, which means the angles on either side are equal. These angles are the same as those measured in the original hyperbolic planes, which proves the lemma.

Geodesics of the bubble geometry must satisfy such a no-kink condition at

the bubble boundary, and be otherwise straight hyperbolic lines of the corresponding hyperbolic plane at any other point. Therefore, the minimal curve from points u and v on the boundary will necessarily be a polygonal of hyperbolic straight segments satisfying no-kink, and our search may be limited to such simpler curves. We can first of all distinguish two[7] classes, or *phases*:

- **Vacuum phase:** the curve does not intersect the bubble. It will therefore be simply the straight segment between u and v in $\mathbb{H}^2_-$.
- **Injection phase:** the curve enters the bubble at one point B (injection point) and exits from another one at $\bar{B}$. The curve is composed of the $\mathbb{H}^2_-$ segment uB, then the $\mathbb{H}^2_+$ segment $B\bar{B}$, and finally the $\mathbb{H}^2_-$ segment $\bar{B}v$. The position of B and $\bar{B}$ on the bubble is determined by the no-kink condition.

For each value of $\theta = \frac{u-v}{2}$, one has to determine the geodesic in each phase, and the actual overall minimal curve will be the shorter one.

Note that if θ is sufficiently close to $\frac{\pi}{2}$, the vacuum phase does not exist as the segment necessarily overlaps with the bubble. In particular, the threshold lies where the vacuum curve is tangent to the bubble, which happens precisely when θ is the angle of parallelism θ^{par} for the outer radius ρ_-. The vacuum

[7] We remark that multiple injections are certainly impossible. The finite segment between an exit and a re-entry point would be a straight segment between two bubble points that is partially external to the bubble itself, which contradicts the fact that the bubble is convex.

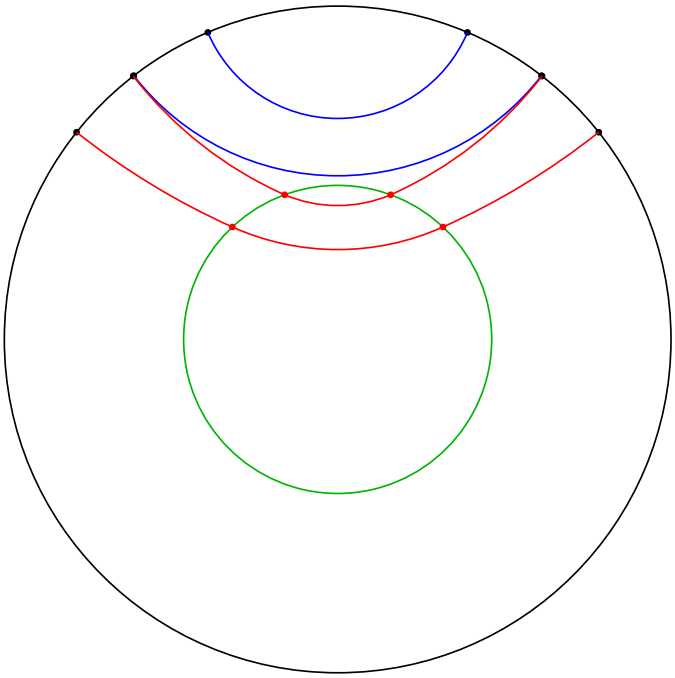

Figure 2.4: A time-slice of the bubble geometry in a "double-Poincaré disk" model. The blue curves are geodesics in the vacuum phase, and the red ones are geodesics in the injection phase. The drawn red and blue curves tangent at infinity are of equal length and mark the location of the phase transition between the two phases.

phase exists only if

$$\cos(\theta) \geq \cos(\theta^{\text{par}}) = \tanh(\rho_+)\,, \tag{2.44}$$

and when this is violated, only the injection phase remains and must therefore trivially be optimal. Nevertheless, we remark that (2.44) does not imply that the vacuum phase is *minimal*, and in principle the true phase transition may occur at a larger $\cos\theta$ than $\cos\theta^{\text{par}}$, as we will verify a posteriori. The shape of geodesics and the location of such a phase transition is depicted visually in Figure 2.4.

2.3.1 Injection geodesic

Let us work out the geodesic(s) in the injection class. This requires determining the location of the points B and $\bar{B}$ on the bubble so as to satisfy the no-kink condition there. By symmetry, the segment $B\bar{B}$ will be concentric with uv. Let C be its midpoint, and O the origin. Define the half-aperture θ_B as the angle BOC. Then the triangle OCB is a right triangle, with a hypotenuse of ρ_+ (in units of L_+) and an angle at O of θ_B. The missing angle at B is the angle α_{in} between the curve and the bubble, measured from the inside. By hyperbolic trigonometry, this is

$$\cosh\rho_+ = \cot\alpha_{\text{in}}\cot\theta_B\,. \tag{2.45}$$

Moving to the outer portion of the geodesic, it will be the segment in $\mathbb{H}^2_-$ from B to v. For the sake of the following argument, we temporarily reinsert the disk of $\mathbb{H}^2_-$ that had been excised back into the interior of the bubble, so

as to work with a complete $\mathbb{H}^2_-$. First, extend the segment OB into a line, then drop the perpendicular from v onto this line to obtain the point D. The triangles ODv and BDv are right with an ideal vertex, therefore the angle $DOv = \theta - \theta_B$ is of parallelism for the leg OD, and the angle $DBv = \alpha_{\text{out}}$, the outer angle between the curve and the bubble, is of parallelism for the leg BD. Since $OB = \rho_-$, we have

$$\rho_- = OD - BD = \cosh^{-1}\csc(\theta - \theta_B) - \cosh^{-1}\csc(\alpha_{\text{out}})\,. \tag{2.46}$$

It is sufficient to set $\alpha_{\text{in}} = \alpha_{\text{out}}$ to result in an equation for θ_B; after some algebra one obtains:

$$\sqrt{1 + (\cosh\rho_+ \tan\theta_B)^2} = \cosh\big(\cosh^{-1}\csc(\theta - \theta_B) - \rho_-\big)\,. \tag{2.47}$$

Equation (2.47) cannot be solved in closed form, and requires numerical methods. Let us establish some bounds on the variables. Without loss of generality, thanks to symmetry, we may take $0 < \theta < \frac{\pi}{2}$. Equation (2.46) necessitates then that $0 < \theta_B < \theta$, if one imposes that $|\alpha| < \frac{\pi}{2}$.

The left-hand side of (2.47) is equal to 1 at $\theta_B = 0$, and is finite and strictly increasing in the interval $0 < \theta_B \leq \theta$. The right hand side equals 1 at the unique special point $\theta_B = \theta^*$ such that $\csc(\theta - \theta^*) = \cosh\rho_-$. It is also strictly larger for any other value of θ_B, always convex, and diverges for $\theta_B = \theta$. All of this information implies that the condition will be satisfied always for exactly two values of θ_B on either side of θ^*. The two solutions are two distinct injection curves without kink, which would appear to imply the existence of two sub-phases, a "grazing" one with a smaller θ_B and a larger impact angle α, and a "direct" one with the larger θ_B and smaller

α. In truth, as we will see shortly, the grazing solution is actually a local *maximum* of the curve length over θ_B, and the direct solution is a minimum. The grazing solution can therefore be discarded[8]. Thus, we observe that no-kink is really a necessary but not sufficient condition for a curve to be a geodesic, and that indeed there is really only one geodesic curve in the class of injecting polygonals, with the injection point given by the larger solution $\theta^* < \theta_B < \theta$ of equation (2.47).

2.3.2 Minimal Length and phase transitions

For each value of θ, one can compute the length of the geodesics in the vacuum phase and in the injection phase, and verify which of the two is shorter. The vacuum phase length can be read off from (2.36):

$$L^{\text{vacuum}} = 2L_- \left(\Lambda + 2\log\sin\theta + \mathcal{O}(e^{-\Lambda})\right) , \tag{2.48}$$

while the length for the injection phase (which must necessarily be given as a function of θ_B, in turn to be determined numerically from solution of the no-kink condition) presents a more involved computation. One relatively easier technique of many is to employ the hyperboloid model for the hyperbolic plane. If $\mathbb{H}^2$ is embedded as the surface $X^\mu X_\mu = -1\,, \quad X^0 > 0$ in $\mathbb{R}^{1,2}$, then the distance between the two points x^μ and y^μ in units of the curvature radius is

$$d(X,Y) = \cosh^{-1}(-X^\mu Y_\mu)\,. \tag{2.49}$$

[8]In [12] we have worded this fact incorrectly by stating that the no-kink condition had one unique solution. To be exact, the no-kink condition has two solutions, as we have just shown, but only one of them is actually a geodesic.

We have the following representation for the points $\bar{B}$, B, v as vectors in the hyperboloid models of $\mathbb{H}^2_+$, $\mathbb{H}^2_-$:

$$\begin{aligned}
\bar{B}^\mu_+ &= (\cosh\rho_+, \sinh\rho_+\cos(\theta_B), -\sinh\rho_+\sin(\theta_B)) \\
B^\mu_+ &= (\cosh\rho_+, \sinh\rho_+\cos(\theta_B), \sinh\rho_+\sin(\theta_B)) \\
B^\mu_- &= (\cosh\rho_-, \sinh\rho_-\cos(\theta_B), \sinh\rho_-\sin(\theta_B)) \\
v^\mu_- &= (\cosh\Lambda, \sinh\Lambda\cos(\theta), \sinh(\Lambda)\sin(\theta))\,,
\end{aligned} \tag{2.50}$$

so that it straightforward to compute the entire length through (2.49) and the asymptotic expansion (2.35):

$$L^{\text{injection}}(\theta_B) = \bar{B}B + 2Bv = L_+\cosh^{-1}(-\bar{B}^\mu_+ B_{+\mu}) + 2L_-\cosh^{-1}(-B^\mu_- v_{-\mu}) \tag{2.51}$$

$$\begin{aligned}
= \quad & 2L_-\Lambda \\
& +2L_-\log(\cosh\rho_- - \sinh\rho_-\cos(\theta-\theta_B)) \\
& +L_+\cosh^{-1}(\cosh^2\rho_+ - \sinh^2\rho_+\cos(2\theta_B)) \\
& +\mathcal{O}(e^{-\Lambda})
\end{aligned} \tag{2.52}$$

There is now a straightforward procedure to determine numerically the length of the injection geodesic for given values of the parameters ρ_+, ρ_-, θ: first one determines the larger θ^*_B of the two solutions of equation (2.47) through a simple root-finding procedure[9]. Then, one simply replaces $\theta \to \theta^*_B$ into (2.52).

The first interesting numerical phenomenon occurs at $\theta = \theta_{\text{par}}$, which is such that the vacuum geodesic is tangent to the bubble. It is found that

[9]Care must be exercised in correctly bounding the search as θ^*_B is often quite close to θ, where the right hand side of the equation diverges

the minimal injection geodesic is shorter than the tangent vacuum geodesic. In other words, the bubble offers a "shortcut" where diving briefly into the bubble can prove optimal over traversing the exterior space undisturbed, if said undisturbed path is within a certain distance from the bubble surface. This is due to the new more highly curved AdS space within, where distances between bubble surface points are shorter than they would be if the bubble was not present. In any case, it physically means that from the point of view of kinematic space, the bubble has an attractive effect that precedes it, being able to engulf geodesics before they come in actual contact.

Let us sketch a "phase diagram" of sort based on this information. For $\theta > \theta_{\text{par}}$, the only existing phase is the injection one, which is thus optimal. We also know that $\theta = \theta_{\text{par}}$ the injection phase is still optimal over the vacuum phase. Note, in addition, that for very small θ it is quite clear geometrically that the vacuum geodesic will be much shorter. Therefore, there must be at least one critical value θ_{crit}, in the interval $0 < \theta_{\text{crit}} < \theta_{\text{par}}$, where a phase transition between vacuum and injecting geodesics occurs. Indeed, the numeric results do display the existence of such a threshold where the lengths of the two possible geodesics are equal. From the point of view of the pattern of the entanglement entropy, it is at θ_{crit}, and not θ_{par}, that the bubble's discontinuity occurs.

Such a discontinuity does not present itself in the entanglement entropy itself, but in its derivatives. In particular, the Crofton form itself:

$$\omega = \frac{\partial^2 L}{\partial u \partial v} du \wedge dv = -\frac{1}{2}\partial_\theta^2 L \, d\theta \wedge d\phi \tag{2.53}$$

presents a δ-function discontinuity at θ_{crit}. This δ-function wall, expanding

to ever-larger $\cos\theta$ as the bubble grows in real space, can for all intents and purposes be understood as the kinematic space equivalent of the bubble itself. We can produce an even more clear understanding by examining numerical results for ω. In particular, since ω is top-rank on $\mathcal{K}$, we can define its scalar ratio with the vacuum Crofton form of $\mathbb{H}_{2,-}$:

$$\omega \equiv \Omega\, \omega_{\mathrm{dS}_{2,-}}\,, \quad \omega_{\mathrm{dS}_{2,-}} = L_- \frac{d\theta \wedge d\phi}{\sin^2\theta}\,. \tag{2.54}$$

The quantity (2.54) can be easily graphed, as we will do in Figure 2.6, and is also conveniently interpreted: in the initial and final states it has the constant values

$$\begin{aligned} \Omega &= 1 \qquad \mathrm{AdS}_- \\ \Omega &= \frac{L_+}{L_-} \qquad \mathrm{AdS}_+ \end{aligned} \tag{2.55}$$

and it will interpolate between these values in some manner for intermediate points.

2.3.3 Shifted bubbles

In the previous section we have proceeded under the assumption of a **centered bubble**, meaning that the vacuum bubble is concentric with the cutoff surface. It may be useful as well to also have control over **shifted bubbles** for which this is not the case. However, in a forward approach, computing directly the entanglement entropy through the Ryu-Takayanagi formula, the computation would quickly turn unwieldy. Thankfully, we now can travel a shortcut through cutoff-invariant quantities. A centered bubble can be transformed into a shifted bubble through the action of an asymptotic $\mathrm{SL}(2,\mathbb{R})$

isometry of the metastable $\mathbb{H}^2_-$, which is the asymptotic metric throughout decay. These maps do no leave the cutoff invariant, of course, so that the entanglement entropy transforms in a complex way, involving a mixing of the infinite and finite. Not so, however, for finite quantities like the Crofton form. The vacuum Crofton form ω_{dS_2} is $\mathrm{SL}(2,\mathbb{R})$ invariant, and the Crofton form ω of a general warped metric will transform covariantly as a 2-form. This implies by (2.54) that Ω is in fact an $\mathrm{SL}(2,\mathbb{R})$ scalar, meaning its transformation simply involves the pullback of the change of coordinates.

Let us perform this transformation explicitly. $\mathrm{SL}(2,\mathbb{R})$ rotations about the center of a round bubble are trivially symmetries of the bubble itself, so that we can restrict to the study of simple hyperbolic translations, which have two opposite boundary points as fixed points and the bulk diameter connecting them as an invariant set. Without loss of generality, fix the coordinates so that $u, v = 0, \pi$ are the fixed points of the transformation. After a change of coordinates on the boundary

$$\cot\frac{u}{2} \equiv x\,, \quad \cot\frac{v}{2} \equiv y\,, \tag{2.56}$$

the vacuum Crofton form can be written as

$$\omega_{\mathrm{dS}_2} = \frac{du \wedge dv}{\sin^2(\frac{u-v}{2})} = 4\frac{dx \wedge dy}{(x-y)^2}\,. \tag{2.57}$$

The sought $\mathrm{SL}(2,\mathbb{R})$ transformations then must act separately on x and y, leave the form invariant, and have fixed points $x, y = 0, +\infty$. It is quite easy to see these must be simple scalings:

$$x \to \lambda x\,, \quad y \to \lambda y \tag{2.58}$$

Which in turn translates straightforwardly into the transformation rule of θ:

$$\theta \to \cot^{-1}\left(\lambda \cot\left(\frac{\phi+\theta}{2}\right)\right) - \cot^{-1}\left(\lambda \cot\left(\frac{\phi-\theta}{2}\right)\right). \tag{2.59}$$

With the explicit transformation in hand, it is now possible to write down the transformation of the scalar Ω from that $\Omega_{\text{central}}(\theta)$ of a centered bubble to that $\Omega_{\text{shifted}}(\theta,\phi)$ of one in general position through a simple pullback:

$$\Omega(\theta,\phi)_{\text{shifted}} = \Omega_{\text{central}}\left(\cot^{-1}\left(\lambda \cot\left(\frac{\phi+\theta}{2}\right)\right) - \cot^{-1}\left(\lambda \cot\left(\frac{\phi-\theta}{2}\right)\right)\right) \tag{2.60}$$

In turn, the Crofton form is reconstructed:

$$\omega_{\text{shifted}} = \Omega_{\text{shifted}}\omega_{\text{dS}_2}\,, \tag{2.61}$$

which encodes the entire bulk geometry through the Crofton formula. If desired, it is possible to also reproduce the entanglement entropy / geodesic length with a cutoff by integrating the Crofton form:

$$L(u,v) = 4G\int_{u^*}\int_{v^*}\omega_{\text{shifted}}(u^*,v^*)\,, \tag{2.62}$$

with the limits of integrations chosen so as to both satisfy equation (2.53) and reproduce the correct infinite part of the length with the cutoff:

$$L(u,v) \sim 2\Lambda + \mathcal{O}(1) \tag{2.63}$$

2.3.4 Horocyclical limit

In the literature, a domain wall separating two different vacua is a more common scenario than the spherical bubbles we have studied so far. By

domain wall in the hyperbolic case (including AdS, Euclidean AdS, or AdS time-slices indiscriminately) it is meant that, having established a Poincaré half-space chart

$$ds^2 = \frac{dz^2 + d\vec{x}^2}{z^2}\,, \tag{2.64}$$

one takes the transition between vacua to happen at a surface of constant z:

$$z = z^*\,. \tag{2.65}$$

Domain walls and spherical bubbles however are not disconnected classes. The surface described by (2.65) is geometrically a **horosphere**, also called horocycle in two dimensions, which are hypersurfaces of vanishing intrinsic curvature and constant extrinsic curvature. Horospheres are by all means to be considered "spheres with their centers at infinity" as they can be obtained as limits of regular spheres by simultaneously sending the radius to infinity and the translating the center to the boundary. Since an expanding vacuum bubble in AdS expands to infinite radius in a finite time as measured by an inertial observer, this limit is quite physically relevant: for an observer in an AdS far away from the nucleation point the vacuum bubble will appear, as soon as it reaches them in a bounded time, as a traveling, intrinsically flat domain wall.

Let us effect such a limit explicitly in the present formalism. We would like to send the radius of the bubble, for example the exterior radius ρ_-, to infinity while simultaneously performing a shift to keep some point S on the surface of the bubble fixed. If the bubble is centered, the tangent to the bubble at S is the line of aperture-center coordinates $(\theta, \phi) = (\theta_{\text{par}}, 0)$, where again θ_{par} is the angle of parallelism for ρ_+. The most useful form of this relationship

in the present case is

$$\cot\theta_{\rm par} = \sinh\rho_- \,. \tag{2.66}$$

The tangent line will be shifted according to (2.59), namely

$$\cot\left(\frac{\theta_{\rm par}}{2}\right) \to \lambda\cot\left(\frac{\theta_{\rm par}}{2}\right), \tag{2.67}$$

which means that if one sends $\lambda \to 0$ in such a way that

$$\lambda\sinh\rho_- \to {\rm const} \tag{2.68}$$

as $\rho_- \to \infty$, the tangent line and the point S will be fixed and the limit will be sensible. Without loss of generality, we may take the constant to be 1, so that the transformed S will lie at the origin[10]. This limit transformation turns the bubble into a horocycle with a center at infinity, in the boundary point π. It would be now possible to compute the relevant limit behaviours of all the expressions for the geodesic lengths of the various phases obtained in the previous sections, and these do indeed simplify greatly in this horocyclical limit. It is however more instructive to simply recognize the well-known set up that is reproduced in this limit, where calculations are more conveniently performed.

2.4 Results

With the formalism set up so far, numerical investigation of the entanglement entropy pattern of the boundary theories throughout bubble expansion is

[10]The arbitrariness in this shift constant geometrically relates to the fact that all horocycles are actually congruent, in accordance with the loss of the size parameter ρ_-.

straightforward. For a central bubble, the entanglement entropy is as said function of the interval half-aperture θ and to the parameters of the geometry of the time-slice, which are the two AdS curvature radii $L_\pm$ and the current size of the bubble, given as the exterior r

2.4.1 Bubble $S_{\mathbf{ent}}$ as a c-function candidate

Now that the necessary formalism has been set up, one can perform a numerical analysis of the holographic entanglement patterns during a centered bubble expansion and make some important observations. As noted in [12], for any given interval size 2θ and for all values of the other parameters the entanglement entropy is monotonically decreasing when considered as a function of the bubble radius ρ_+ or ρ_-. This non-trivial fact implies that for any $0 < \theta < \frac{\pi}{2}$, the entanglement entropy itself acts as a candidate c-function for the dual process to the bubble expansion. The thin-wall approximation produces the artifact of $S_{\text{ent}}(\theta, \rho_-)$ being non-smooth in ρ_-, in fact it is a constant in the interval $0 < \cosh \rho_+ < \csc \theta_{\text{crit}}$ where the vacuum phase is still dominating, after which it is strictly decreasing. In particular, if one takes the interval to be half of the boundary $\theta = \frac{\pi}{2}$, then $\theta_{\text{crit}} = 0$ and the entanglement entropy is actually always strictly decreasing. The schematic nature of these results is reported in Figure 2.7.

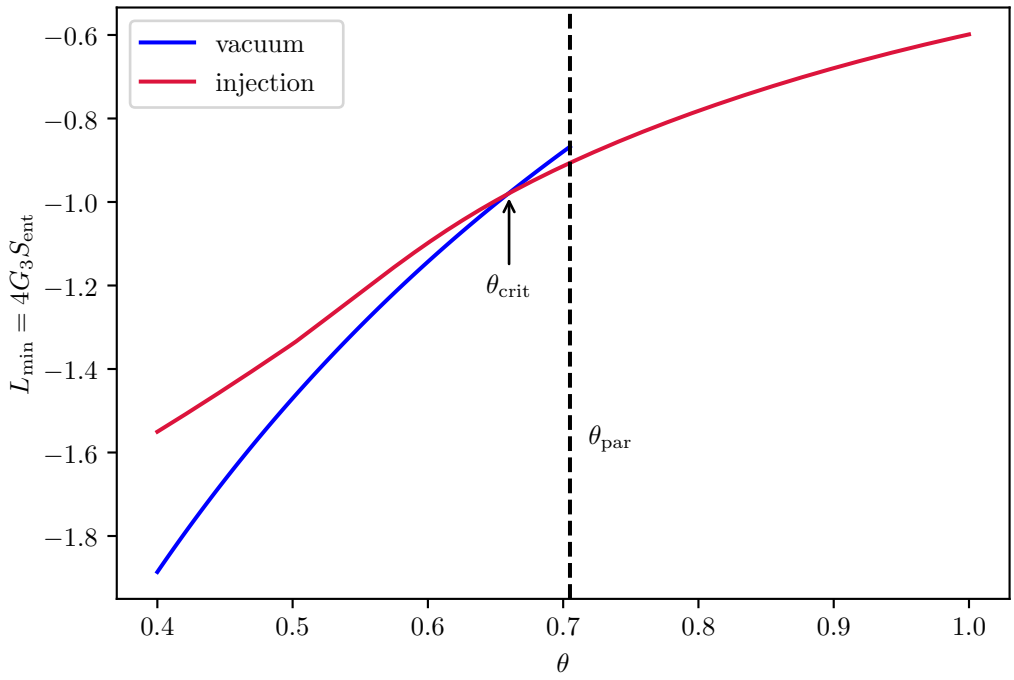

Figure 2.5: Finite part of geodesic length for sample values of the parameters, plotted against half-aperture θ. Observe that the injection phase becomes optimal at the smaller aperture θ_{crit} than the θ_{par} at which the vacuum geodesic becomes tangent to the bubble.

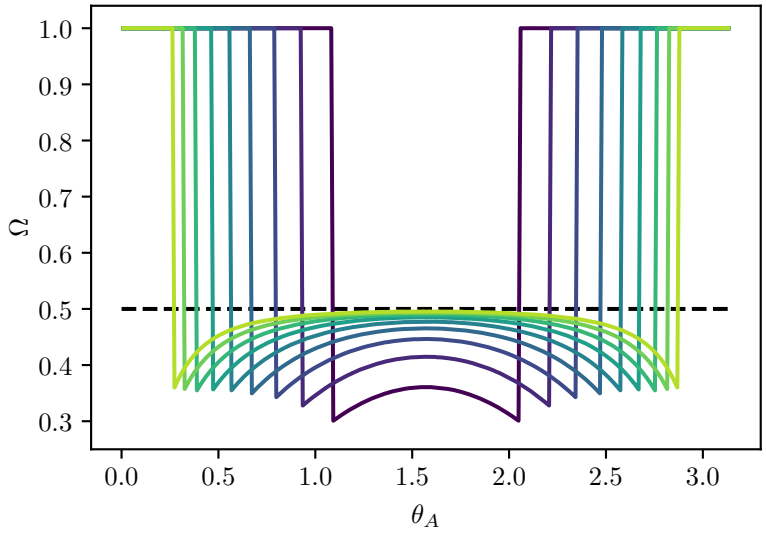

Figure 2.6: The evolution of the Crofton form factor Ω in kinematic space for an expanding bubble, for sample value of the parameters (in this example, the final AdS_+ radius is $\frac{1}{2}$ of the original AdS_- radius). As seen, $\Omega = 1$ for all $\theta > \theta_{\text{crit}}$, since the AdS_- vacuum geodesic is optimal. Then, a δ-function wall (not depicted) occurs at $\theta = \theta_{\text{crit}}$, expanding with the bubble, while the value of Ω inside smoothly approaches the value $\frac{1}{2}$ expected for the AdS_+ vacuum.

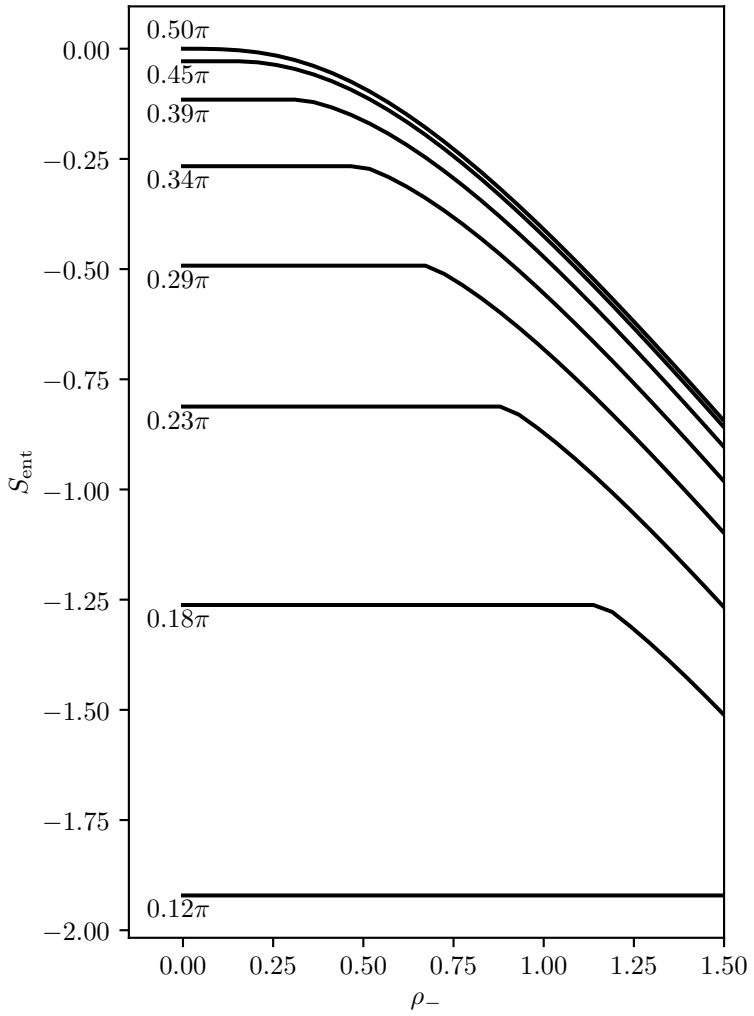

Figure 2.7: The finite part of the entanglement entropy for a central bubble as a function of the bubble's inner radius ρ_-, for sample value 2 of the ratio of cosmological constants. Several curves are plotted for various half-apertures θ.

2.5 RG picture and Conclusions

Motivated by the results obtained through the procedure outlined in this chapter, in [12] we proposed a holographic dictionary for $AdS_- \to AdS_+$ vacuum bubbles, whose full layout is as follows:

- A metastable AdS_- bulk is dual to an "unstable CFT", which is to say a conformal theory which admits an IR-relevant deformation.
- The quantum-gravitational nucleation of a bubble of true AdS_+ vacuum in AdS_- is dual to turning on an IR-relevant deformation.
- The dynamical expansion of the vacuum bubble in the bulk from the center towards the boundary is dual to the subsequent renormalization group flow that the boundary theory undergoes, passing through non-conformal theories. In the boundary, the "bubble" is nucleated initially for zero momentum and then expands in momentum space, moving against the direction of the RG decimation. There is a 1-to-1 correspondence between bulk bubble radius and RG scale.
- The final step, when the vacuum is fully replaced with AdS_+, is dual to the convergence of the boundary RG flow to a final fixed point, which is the CFT_+ dual to that bulk.

The computation of the entanglement pattern for shifted bubbles of Section 2.3.3, in addition, allowed us to propose a more precise conjecture on the relationship between the position of the nucleation event and the relevant

deformation. Briefly stated, the rotational symmetry implies that a centered nucleation must correspond to a relevant operator λ that is uniform on the boundary. Therefore, e.g., for any local CFT$_-$ operator $A(\phi)$ (with ϕ the cylindrical chart on the boundary),

$$\langle \lambda A(\phi) \rangle \tag{2.69}$$

is independent of ϕ. On the other hand, an off-centered nucleation would produce a non-uniform operator, for which the above quantity depends on ϕ (see Figure 2.8). As a shift is effected, a dependence on the half-aperture θ, which acts as a momentum scale, is accompanied by a dependence on ϕ, which is a position variable. The resulting transformation of the dependence can be fully spelled out in terms of the transformation of (θ, ϕ) of eq. (2.59), seen as a chart for dS_2 kinematic space undergoing an $SO(1,3)$ boost.

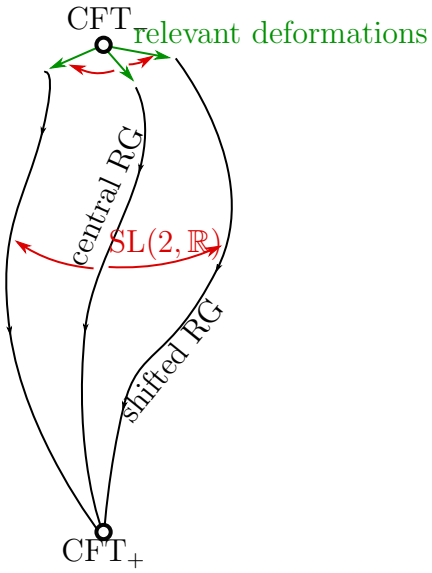

Figure 2.8: Pictorial representation of the "shifted renormalization" scenario. Just as both nucleation and expansion of a shifted bubble are related by $\mathrm{SL}(2,\mathbb{R})$ bulk isometries, and the final AdS_+ is invariant, so in the boundary the relevant deformation and subsequent RG flow are related by kinematic space isometries $\mathrm{SL}(2,\mathbb{R})$ mixing position and momentum, and the final state is an $\mathrm{SL}(2,\mathbb{R})$-invariant CFT_+.

Chapter 3

Self-similar collapse

In a seminal paper[18], a curious gedankenexperiment in classical gravitation was performed, in the simplified simplified setting provided by a massless scalar field minimally coupled to gravity in four dimensions. The experiment consisted in straddling the boundary separating initial conditions that lead eventually to the formation of a black hole from those which do not, and ultimately result in diffusion and flat spacetime. The author's original methodology was to modulate spherically-symmetric initial field amplitudes with an amplitude parameter p, and to study the corresponding evolution numerically. A sufficiently small value of p cannot lead to collapse, since the resulting lies within the linearized regime of the theory, while a sufficiently large value of p must necessarily lead to collapse, as the Schwarzschild criterion is satisfied. Therefore, there must be (at least one) critical value p_* that separates these two phases. By analogy with Statistical Mechanics, the

corresponding time-evolved configuration is termed **critical collapse**.

Two suggestive phenomena are observed in relation to critical collapse:

- The exactly critical solution displays an asymptotic discrete space-time self-similarity, so that there exist an event x_0^μ and a real parameter Λ such that the fields are invariant under a transformation $(x^\mu - x_0^\mu) \to \Lambda(x^\mu - x_0^\mu)$ as x^μ approaches x_0^μ. This periodic repetition is usually called **Choptuik echoing**.

- The near-critical collapses display power-law scalings of observables with the "order parameter" $(p - p_*)$. For example, in numerical simulations the mass of the resulting black hole would scale as

$$M \propto (p - p_*)^\gamma \,. \tag{3.1}$$

  This phenomenon is called **Choptuik scaling** and γ (which was about 0.37 in the specific case of [18]) is called the **Choptuik critical exponent**.

These fascinating observations appeared to point to a Statistical Mechanics framing of classical gravitational collapse, or at the very least are qualitatively reminiscent of statistical arguments. It was implicitly argued that, if the emergence of scale invariance and power-law scaling when approaching critical collapse were analogous, in any way, to the emergence of similar features near a critical point of a statistical system, it should be possible to translate corresponding notions into classical gravity and produce non-trivial

statements. A very natural conjecture would be the universality of critical exponents, namely the expectation that γ be independent of dimension, matter content, and configuration of initial conditions.

A long series of similar experiments were performed in the following years. The critical collapse of a complex scalar field was examined in [58], and [59–62] instead focused on a radiation fluid. Non-linear sigma models are other relevant systems whose critical collapses were studied in detail, albeit limitedly to the hyperbolic plane and the sphere [25]. All these studies confirmed self-similarity properties, thus also making the connection between critical collapse and self-similarity worthy of further investigation.

Universality, in its most naive formulation, appeared a real possibility after [60] extracted the value $\gamma \sim 0.36$ for the critical exponent in the spherically symmetric gravitational collapse of a radiation fluid. Within the available precision, this result seemed indeed consistent with Choptuik's one obtained for a real scalar. The identification was however invalidated shortly thereafter, when it was understood that perturbation theory of the self-similar solution [61] provided a more convenient channel to compute γ. The authors treated the convergence in time of the critical collapse to the self-similar spacetime as akin to a renormalization group flow into a conformal fixed point, and via this approach could prove the following result. Let the field configuration h_0 be a self-similar solution, and consider the spectrum of scaling dimensions of its perturbations. In other words, perturb the system letting

$$h_0 \to h_0 + \epsilon h_{-\kappa}\,, \tag{3.2}$$

where under a scale transformation $x^\mu \to \Lambda x^\mu$, h_0 is invariant and $h_{-\kappa}$ scales as $\Lambda^{-\kappa}$. Explore then all values $\kappa \in \mathbb{C}$ such that a smooth solution exists to first order in ϵ. Then the κ^* with largest real part will mark the most relevant mode, and the Choptuik critical exponent will be

$$\gamma = \frac{1}{\mathrm{Re}\,\kappa^*}\,. \tag{3.3}$$

We report a summary of the proof in Section 3.2.1.

3.1 Critical collapse and scale-invariance

Let us consider in more detail the thought experiment mentioned in the previous section. Take gravity coupled to some continuous stress-energy source in d spacetime dimension (a field, or a fluid), limited to spherical symmetry for the sake of simplicity. It is always possible to choose some initial stress-energy distribution that results in collapse into a black hole, by satisfying the Schwarzschild criterion. Now, we may construct a one-parameter family of related initial conditions simply by modulating field amplitudes $h(t, \vec{x})$ with a multiplier p:

$$h(0, \vec{x}) \to p\, h(0, \vec{x})\,. \tag{3.4}$$

Now, it is clear that both the total initial mass and the local mass density are growing functions of p. Therefore, sufficiently large values of p always lead to a black hole collapse. However, if p is sufficiently small, then a linearized theory must be an accurate description of the physics. In a free theory perturbed by small couplings gravitational collapse is impossible. Therefore,

there is always a finite range of small p such that the final state does *not* include a black hole at all.

We argue there must therefore be a critical value p_* which is such that initial conditions with $p < p_*$ have no final-state black hole, and those with $p > p_*$ do. The interesting puzzle concerns what happens exactly at $p = p_*$. If we assume, as will turn out to be useful, that the final state changes continuously with p when crossing the critical threshold, or in other words that the critical point is "stable", then it stands to reason that the black holes of the supercritical collapses must become small as one approaches criticality, so as to connect continuously with the empty subcritical final states. The conclusion, however, is that the final state of a critical initial condition cannot possess any kind of length/mass scale, since the only one present in collapse is the black hole mass. Thus, critical collapse must eventually display some kind of scale invariance.

A critical final state would have to be a static, scale-invariant, non-empty spacetime of zero mass. This is of course too restrictive a set of requirements, and the conclusion is that critical collapse may not have a final state at all, and a naked singularity must appear that prevents continuation of the solution past its future lightcone[1]. We thus begin to understand from first principles the qualitative structure of critical collapse. As one approaches the naked singularity in critical collapse, the solution approaches one that is spacetime self-similar, namely there exists a chart x^μ such that scalar fields

[1]This is not in contradiction with the standard singularity theorems, since the critical initial conditions are non-generic.

repeat periodically:

$$\phi(\Lambda x^\mu) = \phi(x^\mu)\,, \tag{3.5}$$

for some specific $0 > \Lambda > 1$, while tensor fields scale with the appropriate power of Λ. The point $x^\mu = 0$ is then the aforementioned naked singularity. This phenomenon of asymptotic echoing is general, and the periodic solution that is approached is said to be **discretely self-similar**.

It is possible on special locations of parameter space for the echoing to be promoted to full scale invariance, i.e. **continuous self-similarity** (CSS):

$$\phi(\Lambda x^\mu) = \Lambda^M \phi(x^\mu)\,, \quad \text{for } \textbf{any } \Lambda > 0\,, \tag{3.6}$$

where M is a generator of an internal symmetry[2].

3.2 Continuous self-similarity

A configuration of a classical metric theory is continuously self-similar if two conditions are met:

1. the metric possesses a homothetic Killing vectors ξ, that is to say

$$\mathcal{L}_\xi g_{ab} = 2 g_{ab}\,. \tag{3.7}$$

[2]We may not allow M to be the identity as in the discretely self-similar case, because the only continuously self-similar solution with no mixing with internal symmetries is the trivial Minkowski vacuum. Thus, only theories with internal symmetries may have non-trivial CSS

2. The scalar sector is scale-invariant up to an internal global symmetry of generator M, that is to say

$$\mathcal{L}\phi^I = M^I_J \phi^J \tag{3.8}$$

Given any spacetime event x, the curve

$$\exp(-s\xi)x\,, \quad 0 < s < \infty \tag{3.9}$$

is actually always of finite length, as can be seen from equation (3.7). This means the limit point

$$\lim_{s\to\infty} \exp(-s\xi)x \tag{3.10}$$

which is "always a finite distance away" is either a smooth point of the spacetime itself, or must house a singularity. However, it is easy to see that if the metric is smooth at the limit point, then it is flat to first order in the distance from the point, which implies by equation (3.7) that it actually must be flat everywhere. Therefore, any non-trivial CSS metric has such a **homothetic singularity** in the fixed point of the dilations.

A CSS solution has two null conical horizons where $\xi^2 = 0$, which are precisely the past and future horizons of the singularity. Consider the boundary-value problem of determining a CSS solution. Assume an initial condition is taken on some complete Cauchy surface that the singularity is in the future of. The initial surface can safely intersect the past horizon without passing the singularity, which means this first horizon, the **homothetic horizon**, is merely a coordinate artifact. However, the Cauchy surfaces may not continue past the future horizon while keeping the homothetic singularity in the future.

Therefore, the second surface is actually a Cauchy horizon, and CSS solutions may not be continued past it. Qualitatively, a CSS solution has a structure similar to that exemplified in Figure 3.1.

3.2.1 The link with perturbation theory

Let us review how [61] prove the relation (3.3) between the most relevant mode of the perturbation theory of a CSS solution and the Choptuik critical exponent. The core argument is rather simple. Imagine an initial condition $h(t_0, x)$, $t_0 < 0$ which is sufficiently close to criticality, *i.e.*

$$h(t_0, r) = h_0(z) + \epsilon F(r)\,, \quad \epsilon \ll 1\,. \tag{3.11}$$

During time evolution $t_0 \to t$, with both $t_0 < 0$ and $t < 0$, this solution will initially approach the CSS configuration $h_0(x)$, but then it will diverge again along the unstable manifold. This is possible to derive also by applying linear perturbations to the initial conditions (3.11): after sufficiently large time the perturbation will be dominated by the most relevant mode:

$$h(t, x) = h_0(z) + \epsilon C \left(\frac{t}{t_0}\right)^{-\kappa^*} h_{-\kappa^*}(z) + \mathcal{O}(\epsilon^2)\,, \quad \frac{t}{t_0} \ll 1\,, \tag{3.12}$$

where C is some $\mathcal{O}(1)$ constant involving the coefficient of the most relevant mode in the initial generic perturbation. Now, if a black hole forms due to the perturbation, then collapse will happen at a time such that the perturbation is of the same order as the unperturbed part. This occurs at the time

$$\frac{t}{t_0} = \epsilon^{\frac{1}{\mathrm{Re}\,\kappa^*}}\,, \tag{3.13}$$

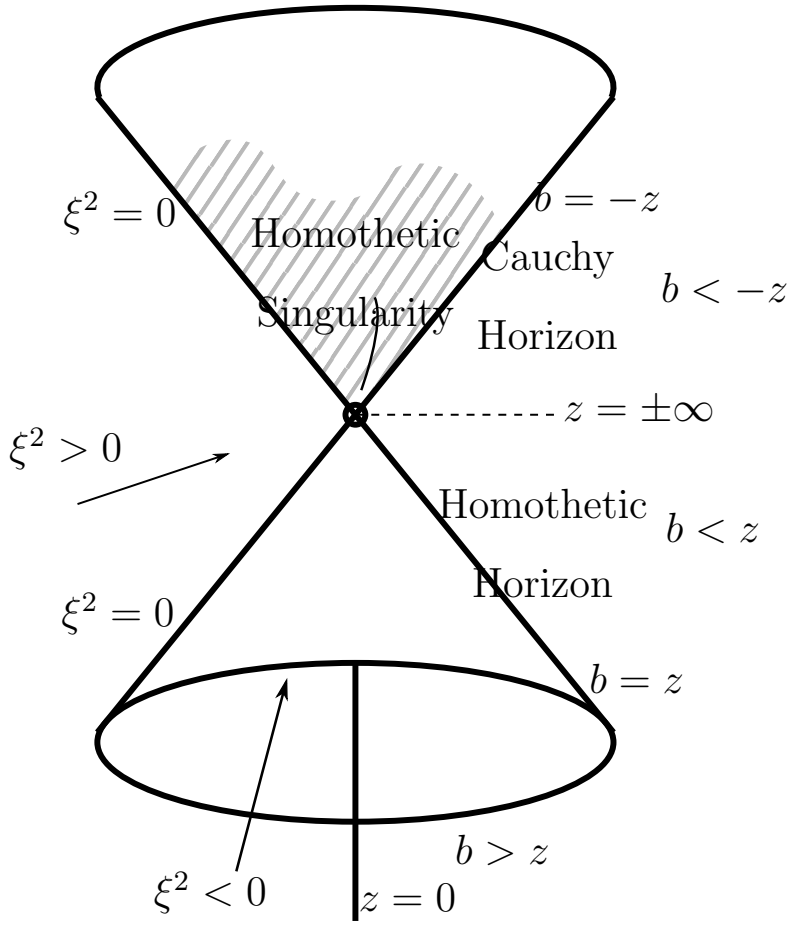

Figure 3.1: Conformal diagram of a CSS solution with important loci marked.

and since, generically, $h_{-\kappa^*}(z) = \mathcal{O}(1)$ for $z = \mathcal{O}(1)$, then the radius r_s of the horizon itself will scale in the same way

$$r_s \sim \epsilon^{-\frac{1}{\kappa^*}} , \tag{3.14}$$

which matches the definition of the Choptuik critical exponent, so that we may conclude

$$\gamma = \frac{1}{\operatorname{Re} \kappa^*} \tag{3.15}$$

3.3 The axion-dilaton system

The Einstein-axion-dilaton system in d dimension appears in (Einstein-frame) low-energy effective theories from type IIB string theory configurations. It consists of a non-linear σ-model over the hyperbolic plane $\mathbb{H}^2$ coupled minimally to gravity

$$S = \int d^d x \sqrt{-g} \left(R - \frac{d\tau d\bar{\tau}}{2(\operatorname{Im} \tau)^2} \right) . \tag{3.16}$$

Where the complex field $\tau(x)$ is limited to the half-plane $\operatorname{Im} \tau > 0$. A more traditional presentation is recovered by decomposing into the real fields of axion and dilaton as $\tau = a + ie^{-\phi}$:

$$S = \int d^d x \sqrt{-g} \left(R - \frac{1}{2} e^{-2\phi} \left((\partial a)^2 + (\partial \phi)^2 \right) \right) . \tag{3.17}$$

ϕ originates as the string theory dilaton, while a is the Ramond-Ramond 0-form potential of type-IIB string theory. It's also noteworthy for comparison with the literature that other equivalent presentations can be obtained by

performing a target-space biholomorphic transformation. For example, if one performs a Cayley transform from the half-plane model to the Poincaré disk:

$$\tau(x) = i\frac{1+F(x)}{1-F(x)} \tag{3.18}$$

then the action is presented with explicit phase symmetry $F \to e^{i\theta}F$:

$$S = \int d^d x\, \sqrt{-g}\left(R - \frac{2\, dF d\overline{F}}{(1-|F|^2)^2}\right) . \tag{3.19}$$

This is the form in which the system appears, in four dimensions, in the survey of σ-models in [25]. We will employ primarily the half-plane action (3.16), though we will make use of the Cayley transform in some computation.

The system enjoys the global internal symmetry of the target-space isometries $\mathrm{PSL}(2,\mathbb{R})$, acting as

$$\tau \to \frac{a\tau + b}{c\tau + d}\,, \quad a,b,c,d \in \mathbb{R}\,, \quad \det\begin{pmatrix} a & b \\ c & d \end{pmatrix} = 1\,. \tag{3.20}$$

As is well-known, $\mathrm{PSL}(2,\mathbb{R})$ is divided into three non-trivial conjugacy classes, up to reflections, classified by the trace $a+d$:

- **Elliptic** elements with $|a+d| < 2$ are $\mathbb{H}^2$ rotations, with one fixed point in $\mathbb{H}^2$, and generate compact one-parameter subgroups.
- **Parabolic** elements with $|a+d| = 2$ are holorations of $\mathbb{H}^2$, with one ideal fixed point, and generate a non-compact one-parameter subgroup.
- **Hyperbolic** elements with $|a+d| > 2$ are $\mathbb{H}^2$ translations, with two ideal fixed points, and generate a non-compact one-parameter subgroup.

By expanding equation (3.20), we can display the generic infinitesimal form of the transformations:

$$\delta\tau = \alpha_0 + \alpha_1\tau + \alpha_2\tau^2\,, \quad \alpha_i \in \mathbb{R}\,, \tag{3.21}$$

and by comparing the roots of the polynomial with the mapping of fixed points, the classification is in terms of the sign of the discriminant $\Delta = \alpha_1^2 - 4\alpha_0\alpha_2$. Elliptic elements have $\Delta < 0$, parabolic elements have $\Delta = 0$, and $\Delta > 0$ is the hyperbolic class. It is useful to choose "canonical" representatives from each class of minimal complexity. All hyperbolic elements are conjugate to a scaling of τ:

$$\tau \to e^{\lambda}\tau\,, \tag{3.22}$$

for some $\lambda \in \mathbb{R}$ (geometrically, λ is the geodesic distance that points are translated by). All parabolic elements are conjugate to a real translation

$$\tau \to \tau + a\,, \quad a \in \mathbb{R}\,. \tag{3.23}$$

The half-plane chart is however not particularly convenient to display elliptic elements explicitly. Arguably the simplest elliptic element is obtained by performing a Cayley transform, then a simple rotation of angle θ around the origin, then transforming back. The result is the following hyperbolic rotation around $\tau = i$:

$$\tau \to \frac{\cos\left(\frac{\theta}{2}\right)\tau + \sin\left(\frac{\theta}{2}\right)}{-\sin\left(\frac{\theta}{2}\right)\tau + \cos\left(\frac{\theta}{2}\right)} \tag{3.24}$$

As detailed in Section 3.2, a configuration (g, τ) of the axion-dilaton system is **continuously self-similar** (CSS) if the metric admits a homothetic Killing

vector ξ satisfying equation (3.7), and the axion-dilaton field τ is invariant under rescalings up to a $\mathrm{PSL}(2,\mathbb{R})$ element, which is to say

$$\mathcal{L}_\xi \tau = \xi^\mu \partial_\mu \tau = \alpha_0 + \alpha_1 \tau + \alpha_2 \tau^2 \tag{3.25}$$

where the α_i act globally, in the sense that they do not depend on the spacetime point. Such spacetimes are thus invariant under a specific combination of dilations and an internal transformation of the scalar sector. Up to an overall conjugation by $\mathrm{PSL}(2,\mathbb{R})$, the CSS configurations are then classified into Elliptic, Parabolic, Hyperbolic according to the class of the compensating transformation, and can be brought to a canonical form corresponding to the infinitesimal versions of the transformations (3.22), (3.23), (3.24):

$$\mathcal{L}_\xi \tau = \begin{cases} \omega\tau & \text{Hyperbolic} \\ \omega & \text{Parabolic} \\ \frac{\omega}{2}(1+\tau^2) & \text{Elliptic} \end{cases} \tag{3.26}$$

where the real parameter ω stands in for the infinitesimal form of the original parameters λ, a or θ. Without loss of generality, $\omega \geq 0$, since one may always apply the discrete S-duality symmetry $\tau \to -\frac{1}{\tau}$ which preserves the condition (3.26) up to a switch in sign $\omega \to -\omega$.

Let us determine a general explicit ansatz for a spherically-symmetric CSS spacetime. Since ξ and rotations commute, it is possible to construct a function z on spacetime which is both rotationally and scale-invariant. In addition, a radius r such that the $(d-2)$-spheres have volume $r^{d-2}\Omega_{d-2}$ can be constructed in the standard fashion. Finally, we define a time coordinate

$$t \equiv -rz\,. \tag{3.27}$$

By equation (3.7), r has scaling dimension 1, and therefore so does t. If one writes a generic spherically-symmetric metric in the (t, r) chart

$$ds^2 = (1 + u(t, r))(-b(t, r)^2 dt^2 + dr^2) + r^2 d\Omega_{d-2}^2 \tag{3.28}$$

then the spacetime will be scale-invariant if the warp factors themselves are:

$$u(t, r) = u(z)\,, \quad b(t, r) = b(z)\,, \quad z = -\frac{r}{t}\,. \tag{3.29}$$

This must be appended with an appropriate ansatz for the axion-dilaton. Consider this field as a function $\tau(t, z)$ and decompose its value on the surface $t = -1$ in terms of a scale invariant function $f(z)$ as follows:

$$\tau(-1, z) \equiv \begin{cases} f(z) & \text{Parabolic, Hyperbolic} \\ -i\frac{1-f(z)}{1+f(z)} & \text{Elliptic} \end{cases}\,. \tag{3.30}$$

Then, the axion-dilaton at any other time is determined uniquely by exponentiating the scale transformation (3.26):

$$\tau(t, z) = \begin{cases} (-t)^{i\omega} f(z) & \text{Hyperbolic} \\ f(z) + \omega \log(-t) & \text{Parabolic} \\ -i\frac{1-(-t)^{i\omega} f(z)}{1+(-t)^{i\omega} f(z)} & \text{Elliptic} \end{cases}\,. \tag{3.31}$$

In conclusion, the general spherically-symmetric self-similar spacetime is uniquely described by the scale invariant functions

$$u(z)\,, \quad b(z)\,, \quad f(z) \tag{3.32}$$

with u, b real, and $f(z)$ in the unit disk or the upper half-plane depending on the class.

If, in addition, the equations of motion stemming from the action (3.16) are satisfied, then we can speak of a CSS solution. The field equations and the axion-dilaton equation take the general form:

$$R_{ab} = \frac{\partial_{\{a}\tau\partial_{b\}}\bar{\tau}}{2(\mathrm{Im}\,\tau)^2}\,, \quad \nabla^2\tau + \frac{i\partial_a\tau\partial^a\tau}{\mathrm{Im}\,\tau} = 0\,. \tag{3.33}$$

The equations can be then specified to the CSS ansatz in the various classes, to obtain ordinary differential equations for b, u and f in the variable z. Any solution to these equation determines an on-shell CSS spacetime.

3.4 Equations of motion and boundary value problem

Because the resulting equations of motion for critical collapse in the axion-dilaton system are impractically complex, within the present section and the following ones we will frequently omit the long explicit forms of these equations, preferring to focus more on the conceptual and methodological aspects. We do remark that we have reported all the full forms of the equations of motion and their perturbations in the works [16, 17].

The first hurdle is the computation of the Ricci tensor for the metric ansatz (3.28) in general dimension d. The computation starts with considering an auxiliary 2-dimensional metric

$$d\tilde{s}^2 = (1 + u(t,r))(-b(t,r)^2dt^2 + dr^2) \tag{3.34}$$

of which one readily determines the two-dimensional Ricci tensor and Christof-

fel symbols. Then, the complete metric is interpreted as a warped product of the auxiliary surface and the q-sphere, with $q = d - 2$:

$$ds^2 = d\tilde{s}^2 + r^2 d\Omega_q^2 \,, \tag{3.35}$$

so that its Ricci tensor can be written as a function of the auxiliary Ricci tensor and Christoffel symbol, the sphere's Ricci tensor $R_{ij} = (q-1)h_{ij}$ and with the explicit full dependence on the unknown dimension through q. Through the same technique one can produce the q-dependent ∇^2 operator to be used in the scalar equation. Finally, relation (3.31) in the relevant class is replaced into all occurrences of τ in the equations of motion.

After imposing that all the fields are only functions of z, this provides us with a system of ODEs of order 1 for $b(z)$ and $u(z)$ and order 2 for $f(z)$. However, it is relatively easy to remove u entirely. The ij equation (where ij are indices on the sphere) is remarkably simple:

$$R_{ij} = 0 \Rightarrow u(z) = \frac{zb'}{(q-1)b} \,, \tag{3.36}$$

while the tr equation will produce a more complex relation, depending on the class, which will however allow to solve directly for $u'(z)$ in terms of at most first derivatives of the axion-dilaton:

$$u'(z) = U(f, f') \,. \tag{3.37}$$

After replacing equations (3.36), (3.37) back into the remaining equations of motion, the u variable is completely removed with no increase in the order for the remaining degrees of freedom. The final system, which is significantly more complicated in form, is of total real order 5, being first-order in $b(z)$

and second-order in the complex $f(z)$. Schematically, it is

$$f''(z) = F(f, f', b)\,, b'(z) = B(f, f', b)\,, \tag{3.38}$$

where the explicit form of the functions $F(f, f', b)$, $B(f, f', b)$ is omitted here for clarity, though reported in full in [16].

The obtained equations of motion must retain a symmetry under global (i.e., z-independent) transformations of $f(z)$ that induce a corresponding $\mathrm{SL}(2,\mathbb{R})$ map in τ. These are

$$f(z) \to \begin{cases} e^{i\theta} f(z) & \text{Elliptic} \\ f(z) + a & \text{Parabolic} \\ e^{\lambda} f(z) & \text{Hyperbolic} \end{cases} . \tag{3.39}$$

In any case, since these changes on $f(z)$ can be compensated by a global $\mathrm{SL}(2,\mathbb{R})$ transformation of τ, one can conclude the existence of a one-parameter group of global symmetries to the system of equations (3.38).

3.4.1 Boundary conditions

The system of ODEs just obtained presents multiple singular points in z, independently on the dimension of spacetime and the class, located at

$$\begin{aligned} &z = \pm 0\,, \\ &z = z_+ \text{ such that } b(z_+) = z_+\,, \\ &z = z_- \text{ such that } b(z_-) = -z_-\,, \\ &z = \pm\infty\,. \end{aligned} \tag{3.40}$$

The singularities at $z = \pm\infty$ are physically simply the hyperplane $t = 0$ and are easily removed by continuing a solution across this plane. This can be done without imposing any additional constraints, so that this singularity introduces no information to the determination of global solutions. On the other hand $z = +0$, that is to say $r = 0$, $t < 0$, is a coordinate singularity akin to that at the origin of a polar chart. For a function $F(z)$ to be smooth in spacetime on the $z = +0$ line, it's necessary that

$$F'(0) = 0\,, \tag{3.41}$$

which means that the fields must satisfy the condition:

$$f'(0) = 0\,. \tag{3.42}$$

It's not necessary to impose $b'(0) = 0$, because the first order equation of motion of b already implies that this vanishes.

The singularity $b(z_+) = z_+$ is actually an horizon where the sign of g_{tt} flips. It is, in fact, the surface where the homothetic Killing vector ξ is null, and it is itself tangent to ξ. We call this null surface a **homothetic horizon**. This horizon is a coordinate singularity and one can continue solutions across it, but because of the requirement of scale invariance, this actually generates some non-trivial constraints. To extract them, physically it would be possible to transform to a local frame which eliminates the coordinate singularity, imposing smoothness of the transformed fields, and to transform back. However, it is much faster to work directly with the equations of motion themselves, which automatically include these notions. The b' equation is regular at the horizon, while the f'' equation is divergent. If we perform a

near-horizon expansion of the equation, of the kind

$$f''(z) = G(f(z_+), f'(z_+), b(z_+))\frac{1}{\beta} + \mathcal{O}(\beta^0)\,, \quad \beta = b(z) - z\,, \tag{3.43}$$

then the second derivative of f will be finite (a necessary and sufficient condition for regularity) if and only if the non-linear function G of the lower-order fields at the horizon vanishes. This establishes a non-linear, complex-valued constraint located at z_+

$$G(f(z_+), f'(z_+), b(z_+)) = 0\,. \tag{3.44}$$

Before one proceeds up to z_-, let us count the free parameters available. The original system of order 5 has 5 integration constants. In addition, the homothetic frequency ω is *a priori* unknown, for a total of 6. However, the complex-valued condition (3.42) removes two. In addition, $b(0)$ is pure gauge, and we can set $b(0) = 1$ with a rescaling of time, removing one additional parameter, and (3.44) does away with other two degrees of freedom. Finally, we can remove the last parameter by making use of the global symmetry (3.39) on f. We choose, for consistency with the literature, to fix the value of f at $z = 0$ in terms of a single real parameter x_0 in the following manner:

$$f(0) = \begin{cases} x_0\,, & 0 < x_0 < 1 & \text{Elliptic} \\ ix_0\,, & x \in \mathbb{R} & \text{Parabolic} \\ 1 + ix_0\,, & x \in \mathbb{R} & \text{Hyperbolic} \end{cases}\,. \tag{3.45}$$

Thus, the system with conditions of regularity at $z = 0$ and the homothetic horizon is actually fully determined, and the solution set has dimension zero. Such discrete points in the space of the only two physical parameters, ω and

x_0, constitute the genuine CSS Einstein-axion-dilaton solutions. One may picture this as a sort of non-linear version of an eigenvalue problem for the homothetic frequency.

In any case, a straightforward procedure is required to perform the solution search. We now sketch the methodology that we employed in [16], which improves over previous techniques to reduce the dimensionality of the search space. First, one defines a complex-valued function $G(\omega, x_0)$ through the following procedure:

- Compute $f(0)$ through (3.45), set $b(0) = 1$, and $f'(0) = 0$ as previously discussed. This completes a set of initial conditions.
- Integrate the equations of motion forward in z with the given ω. Adapt the time-step to the instantaneous magnitude of $b(z) - z$ so as to have increased precision when approaching the horizon.
- Stop the integration when $b(z) - z < 0$ and interpolate the integrated points to determine the precise location z_+ of the horizon.
- Use the integrated solution to compute the constraint $G(f(z_+), f'(z_+), b(z_+))$ and output its value.

The function $G(\omega, x_0)$ vanishes if and only if there exists a CSS solution with those values of ω and x_0. Therefore, the search for solutions has reduced to the simple problem of determining roots in two dimensions to the complex-valued G. Because of the low dimensionality, it is not only relatively agile to determine *a* root, but actually easy to examine a range of values graphically

and observe how many discrete solutions exist. We opted for producing plots of $G(\omega, x_0)$ with the contours $\mathrm{Re}\, G = 0$, $\mathrm{Im}\, G = 0$ marked in different colours. The roots are then identified as intersections. Then a properly-seeded root-finding procedure can determine the exact position of the solution and provide an estimation of its accuracy.

No parabolic solutions

It is worthy of mention that although we have detailed the definition of a parabolic CSS solution, this conjugacy class is a degenerate case that actually does not, generically, contain solutions. This can be seen in several ways. Assume $(b(z), f(z), \omega)$ is a parabolic CSS solution. Note that

$$(b(z), f(z), \omega) \to (b(z), Kf(z), K\omega)\,, \quad K > 0\,, \tag{3.46}$$

is actually a simple dilation of the axion-dilaton $\tau(t, r) \to K\tau(t, r)$, which is a $\mathrm{PSL}(2, \mathbb{R})$ element and therefore a global symmetry. Thus, the transformed configuration must also be a solution. This degeneracy implies that the system is actually overdetermined. In other words, the G-function actually only depends on one variable out of two:

$$G(\omega, x_0) = G(1, \frac{x_0}{\omega})\,, \tag{3.47}$$

but still has two independent components to be made to vanish, so that generically, no zeroes exist.

In practice, it is possible nevertheless to numerically map G over this one parameter and observe whether some unknown considerations or relations

allow the degeneracy to be compensated and solutions may appear. In [17] we have verified over a large range of dimensions $4 \leq d \leq 26$ that this does not, in fact, occur. In light of this, in all of the following we will not include consideration of the parabolic class.

3.4.2 Results for four and five dimensions

In [16] we applied the methodology described so far to the elliptic and hyperbolic classes in $d = 4, 5$, and mapped out continuously self-similar solutions.

In the four dimensional elliptic class, it was well known that a unique solution exists [63, 64], whose parameters we have estimated to be

$$\omega = 1.176\,, \quad |f(0)| = 0.892\,. \tag{3.48}$$

In figure 3.2 we reproduce the "phase plot" where curves of vanishing real and imaginary parts of the function $G(\omega; x_0)$ are represented with alternating colours. Only one intersection can be identified. With this useful tool we were able to provide strong evidence that no other critical points exist.

The surprise comes when moving to any of the other three cases to consider, which are $d = 4$ hyperbolic, $d = 5$ elliptic, and $d = 5$ hyperbolic. In all three of these situations, we have found multiple solutions. In Figures 3.3, 3.4, 3.5 we reproduce the phase plots that evidence these solutions. A peculiarity of the hyperbolic phase diagrams is that they appear to have a series of roots extending past the limits of numerical precision, in the region of small $\mathrm{Im}\{f(0)\}$, so that we find it likely that our survey of the hyperbolic $d = 4, 5$

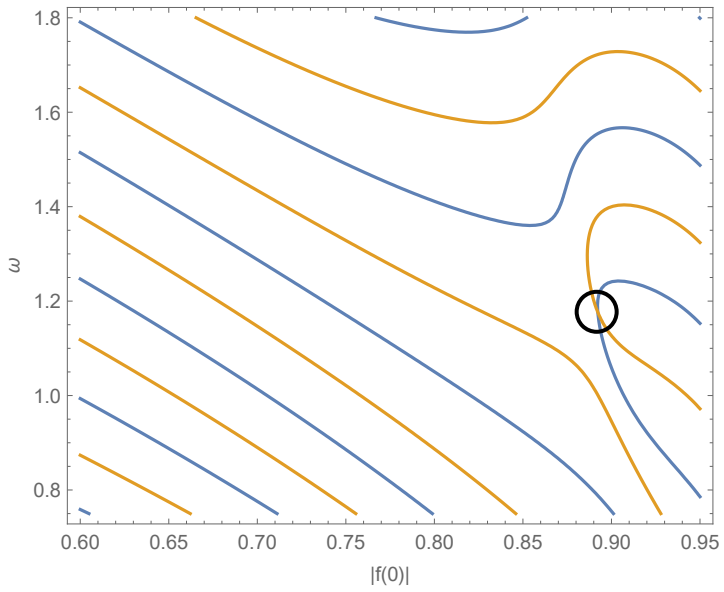

Figure 3.2: The G phase plot for $d = 4$ axion-dilaton CSS solutions in the elliptic class.

CSS solutions is incomplete. It is unknown whether this sequence is finite or whether infinite hyperbolic solutions exist of increasingly smaller $\mathrm{Im}\{f(0)\}$. For the Elliptic class in five dimensions, instead, we are confident that no other solutions exist beyond the three that we have determined.

3.5 Perturbation Theory

The perturbation theory of the CSS solutions is significantly more complicated than the determination of the solutions themselves, since the perturbative modes enjoy neither the background's scale invariance, nor the global residual $\mathrm{SL}(2,\mathbb{R})$ symmetry. Nevertheless, it is feasible to tackle this problem

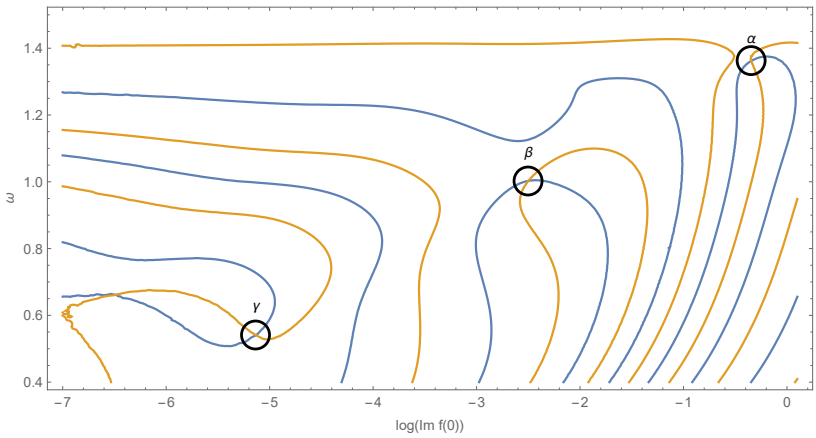

Figure 3.3: The phase plot for $d = 4$ axion-dilaton CSS solutions in the hyperbolic class.

numerically; in this section we present the methodology we employed in [17].

Let's say a CSS solution is given in terms of the scale-invariant fields $h_0(z) = (u_0(z), b_0(z), f_0(z))$. If one perturbs this with a generic, non-CSS perturbation as follows:

$$h(t, z) = h_0(z) + \epsilon h_1(t, z)\,, \tag{3.49}$$

inserts (3.49) into the equations of motion and expands them in powers of ϵ, the leading coefficient will contain the CSS equations of motion, while the next-order term will comprise the linear equations for the perturbation $h_1(t, z)$, with the solution $h_0(z)$ entering in the coefficients. These will be partial differential equations in two variables, for example z and t. However, since the original equations of motion and h_0 are scale-invariant, so will be the linearized equations for h_1. Scale invariance of the equations means equivalently that they are autonomous in $\log(-t)$. This suggests the use of

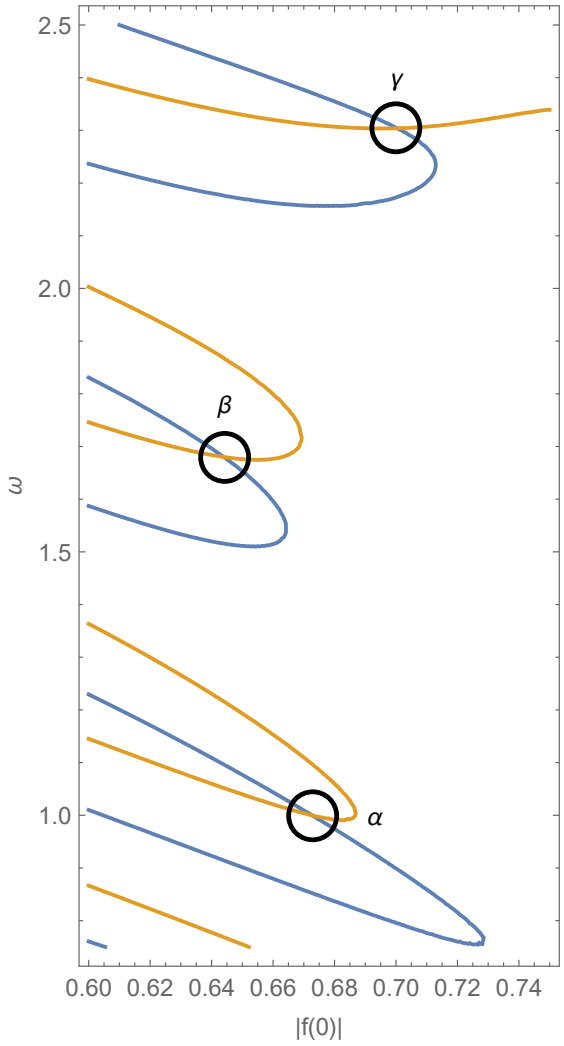

Figure 3.4: The phase plot for $d = 5$ axion-dilaton CSS solutions in the elliptic class.

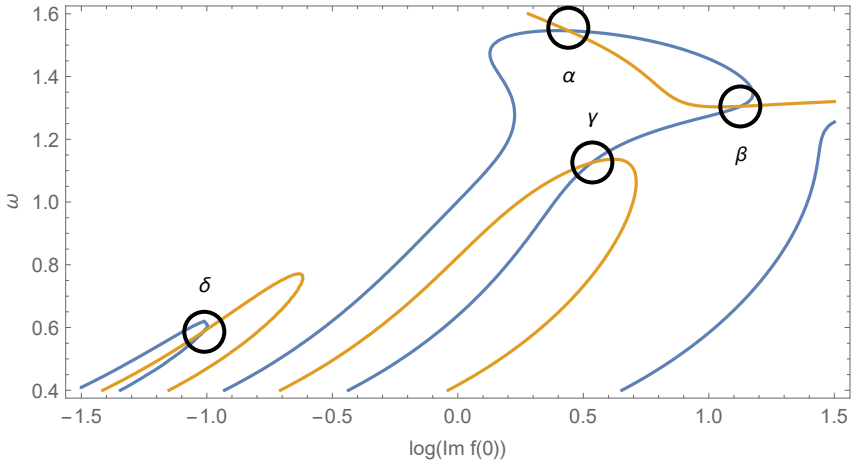

Figure 3.5: The phase plot for $d = 5$ axion-dilaton CSS solutions in the hyperbolic class.

a Fourier-Laplace decomposition of the perturbations in $\log(-t)$:

$$h_1(t, z) = \sum_{\kappa} (-t)^{-\kappa} h_1^{(\kappa)}(z)\,, \tag{3.50}$$

where the sum may run over a certain subset of $\mathbb{C}$. Within such a decomposition, $h_1^{(\kappa)}$ modes of different κ decouple. Thus, because the equations for h_1 are linear, one may as well consider these modes one at a time. Therefore, without loss of generality one may assume the perturbation has a definite scaling dimension, i.e.

$$h(t, z) = h_0(z) + \epsilon\,(-t)^{-\kappa} h_1(z)\,, \tag{3.51}$$

where we have omitted the (κ) superscript. The resulting linearized equations are fully scale invariant, but they possess the additional unknown complex parameter κ.

3.5.1 Linearized equations of motion

The first computationally intensive step is the determination of the linearized equations of motion. In accordance with the previous section, we perturb the scale-invariant fields u, b, f with a perturbation of scaling dimension $-\kappa$:

$$u(t,r) = u_0(z) + \varepsilon\,(-t)^{-\kappa} u_1(z)\ , \tag{3.52}$$

$$b(t,r) = b_0(z) + \varepsilon\,(-t)^{-\kappa} b_1(z)\ , \tag{3.53}$$

$$f(t,r) \equiv f_0(z) + \varepsilon\,(-t)^{-\kappa} f_1(z)\ . \tag{3.54}$$

and the field $\tau(t,r)$ is reconstructed from $f(t,r)$ in the same fashion as defined before:

$$\tau(t,r) = \begin{cases} i\frac{1-(-t)^{i\omega} f(t,r)}{1+(-t)^{i\omega} f(t,r)} & \text{Elliptic} \\ f(t,r) & \text{Hyperbolic} \end{cases}\ . \tag{3.55}$$

These ansätze are inserted into the equations of motion, which are then expanded up to first order in ϵ. The first-order coefficients constitute linearized equations for the perturbed fields. Just as it was possible to eliminate u_0 and its derivatives in the background solution, it is possible to remove u_1 and its derivative from the perturbed equations as well, in an identical fashion by using the equations of motion to rewrite $u_1(z)$ and $u_1'(z)$ as a function of the other first- and zeroeth-order fields.

This long but straightforward procedure, best performed with the help of a computer algebra system, produces a set of ordinary differential equations for the linear perturbations $(b_1(z), f_1(z))$. The system is of first order in the real b_1 and second order in the complex f_1, for a total order of five, again. The

coefficient themselves depend on the unknown parameter κ, and the known values from the background solution of ω and the CSS fields $(b_0(z), f_0(z))$.

Consider again the counting of degrees of freedom in the solutions. The equations have 5 integration constants, to which the additional unknown κ must be added for a total of 6. At the singular point $z = 0$, for $f_1(z)$ to be regular we must again impose $f_1'(0) = 0$, removing two degrees of freedom. By rescaling time, we may completely eliminate the b_1 perturbation and set $b_1(0) = 0$, which takes away another parameter. At the homothetic horizon, we impose as before the finiteness of $f''(z)$, which holds iff both f_0'' and f_1'' are finite there, but this time expanding to higher order in $\beta = b_0(z) - z$:

$$f_0''(\beta) = \frac{1}{\beta} G(h_0) + \mathcal{O}(1)\,, \tag{3.56}$$

$$f_1''(\beta) = \frac{1}{\beta^2} \bar{G}(h_0) + \frac{1}{\beta} H(h_0, h_1|\kappa) + \mathcal{O}(1)\,, \tag{3.57}$$

where h_0, h_1 schematically represent the background fields and perturbations evaluated at z_+. It can be seen that $\overline{G} = 0 \Leftrightarrow G = 0$, so that the original constraint is not contradicted. Instead, we have the new genuine constraint

$$H(h_0(z_+), h_1(z_+)|\kappa) = 0\,, \tag{3.58}$$

where H is by definition linear in the perturbations h_1. This linear, complex-valued constraint removes two more degrees of freedom.

In total, one unknown parameter still remains. We do not possess anymore the luxury of residual internal transformation to remove the last degree of freedom. However, note that since both the equations and the boundary conditions for the $h_1(z)$ are $\mathbb{R}$-linear, then if $(h_1(z), \kappa)$ is a solution, so is

$(Ch_1(z), \kappa)$, for any $C \in \mathbb{R}$. Since we are not interested in determining h_1 but simply κ, this overall rescaling of the mode constitutes the last removable parameter.

To conclude, the problem of determining allowed values of the scaling dimension $-\kappa$ is determined, and the "spectrum" (in a broad sense, as the equations are actually not linear in κ) is generically a discrete subset of $\mathbb{C}$.

3.5.2 Numerical algorithm

Collect all unknowns in the boundary conditions in a real five-vector:

$$X = (\mathrm{Re}\, f_1(0),\, \mathrm{Im}\, f_1(0),\, \mathrm{Re}\, f_1(z_+),\, \mathrm{Im}\, f_1(z_+),\, b_1(z_+))\,. \tag{3.59}$$

The problem can be stated precisely as determining the points in the six-dimensional (κ, X)-space so that a corresponding solution of the linearized equations of motion exists. We define the five-vector-valued "difference function" $D(\kappa; X)$ through the following procedure:

- First solve the linear equation at the homothetic horizon $H = 0$ to determine $f_1'(z_+)$, which completes the boundary conditions at $z = 0$ and $z = z_+$.
- Integrate forward from $z = 0$ to an intermediate point z_{mid}, and also backward from z_+ to z_{mid}.
- Output the difference between the two integrations for the five-vector $(b_1, \mathrm{Re}\, f_1, \mathrm{Im}\, f_1, \mathrm{Re}\, f_1', \mathrm{Im}\, f_1')$, evaluated at z_{mid}.

A smooth solution exists iff the difference function vanishes. Observe that the function $D(\kappa; X)$ is linear in X, as the solutions to a linear differential equations are themselves linear in the boundary conditions, and those in turn are linear in X since the constraint defined by H is linear. If so, then it must be that

$$D(\kappa; X) = A(\kappa)X \tag{3.60}$$

where $A(\kappa)$ is a 5×5 matrix with non-linear dependence on X. If one were to solve the equation $D(\kappa; X) = A(\kappa)X = 0$, a solution ray in X would exist iff

$$\det A(\kappa) = 0\,. \tag{3.61}$$

Therefore, no high-dimensional non-linear search must be performed: all that is necessary to determine modes is to find roots to the determinant (3.61) in the one parameter κ (or two, if complex modes are also sought).

The matrix elements can be computed straightforwardly with 5 evaluations of the difference function on unit vectors:

$$A^i_j(\kappa) = D(\kappa; e^j)^i\,, \tag{3.62}$$

which therefore allows us to efficiently compute $\det A$ as a function of κ. Determining roots is then remarkably easy, and can be performed with a simple algorithm such as bisection.

Being now able to identify the entire spectrum for κ, we may now observe that $\mathrm{Re}\,\kappa$ is bounded from above. We can thus determine the mode κ^* of maximum $\mathrm{Re}\,\kappa$, refine its precise value with further root-finding, and finally

output an estimation of the Choptuik critical exponent:

$$\gamma = \frac{1}{\mathrm{Re}\,\kappa^*}\,, \tag{3.63}$$

with a significantly reduced computational effort and increased precision compared to performing several super-critical collapse simulations.

3.5.3 Results

The improved methodology that we have sketched in the previous sections proves fruitful and can efficiently reconstruct the Choptuik critical exponent for the CSS solutions determined previously. The estimate of the original, well-known value for γ for the unique four-dimensional elliptic solution matches the known result in the literature [63]:

$$\gamma = 0.2641\,. \tag{3.64}$$

Our original contribution was the determination of γ for the other critical collapse solutions that we examined, namely in the four-dimensional hyperbolic class and in the five-dimensional elliptic and hyperbolic classes. The most interesting result is that *the Choptuik exponent is different for all these solutions, even within the same dimension and the same conjugacy class.* To the best of our knowledge, this lack of universality for the critical exponent, even for a given dimension and a given matter content, was not noticed previously. The analogies with Statistical Mechanics apparently do not extend insofar as to encompass gravitational collapse, or perhaps a more sophisticated formulation of universality is needed, one involving not only the raw

critical exponent but also some parameters of the CSS solution. We have not been able to identify this possible generalization so far.

The search for CSS solutions may have some lessons in store also for "vacuumless systems", whose classical description is not encompassed by the doubly–perturbative regime of String Theory, because curvatures or string couplings become too large somewhere. The search for CSS solutions is affected by unusual boundary conditions, against standard notions of a flat asymptotic infinity and standard existence and uniqueness statements. It is precisely these features of the problem that produce an exotic discrete solution space akin to a non-linear operator spectrum. Still, the rationale for the number of solutions in each dimension and class has not found, so far, a convincing physical explanation. It is also important to note that there is no argument granting that at least one solution exist in a given dimension and within a given conjugacy class.

Acknowledgements

Writing this Thesis would have been impossible without the careful, devoted guidance of my advisor, Prof. Augusto Sagnotti, who has not only overseen the production of this document but has patiently helped to correct and revise the published works it is based on. I have to thank him, in particular, for his precise physical insights and for the knowledge he has imparted upon me in terms of academic language and presentation.

My gratitude is also extended to my coauthors. First of all, Ivano Basile, with whom I have authored several papers, shared with me his profound understanding and his wide body of knowledge, not to mention an unwavering enthusiasm for fundamental physics, all of which have proved invaluable resources. I thank Alessandro Bombini for introducing us as gently as possible to the mechanisms of academic research, while also leading us to address poignant, fascinating questions - in particular, for proposing the spark that led to our work on the Bubble/RG conjecture. I also cannot overstate the insightful contributions of Ehsan Hatefi, with whom I collaborated on different topics, only part of which lie within the scope of this thesis.

Finally, I am indebted to Prof. Alberto Zaffaroni for detailed discussions on subtleties of AdS/CFT, and to Prof. Luis Álvarez-Gaumé for illuminating indirect correspondence on the critical collapse of the axion-dilaton system.

Bibliography

[1] L. Alvarez-Gaumé, P. Ginsparg, G. Moore, and C. Vafa, "An O(16) × O(16) heterotic string", Physics Letters B **171**, 155–162 (1986).

[2] L. J. Dixon and J. A. Harvey, "String theories in ten dimensions without spacetime supersymmetry", Nuclear Physics, Section B **274**, 93–105 (1986).

[3] A. Sagnotti, "Some Properties of Open - String Theories", (1995), arXiv:`hep-th/9509080`.

[4] A. Sagnotti, "Surprises in open-string perturbation theory", Nuclear Physics B - Proceedings Supplements **56**, 332–343 (1997), arXiv:`hep-th/9702093`.

[5] S. Sugimoto, "Anomaly cancellations in the type I D9-$\overline{\text{D9}}$ system and the USp(32) string theory", Progress of Theoretical Physics **102**, 685–699 (1999), arXiv:`hep-th/9905159`.

[6] I. Antoniadis, E. Dudas, and A. Sagnotti, "Brane supersymmetry breaking", Physics Letters, Section B: Nuclear, Elementary Particle and High-Energy Physics **464**, 38–45 (1999), arXiv:`hep-th/9908023`.

[7] C. Angelantonj, "Comments on open-string orbifolds with a non-vanishing Bab", Nuclear Physics B **566**, 126–150 (2000), arXiv:hep-th/9908064.

[8] G. Aldazabal and A. M. Uranga, "Tachyon-free non-supersymmetric type IIB orientifolds via brane-antibrane systems", Journal of High Energy Physics **3** (1999), arXiv:hep-th/9908072.

[9] C. Angelantonj, I. Antoniadis, G. D'Appollonio, E. Dudas, and A. Sagnotti, "Type I vacua with brane supersymmetry breaking", Nuclear Physics B **572**, 36–70 (2000), arXiv:hep-th/9911081.

[10] E. Dudas, J. Mourad, and A. Sagnotti, "Charged and uncharged D-branes in various string theories", Nuclear Physics B **620**, 109–151 (2002), arXiv:hep-th/0107081.

[11] R. Antonelli and I. Basile, "Brane annihilation in non-supersymmetric strings", Journal of High Energy Physics **2019** (2019), arXiv:1908.04352.

[12] R. Antonelli, I. Basile, and A. Bombini, "AdS vacuum bubbles, holography and dual RG flows", Classical and Quantum Gravity **36** (2019), arXiv:1806.02289.

[13] S. Coleman, "Fate of the false vacuum: Semiclassical theory", Physical Review D **15**, 2929–2936 (1977).

[14] S. Coleman and F. De Luccia, "Gravitational effects on and of vacuum decay", Physical Review D **21**, 3305–3315 (1980).

[15] S. Ryu and T. Takayanagi, "Holographic derivation of entanglement entropy from the anti-de sitter space/conformal field theory correspondence", Physical Review Letters **96** (2006), arXiv:hep-th/0603001.

[16] R. Antonelli and E. Hatefi, "On self-similar axion-dilaton configurations", Journal of High Energy Physics **2020** (2020), arXiv:1912.00078.

[17] R. Antonelli and E. Hatefi, "On critical exponents for self-similar collapse", Journal of High Energy Physics **2020** (2020), arXiv:1912.06103.

[18] M. W. Choptuik, "Universality and scaling in gravitational collapse of a massless scalar field", Physical Review Letters **70**, 9–12 (1993).

[19] L. Álvarez-Gaumé, C. Gómez, A. S. Vera, A. Tavanfar, and M. A. Vázquez-Mozo, "Critical formation of trapped surfaces in the collision of gravitational shock waves", Journal of High Energy Physics **2009** (2009), arXiv:0811.3969.

[20] R. S. Hamadé and J. M. Stewart, "The spherically symmetric collapse of a massless scalar field", Classical and Quantum Gravity **13**, 497–512 (1996), arXiv:gr-qc/9506044.

[21] E. W. Hirschmann and D. M. Eardley, "Universal scaling and echoing in the gravitational collapse of a complex scalar field", Physical Review D **51**, 4198–4207 (1995), arXiv:gr-qc/9412066.

[22] L. Álvarez-Gaumé, C. Gómez, A. Sabio Vera, A. Tavanfar, and M. A. Vázquez-Mozo, "Critical gravitational collapse: Towards a holographic understanding of the Regge region", Nuclear Physics B **806**, 327–385 (2009), arXiv:0804.1464.

[23] C. R. Evans and J. S. Coleman, "Critical phenomena and self-similarity in the gravitational collapse of radiation fluid", Physical Review Letters **72**, 1782–1785 (1994), arXiv:gr-qc/9402041.

[24] T. Koike, T. Hara, and S. Adachi, "Critical behavior in gravitational collapse of radiation fluid: A renormalization group (linear perturbation) analysis", Physical Review Letters **74**, 5170–5173 (1995), arXiv:gr-qc/9503007.

[25] E. W. Hirschmann and D. M. Eardley, "Criticality and bifurcation in the gravitational collapse of a self-coupled scalar field", Physical Review D - Particles, Fields, Gravitation and Cosmology **56**, 4696–4705 (1997), arXiv:gr-qc/9511052.

[26] A. M. Abrahams and C. R. Evans, "Critical behavior and scaling in vacuum axisymmetric gravitational collapse", Physical Review Letters **70**, 2980–2983 (1993).

[27] J. Scherk and J. H. Schwarz, "How to get masses from extra dimensions", Nuclear Physics, Section B **153**, 61–88 (1979).

[28] E. Cremmer, J. Scherk, and J. H. Schwarz, "Spontaneously broken N = 8 supergravity", Physics Letters B **84**, 83–86 (1979).

[29] R. Rohm, "Spontaneous supersymmetry breaking in supersymmetric string theories", Nuclear Physics, Section B **237**, 553–572 (1984).

[30] C. Kounnas and M. Porrati, "Spontaneous supersymmetry breaking in string theory", Nuclear Physics, Section B **310**, 355–370 (1988).

[31] S. Ferrara, C. Kounnas, M. Porrati, and F. Zwirner, "Superstrings with spontaneously broken supersymmetry and their effective theories", Nuclear Physics, Section B **318**, 75–105 (1989).

[32] I. Antoniadis and C. Kounnas, "Superstring phase transition at high temperature", Physics Letters B **261**, 369–378 (1991).

[33] E. Kiritsis and C. Kounnas, "Perturbative and non-perturbative partial supersymmetry breaking: N = 4 → N = 2 → N = 1", Nuclear Physics B **503**, 117–156 (1997).

[34] M. B. Green, J. H. Schwarz, and E. Witten, *Superstring theory: 25th anniversary edition*, Vol. 1, Cambridge Monographs on Mathematical Physics (Cambridge University Press, 2012).

[35] K. Becker, M. Becker, and J. Schwarz, *String theory and M-theory: A modern introduction* (Cambridge University Press, Dec. 2006).

[36] J. Wess and J. Bagger, *Supersymmetry and supergravity* (Princeton University Press, Princeton, NJ, USA, 1992).

[37] J. Terning, *Modern supersymmetry: Dynamics and duality* (Apr. 2006).

[38] D. Z. Freedman and A. Van Proeyen, *Supergravity* (Cambridge University Press, 2012).

[39] E. Dudas, M. Nicolosi, G. Pradisi, and A. Sagnotti, "On tadpoles and vacuum redefinitions in String Theory", Nuclear Physics B **708**, 3–44 (2005), arXiv:hep-th/0410101.

[40] E. Dudas, N. Kitazawa, and A. Sagnotti, "On climbing scalars in String Theory", Physics Letters, Section B: Nuclear, Elementary Particle and High-Energy Physics **694**, 80–88 (2010), arXiv:1009.0874.

[41] A. Gruppuso, N. Kitazawa, N. Mandolesi, P. Natoli, and A. Sagnotti, "Pre-inflationary relics in the CMB?", Physics of the Dark Universe **11**, 68–73 (2016), arXiv:1508.00411.

[42] A. Sagnotti, *Low-l CMB from string-scale SUSY breaking?*, Sept. 2017, arXiv:1509.08204.

[43] J. Mourad and A. Sagnotti, "An Update on Brane Supersymmetry Breaking", International School of Subnuclear Physics (2017), arXiv:1711.11494.

[44] J. Mourad and A. Sagnotti, "AdS vacua from dilaton tadpoles and form fluxes", Physics Letters, Section B: Nuclear, Elementary Particle and High-Energy Physics **768**, 92–96 (2017), arXiv:1612.08566.

[45] D. L. Wiltshire, "Dilaton black holes with a cosmological term", Journal of the Australian Mathematical Society Series B-Applied Mathematics **41**, 198–216 (1999), arXiv:gr-qc/9502038.

[46] I. R. Klebanov and A. A. Tseytlin, "D-branes and dual gauge theories in type 0 strings", Nuclear Physics B **546**, 155–181 (1999).

[47] S. J. Poletti, J. Twamley, and D. L. Wiltshire, "Charged dilaton black holes with a cosmological constant", Physical Review D **51**, 5720–5724 (1995).

[48] S. S. Gubser and I. Mitra, "Some interesting violations of the Breitenlohner-Freedman bound", Journal of High Energy Physics **6**, 1145–1159 (2002), arXiv:hep-th/0108239.

[49] I. Basile, J. Mourad, and A. Sagnotti, "On classical stability with broken supersymmetry", Journal of High Energy Physics **2019**, 174 (2019).

[50] E. Dudas and J. Mourad, "Brane solutions in strings with broken supersymmetry and dilaton tadpoles", Physics Letters, Section B: Nuclear, Elementary Particle and High-Energy Physics **486**, 172–178 (2000), arXiv:hep-th/0004165.

[51] J. Maldacena, "The large-N limit of superconformal field theories and supergravity", International Journal of Theoretical Physics **38**, 1113–1133 (1999), arXiv:hep-th/9711200.

[52] A. B. Zamolodchikov, *Irreversibility of the Flux of the Renormalization Group in a 2D Field Theory*, 1986.

[53] C. Holzhey, F. Larsen, and F. Wilczek, "Geometric and renormalized entropy in conformal field theory", Nuclear Physics, Section B **424**, 443–467 (1994), arXiv:hep-th/9403108.

[54] P. Calabrese and J. Cardy, "Entanglement entropy and quantum field theory", Journal of Statistical Mechanics: Theory and Experiment (2004), arXiv:hep-th/0405152.

[55] L. F. Abbott and S. Coleman, "The collapse of an anti-de sitter bubble", Nuclear Physics, Section B **259**, 170–174 (1985).

[56] B. Czech, L. Lamprou, S. Mccandlish, and J. Sully, "Integral Geometry and Holography", (2015), arXiv:arXiv:1505.05515v1.

[57] J. D. Brown and M. Henneaux, *Central Charges in the Canonical Realization of Asymptotic Symmetries: An Example from Three Dimensional Gravity*, tech. rep. 2 (1986), pp. 207–226.

[58] E. W. Hirschmann and D. M. Eardley, "Universal scaling and echoing in the gravitational collapse of a complex scalar field", Physical Review D **51**, 4198–4207 (1995), arXiv:gr-qc/9412066.

[59] L. Álvarez-Gaumé, C. Gómez, A. Sabio Vera, A. Tavanfar, and M. A. Vázquez-Mozo, "Critical gravitational collapse: Towards a holographic

understanding of the Regge region", Nuclear Physics B **806**, 327–385 (2009), arXiv:0804.1464.

[60] C. R. Evans and J. S. Coleman, "Critical phenomena and self-similarity in the gravitational collapse of radiation fluid", Physical Review Letters **72**, 1782–1785 (1994), arXiv:gr-qc/9402041.

[61] T. Koike, T. Hara, and S. Adachi, "Critical behavior in gravitational collapse of radiation fluid: A renormalization group (linear perturbation) analysis", Physical Review Letters **74**, 5170–5173 (1995), arXiv:gr-qc/9503007.

[62] D. Maison, "Non-universality of critical behaviour in spherically symmetric gravitational collapse", Physics Letters, Section B: Nuclear, Elementary Particle and High-Energy Physics **366**, 82–84 (1996), arXiv:gr-qc/9504008.

[63] D. M. Eardley, E. W. Hirschmann, and J. H. Horne, "S duality at the black hole threshold in gravitational collapse", Physical Review D **52** (1995), arXiv:gr-qc/9505041.

[64] L. Álvarez-Gaumé and E. Hatefi, "Critical collapse in the axion-dilaton system in diverse dimensions", Classical and Quantum Gravity **29** (2012), arXiv:1108.0078.